UNIVERSIDADE DE SÃO PAULO
FACULDADE DE MEDICINA

PÓS-GRADUAÇÃO EM ALERGIA E IMUNOPATOLOGIA

GIULIANA XAVIER DE MEDEIROS

Avaliação da resposta imunológica contra SARS-CoV-2 em
grupos de risco vacinados com CoronaVac

São Paulo
2024

GIULIANA XAVIER DE MEDEIROS

Avaliação da resposta imunológica contra SARS-CoV-2 em grupos de risco vacinados com CoronaVac

Tese apresentada à Faculdade de Medicina da Universidade de São Paulo para obtenção do título de Doutor em Ciências

Programa de Alergia e Imunopatologia

Orientador: Prof. Dr. Edecio Cunha-Neto

Versão corrigida. Resolução CoPGr6018/11, de 13 de outubro de 2011. A versão

original está disponível na Biblioteca FMUSP

São Paulo
2024

Agradecimentos

Agradeço, primeiramente, aos meus pais, por todo o apoio, incentivo e amor incondicional.

Ao meu marido, Roberto, por estar sempre ao meu lado.

À Luri Sasahara, Fernanda Bruno e Safiri Paiva, por serem o melhor presente da Pós-Graduação.

À Loisi de Carvalho, pela ajuda na realização dos experimentos.

Ao meu orientador, Edecio Cunha-Neto, pelos ensinamentos e orientação.

À Keity Souza Santos, por todos os conselhos.

À Andreia Kuramoto, sem a qual nenhum dos resultados aqui apresentados seriam possíveis.

Aos membros do Laboratório de Imunologia do Incor, pelo apoio, risadas e companheirismo.

À Susan Ribeiro, pelo acolhimento e contribuição para meu crescimento científico e pessoal.

Aos amigos da Emory University, por serem minha família longe de casa.

À todos os pacientes e seus familiares que tornaram a realização deste trabalho possível.

"I would rather have questions that can't be answered
than answers that can't be questioned."
- Richard Feynman

RESUMO

Medeiros GX. Avaliação da resposta imunológica contra SARS-CoV-2 em grupos de risco vacinados com CoronaVac [tese]. São Paulo: Faculdade de Medicina, Universidade de São Paulo; 2024.

Neste trabalho, tivemos como objetivo avaliar a resposta de grupos vulneráveis à COVID-19, como idosos e pacientes com Imunodeficiência Comum Variável (ICV), vacinados com CoronaVac. Além da resposta ao regime inicial de 2doses, também foi avaliada a resposta ao reforço vacinal com a vacina de RNAm BNT162b2. Níveis de IgG anti-RBD e Spike de SARS-CoV-2, IFN-γ e IL-2 após ensaio de liberação de citocinas induzido por antígeno, foram determinados por ELISA. Título de neutralização foram quantificados por teste de neutralização baseado em efeito citopático (CPE-VNT) para os dois grupos. Na coorte de idosos, foram incluídos indivíduos vacinados com 2 doses de CoronaVac (N=101, dos quais 54% estão acima dos 55 anos), ou 2 CoronaVac + 1 BNT162b2 (N=31), convalescentes foram recrutados como controles positivos (N=72) e amostras pré-pandêmicas foram incluídas como controle negativo (N=36). Não foi observada diferença na produção de IFN-γ e IL-2 entre vacinados com 2 doses e convalescentes. Vacinados tiveram maior produção de IgG anti-RBD de SARS-CoV-2, entretanto convalescentes apresentaram maiores títulos de anticorpos neutralizantes. Foi observada uma correlação negativa significativa entre produção de citocinas e anticorpos e idade dos participantes. Mulheres e homens mais jovens apresentaram maior produção de IL-2 em relação aos participantes acima de 55 anos. Homens acima de 55 anos tiveram níveis de IgG anti-RBD diminuídos em comparação àqueles abaixo de 55 anos. Mulheres acima de 55 apresentaram menor produção de anticorpos neutralizantes em comparação às mais jovens. A terceira dose (BNT162b2) levou à um aumento significativo na produção de anticorpos específicos e neutralizantes. O aumento foi observado tanto em indivíduos acima quanto abaixo de 55 anos em relação à 2a dose. Na coorte de imunodeficiência, foram incluídos 26 pacientes com ICV vacinados com 2 doses de CoronaVac (N=14) ou ChAdOx1 (N=9) e vacinados com 2 CoronaVac + 1 BNT162b2 (N=14). Indivíduos saudáveis vacinados com CoronaVac (N=60) e após reforço com BNT162b2 foram incluídos como controles (N=16). Pacientes ICV vacinados com 2 doses ChAdOx1 apresentaram maiores dos níveis de anticorpo anti-RBD e -S em relação aos vacinados com CoronaVac. Vacinados com ChAdOx1 foram os únicos a produzirem anticorpos neutralizantes contra as linhagens Wuhan, Delta e Gama. A resposta celular foi baixa independentemente da plataforma vacinal. O regime de 3 doses (2 CoronaVac + 1 BNT162b2) induziu resposta imune menor do que 2 doses de ChAdOx1. A resposta vacinal de pacientes ICV foi menor do que a de indivíduos saudáveis. Nossos resultados indicam que idosos se beneficiaram da dose heteróloga de BNT162b2, porém a duração desta resposta deve ser avaliada em estudos longitudinais para garantir o calendário ótimo de doses adicionais para este grupo. Os pacientes ICV tiveram uma melhor resposta ao regime de duas doses de ChAdOx1 em comparação ao de 3 doses, sugerindo

que aqueles inicialmente vacinados com CoronaVac podem não estar adequadamente protegidos contra a infecção por SARS-CoV-2 e suas complicações.

ABSTRACT

Medeiros, GX. Evaluation of immunological response Against SARS-CoV-2 in risk groups vaccinated with CoronaVac [thesis]. São Paulo: Faculdade de Medicina, Universidade de São Paulo; 2024.

In this study, our objective was to evaluate the response of vulnerable groups to COVID-19, such as the elderly and patients with Common Variable Immunodeficiency (CVID), who were vaccinated with CoronaVac. In addition to the response to the initial 2-dose regimen, the response to booster vaccination with the mRNA vaccine BNT162b2 was also assessed. Levels of anti-RBD and Spike IgG antibodies against SARS-CoV-2, as well as IFN-γ and IL-2 levels after antigen-induced cytokine release assay, were determined by ELISA. Neutralization titers were quantified using a cytopathic effect-based neutralization test (CPE-VNT) for both groups. In the elderly cohort, individuals vaccinated with 2 doses of CoronaVac (N=101, of which 54% were above 55 years old) or 2 CoronaVac + 1 BNT162b2 (N=31) were included. Convalescent individuals were recruited as positive controls (N=72), and pre-pandemic samples were included as negative controls (N=36). No difference was observed in the production of IFN-γ and IL-2 between individuals vaccinated with 2 doses and convalescent individuals. Vaccinated individuals had higher production of anti-RBD IgG antibodies against SARS-CoV-2; however, convalescent individuals exhibited higher titers of neutralizing antibodies. A significant negative correlation was observed between cytokine production and antibody levels, as well as the age of participants. Women and younger men showed higher IL-2 production compared to participants above 55 years old. Men above 55 years old had decreased levels of anti-RBD IgG compared to those below 55 years old. Neutralizing antibody titers were lower in women above 55 compared to younger women. The third dose (BNT162b2) led to a significant increase in the production of specific and neutralizing antibodies. This increase was observed in both individuals above and below 55 years old compared to the second dose. In the immunodeficiency cohort, 26 CVID patients vaccinated with 2 doses of CoronaVac (N=14) or ChAdOx1 (N=9) and 2 CoronaVac + 1 BNT162b2 (N=14) were included. Healthy individuals vaccinated with CoronaVac (N=60) and boosted with BNT162b2 were included as controls (N=16). CVID patients vaccinated with 2 doses of ChAdOx1 showed higher levels of anti-RBD and –S antibodies compared to those vaccinated with CoronaVac. Only individuals vaccinated with ChAdOx1 produced neutralizing antibodies against the Wuhan, Delta, and Gamma variants. Cellular response was low regardless of the vaccine platform. The 3-dose regimen (2 CoronaVac + 1 BNT162b2) induced a lower immune response than 2 doses of ChAdOx1. The vaccine response in CVID patients was lower than in healthy individuals. Our results indicate that the elderly benefited from the heterologous dose of BNT162b2; however, the duration of this response should be evaluated in longitudinal studies to ensure the optimal schedule for additional doses in this group. CVID patients had a better response to the two-dose regimen of ChAdOx1 compared to the 3-dose regimen, suggesting that those initially vaccinated with CoronaVac may not be adequately protected against SARS-CoV-2 infection and its complications.

Lista de figuras

Lista de abreviações

cDNA – ácido desoxirribonucleico complementar (do inglês, *complementary desoxiribonucleic acid*)

DP – desvio padrão

ELISPOT – ensaio de imunoadsorção ligado a enzima em pontos (do inglês, enzyme-linked immunospot assay)

HCoV – coronavírus humano (do inglês, human coronavírus)

IIQ – intervalo interquartil

ICS – marcação de citocina intracelular (do inglês, *intracelular cytokine staining*)

IL-2 – interleucina 2

IFN-y – interferon gamma

Kb – quilo bases

MCP1 – proteína quimioatrativa de monócitos-1 (do inglês, *monocyte chemoattractant protein-1*)

NA – não se aplica

NAb – anticorpos neutralizantes (do inglês, *neutralizing antibodies*)

NLR – receptor do tipo NOD (do inglês, *NOD-like receptor*)

NSP – proteínas não estruturais (do inglês, *non-structural protein*)

ORF – fase de leitura aberta (do inglês, *open reading frame*)

PBMC – células mononucleares do sangue periférico (do inglês, *peripheral blood mononuclear cells*)

RLR – receptor do tipo RIG (*RIG-like receptor*)

RNA – ácido ribonucleico (do inglês, *ribonucleic acid*)

RT-qPCR – reação em cadeira da polimerase quantitativa em tempo real (do inglês, *real time quantitative polymerase chain reaction*)

SARS-CoV-2 - coronavírus da síndrome respiratória aguda grave 2 (do inglês, *severe acute respiratory syndrome coronavirus 2*)

TLR – receptor do tipo toll (do inglês, *toll-like receptor*)

TMPRSS2 – serina protease transmembrana (do inglês, *transmembrane protease serine 2*)

TNF-α – fator de necrose tumoral alfa (do inglês, *tumor necrosis fator alpha*)

VOC – variantes de preocupação (do inglês, variants of concern)

Sumário

1. Introdução

A pandemia de COVID-19 teve início em dezembro de 2019 em Wuhan, na China, e rapidamente se espalhou por todos os continentes. Desde 2019, já houve mais 700 milhões de casos e quase 7 milhões de mortes mundialmente, de acordo com a Organização Mundial de Saúde (OMS, 2023). A COVID-19 é causada pelo coronavírus da síndrome respiratória aguda grave 2 (SARS-CoV-2), identificado em janeiro de 2020 (WU, Fan *et al.*, 2020).

O SARS-CoV-2 pertence ao gênero Coronavirus, família Coronaviridae e à classe dos Betacoronavirus, caracterizada por vírus envelopados de RNA fita simples com genomas longos, contendo 28 a 34kb. Outros vírus da mesma família já foram responsáveis por epidemias de infecções respiratórias no passado, como o SARS-CoV e MERS-CoV, em 2002 e 2012 respectivamente, e outros são responsáveis pelos resfriados sazonais, como OC43, HKU-1, 293E e NL63 (FEHR; PERLMAN, 2015). Assim como a dos demais coronavírus patogênicos, a transmissão do SARS-CoV-2 ocorre, principalmente, através do contato próximo com pessoas infectadas, por meio da tosse, espirro e gotículas respiratórias contendo o vírus (LOTFI; HAMBLIN; REZAEI, 2020).

A maioria dos indivíduos infectados por SARS-CoV-2 apresenta doença assintomática ou leve (DIAMOND; KANNEGANTI, 2022), sendo os sintomas mais comuns tosse, dor de garganta ou coriza, seguido ou não de anosmia, ageusia, diarreia, dor abdominal, febre, fadiga e/ou cefaleia. Os casos moderados são aqueles com persistência dos sintomas leves com uma piora progressiva e pneumonia. A doença é considerada grave quando, além da persistência dos sintomas iniciais, tem-se síndrome respiratória aguda grave, caracterizada por desconforto respiratório e/ou saturação de oxigênio abaixo de 94% (OMS, 2023). Os casos graves ou que evoluem para óbito geralmente estão associados ao sexo, fatores genéticos, comorbidades, imunodeficiências e idade avançada (DIAMOND; KANNEGANTI, 2022; WRAY; ARROWSMITH, 2021).

A infecção tem início nas vias orais, após a inalação do vírus. O SARS-CoV-2 codifica proteínas específicas que permitem que ele interaja com receptores das células epiteliais do trato respiratório e inicie sua replicação intracelular (TAY *et al.*, 2020). O genoma do SARS-CoV-2 codifica 29 proteínas virais e contém 14 fases de leitura aberta (ORFs). Dois terços do genoma codificam duas poliproteínas (pp1a e pp1ab),

que são digeridas por proteases em 16 proteínas não-estruturais (NSPs), essenciais para replicação e transcrição viral (WANG *et al.*, 2020). O terço restante codifica as proteínas estruturais spike, envelope, membrana e nucleocapsídeo, responsáveis pela montagem do vírion e entrada na célula. Genes acessórios codificam proteínas acessórias (ORF3a, ORF3b, ORF6, ORF7a, ORF7b, ORF8b, ORF9b e ORF14), envolvidas na regulação da infecção viral (YANG; RAO, 2021).

A proteína spike tem um papel importante na patogênese da COVID-19, pois medeia a entrada do vírus na célula hospedeira. A spike forma trímeros na superfície da célula e é clivada pela serina protease transmembrana 2 (TMPRSS2) em duas subunidades (S1 e S2) (NAQVI *et al.*, 2020). A subunidade S1 está envolvida na adesão dos vírus à membrana da célula hospedeira por interação do domínio de ligação ao receptor (RBD) com a enzima conversora da angiotensina 2 (ACE2), expressa nas células epiteliais (WAN *et al.*, 2020). Após a ligação da RBD com a ACE2, a subunidade S2 auxilia a fusão do vírus com a membrana da célula. Durante este processo, a subunidade S2 apresenta 3 conformações: 1) estado pré-fusional, 2) estado intermediário pré-grampo e 3) grampo pós fusional (QING; GALLAGHER, 2020). Essas mudanças conformacionais estão associadas com a antigenicidade do vírus (WALLS *et al.*, 2020).

Após a entrada na célula, o vírus inicia sua montagem (Figura 1). Os ribossomos do hospedeiro são utilizados para a produção das poliproteases pp1a e pp1ab, que serão processadas nas 16 NSPs. As NSPs formarão o complexo de replicação e transcrição (RTC) e iniciarão o processo de transcrição e replicação do RNA viral. O RNA genômico e proteínas estruturais formam vírions maduros, que serão liberados por exocitose para iniciar outro ciclo de infecção (DIAMOND; KANNEGANTI, 2022).
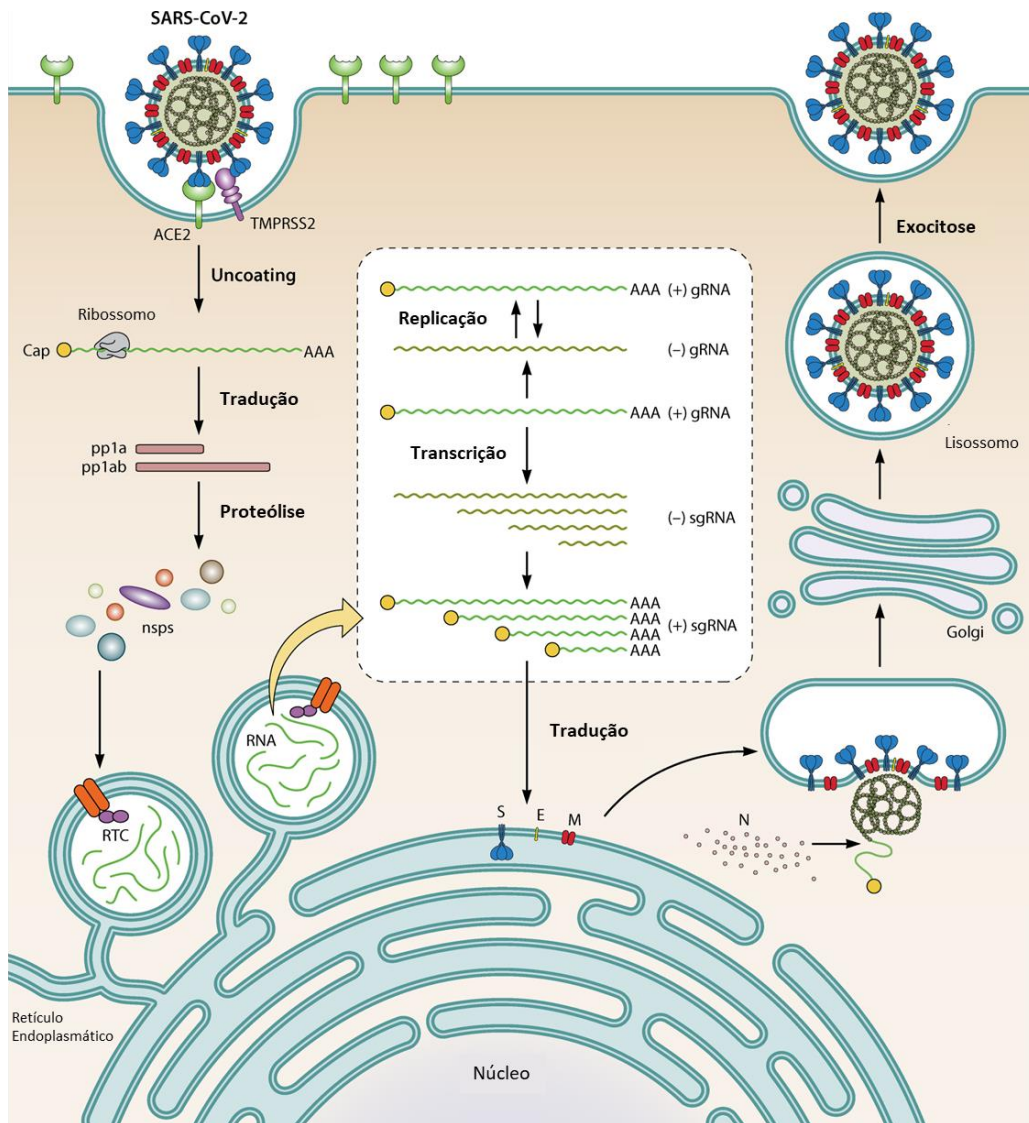
Figura 1. Etapas da replicação do vírus SARS-CoV-2. Adaptado de KUNG *et al.*, 2022.

2.1. Resposta imune adaptativa contra SARS-CoV-2

A resposta imune adaptativa contra o SARS-CoV-2 surge entre o 5º e 10º dia de infecção, devido a necessidade de expansão e diferenciação dos linfócitos naive em linfócitos efetores. Quando há uma população suficiente de linfócitos T (auxiliares e citotóxicos) e B (células secretoras de anticorpos, chamadas de plasmócitos), eles trabalham juntos para eliminar as células infectadas e os vírus circulantes (SETTE; CROTTY, 2020).

A resposta humoral tem um papel importante na defesa contra infecções virais. No geral, a resposta pode ser dividida em duas fases: extra-folicular e centro germinativo (ELSNER; SHLOMCHIK, 2020). Na primeira fase, linfócitos B são ativados e se

diferenciam em plasmócitos nos linfonodos – especificamente, na parte externa do folículo – poucos dias após a infecção. Os plasmócitos produzem anticorpos com afinidade baixa, mas suficiente para neutralizar o vírus (LAM; SMITH; BAUMGARTH, 2020). A maior parte desses linfócitos são produtores de IgM, e tem vida curta na circulação. A segunda fase ocorre no centro germinativo, e é mais demorada e complexa que a primeira. Nesta, linfócitos B antígeno-específicos passam por hipermutação somática e seleção baseada em afinidade para gerar células de memória longevas e com alta afinidade (ELSNER; SHLOMCHIK, 2020).

A maioria dos indivíduos infectados por SARS-CoV-2 produz anticorpos específicos – processo chamado de soroconversão – dentro de 1 a 2 semanas após a infecção, sendo os principais alvos as proteínas spike e nucleocapsídeo (PICCOLI *et al.*, 2020; QI *et al.*, 2022). A produção de IgG, IgM e IgA é praticamente simultânea, porém IgM e IgA decaem rapidamente, enquanto a produção de IgG persiste por mais tempo (ISHO *et al.*, 2020).

O aparecimento de anticorpos neutralizantes (NAb) é rápido e geralmente ocorre simultaneamente à soroconversão (SEOW *et al.*, 2020). Os anticorpos neutralizantes têm como principal alvo a RBD, responsável pela entrada no vírus na célula hospedeira, chegando a 90% da atividade neutralizante do soro (PICCOLI *et al.*, 2020). Os níveis séricos de NAbs atingem seu pico poucas semanas após a infecção e caem significativamente durante os meses subsequentes (COHEN *et al.*, 2021; SEOW *et al.*, 2020). Interessantemente, diversos estudos relatam que indivíduos sem anticorpos neutralizantes após infecção conseguiram se recuperar da COVID-19, devido a uma resposta celular considerável (RYDYZNSKI MODERBACHER *et al.*, 2020; SCHULIEN *et al.*, 2021). A presença de linfócitos T específicos para SARS-CoV-2 em indivíduos convalescentes na ausência de anticorpos é chamada de "sensibilização celular sem soroconversão" (MOSS, 2022; SWADLING *et al.*, 2021).

A resposta celular na COVID-19 é caracterizada pela presença de linfócitos T CD4+ e CD8+ (SETTE; CROTTY, 2020). Linfócitos T CD4+ estão presentes após quase toda infecção por SARS-CoV-2 e são mais proeminentes que respostas T CD8+ (GRIFONI *et al.*, 2020; SEKINE *et al.*, 2020). Ao contrário da resposta de anticorpos, linfócitos T CD4+ específicos foram encontrados contra quase todas as proteínas da linhagem ancestral de SARS-CoV-2 (21 em 24), ainda que com reconhecimento maior das proteínas spike, membrana e nucleocapsídeo (GRIFONI *et al.*, 2020). Estudos observacionais de pacientes com COVID-19 aguda e convalescentes mostraram que

a resposta de linfócitos T está associada à doença leve, indicando a importância da resposta celular para controle da doença (SEKINE et al., 2020; TARKE et al., 2022). A resposta de linfócitos T CD4+ contra SARS-CoV-2 é caracterizada pela alta produção das citocinas IFN-γ, IL-2, TNF-α, IL-6 e IL-17A, característicos de um perfil Th1 (SHAH *et al.*, 2020; SONG *et al.*, 2020). Uma das funções dos linfócitos T CD4+ é a de recrutar outras células efetoras para o sítio da infecção e, para isso, expressam também quimiocinas que auxiliam nessa função, como CCL-3, CCL-4 e CCL-5 (MECKIFF *et al.*, 2020). Já os linfócitos T CD8+, apresentam alta capacidade proliferativa e citotóxica, com alta produção de IFN-γ, granzima B, perforina e CD107a (RYDYZNSKI MODERBACHER *et al.*, 2020; SCHULIEN *et al.*, 2021; SEKINE *et al.*, 2020).

Estudos longitudinais realizados após a epidemia de SARS-CoV-1 em 2002 mostraram que a resposta de anticorpos se tornou indetectável após 4 anos (TANG *et al.*, 2011), enquanto linfócitos T de memória contra o vírus foram detectados até 17 anos após a infecção (LE BERT *et al.*, 2020). No caso da atual pandemia de SAR-CoV-2, foi observado que a produção de anticorpos neutralizantes diminui 4-6 meses após a infecção natural (DAN *et al.*, 2021; WHEATLEY *et al.*, 2021), mas a resposta celular permaneceu detectável 12 meses após infecção (GUO *et al.*, 2022).

Outro grande desafio a pandemia de COVID-19 foi o aparecimento de variantes virais. Nos últimos meses, diversas variantes de SARS-CoV-2 emergiram, como a alpha, beta, gamma, delta e, mais recentemente, omicron (OMS, 2023). Todas estiveram associadas a aumento da transmissibilidade, maior risco de reinfecção, resposta de NAbs reduzida e redução da efetividade das vacinas, e por isso foram classificadas como variantes de preocupação (VOCs) (OMS, 2023). Estratégias para combater o aparecimento de novas variantes são de extrema urgência e, em grande parte, não dependem somente do sistema imune, mas sim da adesão da população às vacinas desenvolvidas contra COVID-19 e a formulação de novos imunizantes capazes de eliminar o vírus mutante.

1.1. Vacinas contra COVID-19

O desenvolvimento de vacinas contra a COVID-19 foi extremamente rápido e bem-sucedido. Graças ao conhecimento adquirido durante as epidemias de SARS e MERS, diversos laboratórios possuíam pesquisas avançadas sobre a patogênese dos

coronavírus, o que permitiu o desenvolvimento de vacinas em menos de 1 ano da identificação do SARS-CoV-2. Desde o início da vacinação em dezembro de 2020, mais de 13 bilhões de doses foram aplicadas no mundo todo. No Brasil, já foram mais de 510 milhões de doses, com a taxa de imunização completa chegando a 80% em junho de 2023 (SAÚDE, 2023).

Atualmente, temos 11 vacinas aprovadas para uso emergencial, e mais de 180 em fase de testes clínicos (OMS, 2023). Dentre as vacinas aprovadas, incluem-se: (i) vacinas de RNA mensageiro (RNAm); (ii) vacinas de vetores virais não replicantes; (iii) vacina de subunidade proteica; (iv) vacina de vírus inativado. As características de cada tipo de vacina estão resumidas na tabela 1 (SADARANGANI; MARCHANT; KOLLMANN, 2021; TREGONING et al., 2021).

A maioria das vacinas baseia-se na apresentação da proteína spike. Isso se deve ao fato de que em indivíduos hospitalizados com COVID-19, a presença de anticorpos específicos contra a spike se correlacionou com sobrevivência (ATYEO et al., 2020). Ainda, NAbs contra a spike estão presentes na maioria dos indivíduos após a infecção (LEE et al., 2021; ROBBIANI et al., 2020). Em estudos vacinais preliminares, a quantidade de NAbs contra a proteína spike foi demonstrada como o correlato de proteção mais promissor (CHANDRASHEKAR et al., 2020).

A vacina de RNAm BNT162b2 foi a mais utilizada no mundo (OMS, 2023). Sua eficácia no "mundo real" foi considerada similar àquela relatada pelo ensaio clínico de fase III (CHODICK et al., 2021). Duas semanas após a 2ª dose da BNT162b2, tem-se um aumento significativo dos níveis de anticorpos neutralizantes e de IgG nos indivíduos vacinados (LUSTIG et al., 2021). Além da resposta humoral, foi observada a presença de linfócitos T CD4+ e CD8+ IFN-γ+ e/ou IL-2+ após a 2ª dose (SAHIN et al., 2021). A vacina foi também associada a redução de hospitalizações e mortes relacionadas à COVID-19 (CHODICK et al., 2021; HAAS et al., 2021). A vacina de vírus inativado CoronaVac foi utilizada para vacinação em massa na maioria dos países de média e baixa renda, incluindo o Brasil. Resultados de estudos clínicos randomizados demonstraram uma eficácia de 51 a 84% contra infecção sintomática em adultos de 18-59 anos (HITCHINGS et al., 2021; JARA et al., 2021; TANRIOVER et al., 2021), chegando a 90% de eficácia na prevenção de hospitalização na UTI (JARA et al., 2021). Estudos relataram uma alta taxa de soroconversão após 2 doses de CoronaVac, com a presença de IgG anti-RBD em 99-100% dos vacinados 28 dias após a segunda dose (WU, Zhiwei et al., 2021; YALÇIN et al., 2022). Anticorpos

neutralizantes foram detectados em 94-100% dos indivíduos após o mesmo intervalo (WU, Zhiwei *et al.*, 2021; YALÇIN *et al.*, 2022; ZHANG *et al.*, 2021). Quando comparando a magnitude da resposta humoral entre vacinas, diferentes estudos detectaram menores títulos de NAbs em indivíduos vacinados com CoronaVac em relação aos vacinados com BNT162b2 (LU *et al.*, 2021; PENG *et al.*, 2022).

Quanto à duração da resposta imunológica induzida pela vacina, foi observada uma redução da resposta humoral 6 meses após a segunda dose de BNT162b2, sendo essa redução mais acentuada em homens e idosos (LEVIN *et al.*, 2021). Anticorpos contra as VOCs circulantes não foram detectados em indivíduos vacinados com 2 doses de CoronaVac ou 2 doses de vacina de RNAm (PENG *et al.*, 2022). A resposta celular se manteve estável frente às variantes em indivíduos vacinados com vacina de RNAm (MOSS, 2022).

Devido à queda da proteção contra a infecção ao longo do tempo, redução da proteção contra variantes e proteção reduzida em grupos de risco, mesmo após 2 doses da vacina – seja ela de RNAm ou vírus inativado –, a OMS passou a recomendar de doses de reforço.

Considerando a importância da resposta celular para a proteção contra COVID-19, estudos longitudinais que acompanham a resposta imunológica das doses adicionais serão essenciais para guiar o desenvolvimento do plano de imunização e manutenção da proteção contra as atuais e possíveis novas variantes de SARS-CoV-2.

Tabela 1. Características das principais vacinas contra COVID-19. Adaptada de Sadarangani et al. 2020

Vacina	Fabricante	Formulação	Eficácia contra infecção sintomática
RNAm			
BNT162b2	Pfizer/BioNTech	Nanopartículas lipídicas de mRNA codificando a proteína S completa, modificada por 2 mutações na prolina para manter conformação pré-fusão da proteína.	95% após 2 doses
mRNA-1273	Moderna	Nanopartículas lipídicas de mRNA codificando a proteína S completa, modificada por 2 mutações na prolina para manter conformação pré-fusão da proteína.	95% após 2 doses
Vetor viral			
ChAdOx1 nCoV-19	Universidade de Oxford/AstraZeneca	Vetor de adenovírus símio recombinante com replicação deficiente expressando a proteína S completa com uma sequencia tPA inicial	91% após 2 doses
Gam-COVID-Vac	Gamaleya Research Institute	Vetor de adenovírus humano 26 (dose 1) e adenovírus humano 5 (dose 2) recombinante com replicação deficiente expressando a proteína S completa	91% após 2 doses
Ad26. COV2.S	Janssen	Vetor de adenovírus humano 26 recombinante com replicação deficiente expressando a proteína S completa com mutação em 2 aminoácidos na junção S1/S2	67% após 1 dose
Subunidade proteica			
NBX-CoV2372	Novavax	Nanopartícula recombinante da proteína S com mutações nos sítios de clivagem S1/S2 e duas substituições de prolina para estabilizar na conformação pré fusão. Adjuvante com base de saponina (Matriz-M1)	90% após 2 doses
Vírus inativado			
CoronaVac	Sinovac Biotech	SARS-CoV-2 cultivado em células Vero, inativado com B-propiolactona e adsorbido em hidróxido de alumínio	50-84% após 2 doses

1.2. Resposta vacinal em grupos de risco

1.2.1. Idosos

Idosos são mais suscetíveis a infecções e, devido ao declínio do sistema imunológico, a eficácia das vacinas também é reduzida com a idade. Esse declínio na capacidade do sistema imunológico em gerar imunidade protetora contra vacinas e infecções ao longo dos anos é denominado "imunosenescência" (ALLEN *et al.*, 2020; FRASCA; BLOMBERG, 2020). Por este motivo, idosos foram incluídos como um grupo de risco na pandemia da COVID-10.

À medida que envelhecemos, o sistema imunológico inato começa a produzir respostas inflamatórias cronicamente, processo conhecido como "inflammaging", que contribui, entre outros fatores, para doenças relacionadas ao envelhecimento (FRANCESCHI *et al.*, 2018). Apesar dessa inflamação, a capacidade do sistema imunológico inato de se ativar e, consequentemente, ativar a resposta adaptativa é reduzida (SHAW; GOLDSTEIN; MONTGOMERY, 2013). Na resposta imune inata, observa-se que a subpopulação de monócitos CD14+16+, que produz citocinas pró-inflamatórias, aumenta com a idade, contribuindo para o inflammaging (MERINO *et al.*, 2011). No entanto, apesar do aumento basal na produção de citocinas pró-inflamatórias, a resposta inflamatória aos antígenos é reduzida em idosos, possivelmente devido à diminuição da capacidade fagocítica desses monócitos (PENCE, 2020).

Estudos em macrófagos de pacientes idosos mostraram redução na capacidade de apresentação de antígenos após a vacinação (JACKAMAN *et al.*, 2013; KELLY *et al.*, 2007). Isso pode ser explicado pela redução na produção de IFN-γ, citocina responsável pela ativação de macrófagos e pela função fagocítica. Estudos em camundongos também demonstraram que macrófagos de animais mais velhos apresentam expressão reduzida de MHC-II após o tratamento com IFN-γ (HERRERO *et al.*, 2001). Além disso, foi demonstrado que células dendríticas derivadas de monócitos (moDCs) apresentam capacidade fagocítica e migração reduzidas, o que pode ter um impacto negativo na capacidade dessas células de capturar antígenos e apresentá-los aos linfócitos T nos linfonodos, resultando na redução da ativação da resposta adaptativa (AGRAWAL *et al.*, 2007).

À medida que envelhecemos, ocorre um declínio progressivo na produção de linfócitos T naive pelo timo e nas células T progenitoras da medula óssea (KYOIZUMI *et al.*, 2013). A redução na quantidade de linfócitos T naive resulta em um menor repertório do receptor de células T (TCR), o que afeta a capacidade dessas células de reconhecer antígenos novos (BEKTAS *et al.*, 2017). Ainda, a expressão de moléculas coestimuladoras também é afetada pela idade (PLUNKETT *et al.*, 2007). A redução da expressão das moléculas co-estimuladores CD28 e CD27 nos linfócitos T leva a queda na proliferação e sinalização da via de IL-2 (PLUNKETT *et al.*, 2007)
A frequência de linfócitos B de memória e plasmócitos na periferia e na medula óssea é também reduzida em idosos (PRITZ *et al.*, 2015). Esse declínio na frequência pode ser uma das causas da rápida diminuição dos títulos de anticorpos protetores após a imunização em idosos em comparação com adultos, uma vez que a idade não afeta a função efetora dos plasmócitos (SASAKI *et al.*, 2011).

1.2.2. Imunodefiência comum variável

A imunodeficiência comum variável (ICV) é o erro inato da imunidade (EII) mais prevalente e e clinicamente relevante (CUNNINGHAM-RUNDLES, 2019; SEIDEL *et al.*, 2019). A ICV é caracterizada por hipogamaglobulinemia e defeitos na produção de anticorpos específicos, uma vez que linfócitos B falham em se diferenciar em linfócitos B de memória e plasmócitos (GATHMANN *et al.*, 2014). Diversas anomalias na produção de linfócitos T também foram relatadas em pacientes com ICV, incluindo expansão oligoclonal de linfócitos T CD8+, número reduzido de linfócitos T CD4+, bem como defeitos na ativação dessas células (MEYTS *et al.*, 2021; RAMESH *et al.*, 2017). Como sugerido pelo nome, a manifestação clínica da doença é variável e, apesar da maioria pacientes apresentarem infecções bacterianas recorrentes características, muitos apresentam outros sinais de desregulação imune, como autoimunidade, doença pulmonar, enteropatias, linfoproliferação e alergias. Atualmente, terapia de reposição de imunoglobulina é o principal tratamento para a condição (SEIDEL *et al.*, 2019).
Considerando que o excesso de anticorpos pode ser um agravante da COVID-19 devido à citotoxicidade mediada por células dependente de anticorpos (ADCC) (ZHOU *et al.*, 2021), o fato de pacientes ICV terem sua produção comprometida pode ser algo positivo. Entretanto, pacientes que também apresentam defeitos nos

linfócitos T, podem estar em risco elevado de infecção grave e reduzida resposta vacinal (DELAVARI *et al.*, 2021).

Indivíduos imunocomprometidos estão em maior risco de infecção, e, por isso, a pandemia de COVID-19 apresentou um grande potencial desafio para este grupo (MEYTS *et al.*, 2021). Diversos casos de COVID-19 em pacientes ICV foram reportados: ~29% tiveram doença moderada a grave e ~13% foram casos fatais, uma porcentagem mais alta que a população geral (HAUSER *et al.*, 2020; KATZENSTEIN *et al.*, 2022; WEIFENBACH; JUNG; LÖTTERS, 2021). Entretanto, o fato de ~87% dos pacientes se recuperarem da infecção, sugere que a resposta imune, ainda que comprometida, tem um papel importante protegendo esses indivíduos da COVID-19 fatal.

Vacinas contra COVID-19 tiveram sucesso para conter a pandemia de SARS-CoV-2, uma vez que, em geral, induziram resposta suficiente para reduzir hospitalizações e transmissão da doença (TREGONING *et al.*, 2021). Em geral, pacientes ICV apresentam resposta vacinal subótima, porém pacientes com condições imuno-mediadas leves, como defeitos nos fagócitos e deficiências de anticorpos, apresentam resposta vacinal adequada (LEEUWEN; GEURTSVANKESSEL; ELLERBROEK, 2022). Pacientes ICV responderam à vacina contra influenza tipo B (HIB) e à vacina do tétano, porém tiveram baixas respostas à vacina contra difteria e *S. pneumoniae*, indicando uma heterogeneidade significativa na resposta vacinal destes pacientes (AMERATUNGA; LONGHURST; LEHNERT, 2021). Quanto às vacinas contra COVID-19, também é esperado uma resposta heterogênea, a depender da condição de cada paciente e da plataforma vacina utilizada. Não é possível estimar qual tecnologia vacinal terá maior eficácia, porém foi observada uma soroconversão de 72% de pacientes com EII produziram após vacina de mRNA (DURKEE-SHOCK; KELLER, 2022).

Com o aumento crescente da porcentagem da população com anticorpos contra SARS-CoV-2 devido à infecção e vacinação, é esperada a transferência passiva destes para os pacientes ICV durante tratamento de reposição de imunoglobulina (MANIAN *et al.*, 2021). Porém ainda não se sabe se estes anticorpos serão funcionais e auxiliarão na proteção à longo prazo.

2. Objetivos

2.1. Objetivo geral

Quantificar a resposta imunológica humoral e celular em indivíduos idosos e pacientes com Imunodeficiência Comum Variável vacinados com diferentes plataformas e regimes vacinais.

2.2. Objetivos específicos

- Identificar a influência do sexo e da idade na resposta celular à vacina em idosos após 2 doses de vacina;
- Avaliar a magnitude da resposta de pacientes ICV após 2 e 3 doses de vacina;
- Comparar a resposta vacinal elicitada por CoronaVac e a vacina de adenovírus ChAdOx1 em pacientes ICV;
- Avaliar a imunogenicidade do reforço vacinal após regime inicial de CoronaVac.

3. Métodos

3.1. Participantes

Para a quantificação da resposta celular em idosos, foi realizado um estudo transversal com profissionais da saúde do Instituto do Coração de São Paulo imunizados com 2 doses de CoronaVac (3µg vacina/imunização), com intervalo de 3 semanas entre as doses (n = 101, mediana da idade = 55, IIQ = 28), ou 2 doses de CoronaVac + 1 dose de BNT162b2, 230 dias (IIQ = 30) após as duas doses iniciais (n = 39, mediana da idade = 49, IIQ = 23). Os indivíduos relataram não terem sido infectados previamente com SARS-CoV-2. Coleta de sangue venoso foi realizada pelo menos 21 dias após a última imunização (mediana = 37, IIQ = 40). Indivíduos convalescentes (confirmados por RT-PCR para SARS-CoV-2, n = 72; mediana da idade = 40, IIQ = 15) com doença leve e 150 dias pós sintomas foram incluídos como controle positivo. Amostras soronegativas sem resposta celular específica para SARS-CoV-2 obtidas durante a pandemia foram incluídas como controle negativo (n = 36; mediana da idade = 36, IIQ = 17).

Para avaliação da resposta de indivíduos imunodeficientes, foram recrutados 26 pacientes ICV acompanhados no Hospital das Clínicas da Faculdade de Medicina da Universidade de São Paulo (HC-FMUSP) entre maio e novembro de 2021, durante a circulação das variantes Delta e Gamma no Brasil. Todos os pacientes preenchiam os critérios diagnósticos estabelecidos por Bonilla et al. Dentre os 26 indivíduos incluídos, 15 foram vacinados com 2 doses de CoronaVac, 9 com 2 doses de ChAdOx1 e 14 tomaram dose reforço BNT162b2 após 2 doses de CoronaVac. Indivíduos saudáveis vacinados com 2 doses de CoronaVac (N=60) ou após reforço com BNT162b2 (N=17) foram incluídos como controles. Todas as amostras foram coletadas imediatamente antes da infusão mensal de imunoglobulina.

Todos os voluntários assinaram termo de consentimento e o estudo foi aprovado pelo Comitê de Ética do Hospital das Clínicas da Universidade de São Paulo (CAPPesq CAAE30155220.30000.0068).

3.2. Ensaio de liberação de citocina induzido por antígeno

O ensaio de liberação de citocina induzido por antígeno foi realizado incubando 250ul de sangue periférico heparinizado em placas de 96 poços de fundo U por 48h em incubadora 37°C, 5%CO_2 na presença de pool de epítopos de linfócitos T CD4+. Os vinte epítopos usados como estímulo específico foram identificados por análise bioinformática e sintetizados escaneando o proteoma completo do genoma de referência de SARS-CoV-2 (RefSeq: NC_045512.2) usando a abordagem de ligação de HLA-DR promíscuo. As placas foram centrifugadas e o sobrenadante foi coletado e armazenado a -80°C até o uso. A quantificação de IFN-γ e IL-2 no sobrenadante foi avaliada por ELISA, de acordo com as instruções do fabricante (R&D Systems, Minneapolis, MN). Os valores de *cutoff* foram obtidos por análise de curva ROC com diagnóstico como valores de referência, e valores IFN-γ ou IL-2 como preditores. Valores de citocinas foram subtraídos do controle de DMSO. O limite de quantificação do teste para IFN-γ foi de 1,17pg/ml e 0,98pg/ml para IL-2.

3.3. Ensaio Imunoadsorvente Ligado à Enzima (ELISA)

ELISA foi realizado em placas de poliestireno de 96 poços de alta aderência cobertas com 4mg/ml de proteína Spike, 2mg/ml de proteína Nucleocapsídeo ou 0.8mg/ml de RBD de SARS-CoV-2, expressas em células HEK293T (gentilmente cedidas por Dr. Ricardo Gazzinelli, UFMG) por 18h a 4°C. Resumidamente, 50µl de soro diluído (1:100) foram incubados a 37°C por 45min. O anticorpo secundário IgG de cabra anti-humano conjugado com peroxidase foi diluído 1:10.000 e incubado a 37°C por 30min. A densidade ótica (DO) a 492nm foi medida com leitor de microplaca (Epoch, BioTek, EUA). Valores foram determinados como DO menos branco e o ponto de corte foi determinado como a média da DO média de 12 amostras pré-pandêmicas + 3x desvio padrão. Resultados são mostrados como razão da DO amostra/ponto de corte. Razão de anticorpo > 1,2 foi considerada como positiva.

3.4. Ensaio de neutralização viral

Os ensaios de neutralização viral foram realizados em parceria com laboratório de Virologia Clínica e Molecular da USP. Para tal, SARS-CoV-2 (GenBank: MT

MT350282) foi usado para conduzir o teste de neutralização de vírus de efeito citopático (CPE-VNT). As propriedades da linhagem viral foram previamente descritas em Araujo et al. ((ARAUJO *et al.*, 2020)). Foram utilizadas placas de 96 poços contendo células Vero a 5x10^6 células/ml (ATCC CCL-81). Uma série de diluições (1:20 a 1:2.560) foram preparadas para o ensaio. Soro diluído foi misturado em igual volume com o vírus (100 doses de cultura infecciosa, 100% endpoint por poço – VNT100) e pré incubados para neutralização viral por 1h a 37°C. A mistura contendo soro e vírus foi transferida para uma monocamada confluente de células e incubadas a 37°C 5% CO_2 por 3 dias. Todos os procedimentos foram realizados em Laboratório de Biossegurança Nível 3. Após 72h, placas foram analisadas por microscopia de luz. CPE total foi observado em células Vero, distinguindo a presença/ausência de CPE-VNT contra linhagem referência Wuhan ou variantes Delta e Gamma. Para determinar os títulos de VNT, foi considerada a diluição de soro mais alta capaz de neutralizar o soro. Como controle positivo, foi utilizado um soro referência de amostra de indivíduo RT-qPCR positivo.

3.5.   Análise estatística

Análises estatísticas foram realizadas usando GraphPad Prism versão 9 e plataforma R versão 4.0.3. Variáveis contínuas foram analisadas usando teste de Shapiro-Wilk para avaliação da normalidade da distribuição. Comparações de variáveis contínuas entre vários grupos foram feitas usando teste de Kruskal-Wallis com teste de Dunn post-hoc e Mann-Whitney foi utilizado para comparação de dois grupos. Teste de qui-quadrado foi realizado para associação de dados categóricos. Correlações foram avaliadas pelo coeficiente de Spearman. O limite de idade usado para caracterizar os grupos de resposta imune foram estabelecidos após duas etapas: (i) análise de k-means cluster baseada em cinco variáveis contínuas (razão de IgG de NP, RBD, Spike e níveis de IFN-γ e IL-2) foi usada para identificar dois grupos com resposta imune diferentes, de acordo com o algoritmo de Hartigan e Wong (J. A. HARTIGAN AND M. A. WONG, 1979); (ii) análise de curva ROC com os clusters de referência e idade como preditor foi utilizada para determinar o threshold de idade que poderia distinguir os dois grupos com maior acurácia. Um valor de $p < 0,05$ foi considerado como estatisticamente significativo para todas as análises.

4. Resultados

4.1. Idosos

Dados demográficos e medianas das quantificações estão descritos na tabela 2. Foi avaliada a resposta celular, representada pela produção de IFN-γ e IL-2, e humoral, representada por anticorpos vírus-específicos e neutralizantes, em indivíduos saudáveis não infectados (amostras pré-pandêmicas), em vacinados com 2 doses de CoronaVac e em convalescentes (previamente infectados). A produção de IFN-γ e IL-2 foi maior nos grupos vacinado e convalescente em relação ao grupo controle, mas não apresentaram diferenças entre si (Fig. 2A). A produção de IgG anti-RBD foi maior no grupo vacinado em comparação com o grupo controle e convalescente, que também apresentou maior produção de IgG em relação aos controles (Fig.2B). Indivíduos convalescentes apresentaram maior produção de anticorpos neutralizantes contra linhagem Wuhan do que indivíduos vacinados com 2 doses de CoronaVac (Fig.2C).

Tabela 2. Características dos participantes

	Vacinado		Convalescente	Controle
	2 doses	3 doses		
n	101	31	72	36
Idade, média ± dp (intervalo)	54 ± 16.3 (23-90)	54 ± 16.3 (28-77)	40.5 ± 10.5 (24-68)	39 ± 12.3 (22-44)
Sexo, n (%)				
Mulher	70 (71)	19 (61)	54 (75)	26 (72)
Homem	30 (29)	12 (39)	18 (25)	10 (28)
Intervalo entre coleta e vacina ou sintomas, mediana (intervalo)	37 (21-80)	120 (64-143)	207 (159-240)	NA
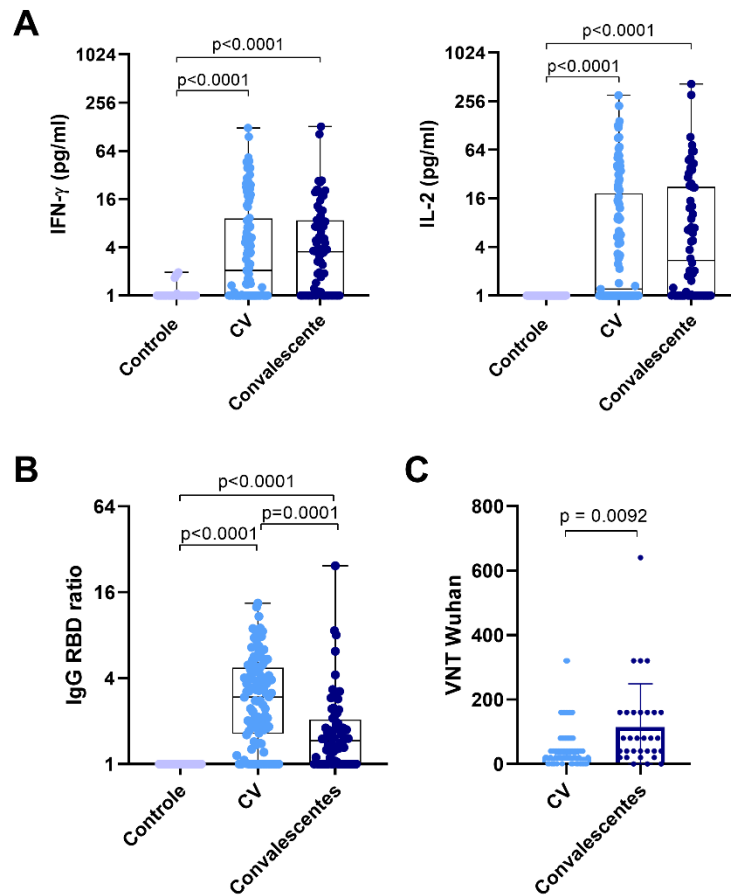
Figura 2. Produção de citocinas e anticorpos em indivíduos vacinados e convalescentes. (A) Produção de IFN-γ e IL-2 em indivíduos saudáveis sem infecção prévia (Controle), vacinados com 2 doses de CoronaVac (CV) e convalescentes após estímulo de sangue total com peptídeos específicos de SARS-CoV-2. (B) Produção de IgG anti-RBD de SARS-CoV-2 em indivíduos saudáveis sem infecção prévia (Controle), vacinados com 2 doses de CoronaVac (CV) e convalescentes. (C) Títulos de neutralização viral contra linhagem Wuhan de SARS-CoV-2 em indivíduos vacinados com 2 doses de CoronaVac (CV) e convalescentes. Box plots mostram mediana e IIQ, barras de erro mostram valores min e max; Para VNT, barras mostram média geométrica e barras de erros indicam IC 95%. VNT abaixo de 1:20 foi considerado 1 nos gráficos. Kruskal–Wallis com post hoc test Dunn; Mann-Whitney test.

Para avaliar se o tempo até a coleta interferiu nos resultados, avaliamos a correlação do intervalo entre vacinação e coleta. Não foi encontrada correlação no tempo entre coleta e vacinação (Fig.3A-C).

Figura 3. Correlação entre tempo até coleta e parâmetros imunológicos em indivíduos vacinados com 2 doses de CoronaVac. (A) Correlação entre a produção de IFN-γ e IL-2 e o tempo até 2ª dose de CoronaVac. (B) Correlação entre a produção de IgG anti-RBD e o tempo até 2ª dose de CoronaVac. (C). Correlação entre títulos de anticorpos neutralizantes e o tempo até 2ª dose de CoronaVac. Teste de correlação de Spearman.

Considerando o impacto da idade na resposta imunológica, avaliamos a correlação entre a idade dos indivíduos vacinados com 2 doses e os parâmetros imunológicos. Observamos uma correlação significativamente negativa entre idade e produção de IL-2, mas não para IFN-γ (Fig. 4A). A produção de IgG anti-RBD apresentou uma correlação significativamente negativa com a idade (Fig. 4B), bem como os anticorpos neutralizantes contra as linhagens Wuhan e Beta (Fig. 4C).
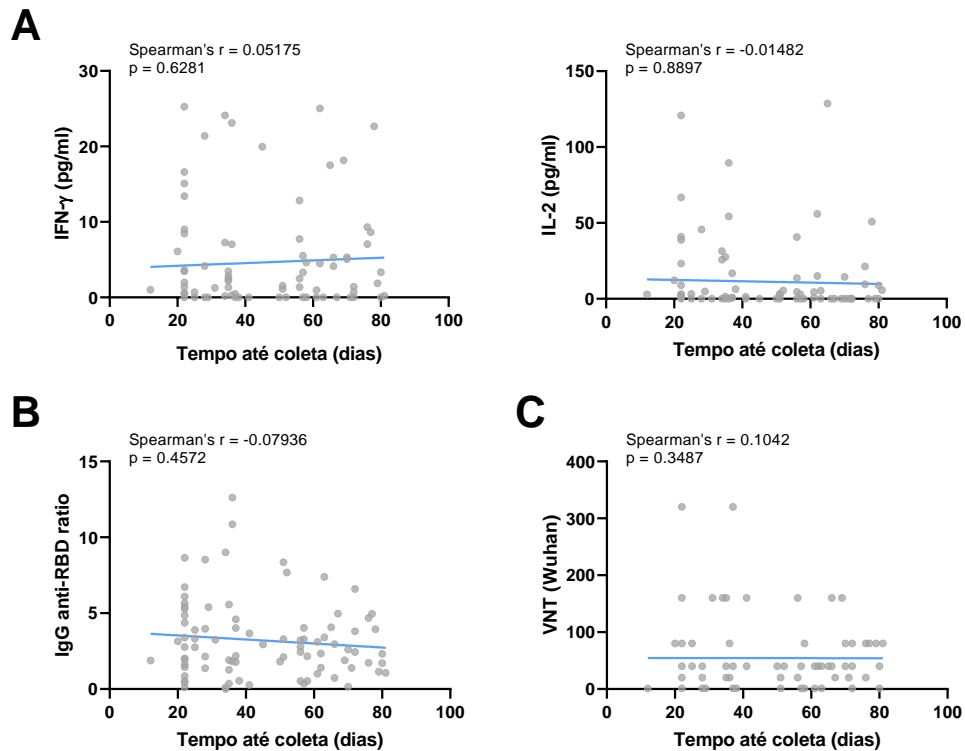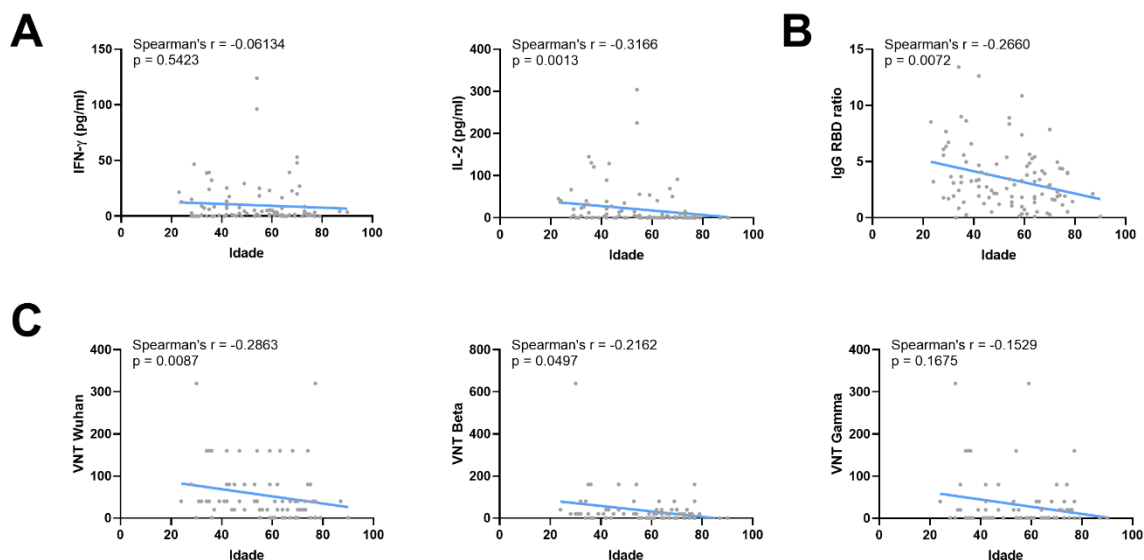
Figura 4. Correlação entre idade e parâmetros imunológicos em indivíduos vacinados com 2 doses de CoronaVac. (A) Correlação entre idade e a produção de IFN-γ e IL-2 após estímulo do sangue total em indivíduos vacinados com 2 doses de CoronaVac. (C-D) Correlação entre idade e a produção de IgG anti-RBD em indivíduos vacinados com 2 doses de CoronaVac. (C) Correlação entre idade e títulos de neutralização viral contra linhagens Wuhan, Beta e Gamma, respectivamente, em indivíduos vacinados com 2 doses de CoronaVac. Teste de correlação de Spearman.

A partir do resultado de correlação negativo entre idade e resposta imunológica após 2 doses, utilizamos as variáveis numéricas (IFN-γ, IL-2, IgG anti-RBD, -Spike, -NP) como preditoras e a idade dos participantes vacinados, para identificar clusters distintos de resposta, e encontramos a idade de 55 anos como aquela que melhor divide os resultados. Portanto, comparamos dois grupos: indivíduos vacinados com idade <55 anos e ≥55. No geral, observamos que mulheres e homens jovens produziram citocinas ou anticorpos específicos/neutralizantes contra SARS-CoV-2, enquanto 17% dos homens acima de 55 não produziram citocinas nem anticorpos, em comparação com 3% das mulheres do mesmo grupo (Fig.5A). A produção de IL-2 em homens acima de 55 anos foi significativamente menor do que daqueles abaixo de 55, bem como em relação às mulheres mais velhas e as mais novas (Fig. 5B). Não foram encontradas diferenças na produção IFN-γ entre os grupos (Fig. 5B). Os níveis de IgG anti-RBD também foram menores em homens acima de 55 em relação aos mais novos (Fig. 5C). Quanto aos NAbs, observamos que mulheres acima de 55 anos possuem menos NAbs contra linhagem Wuhan quando comparadas às mais novas

(Fig. 5D). Para as linhagens Beta e Gamma, não foram observadas diferenças (Fig. 5D).
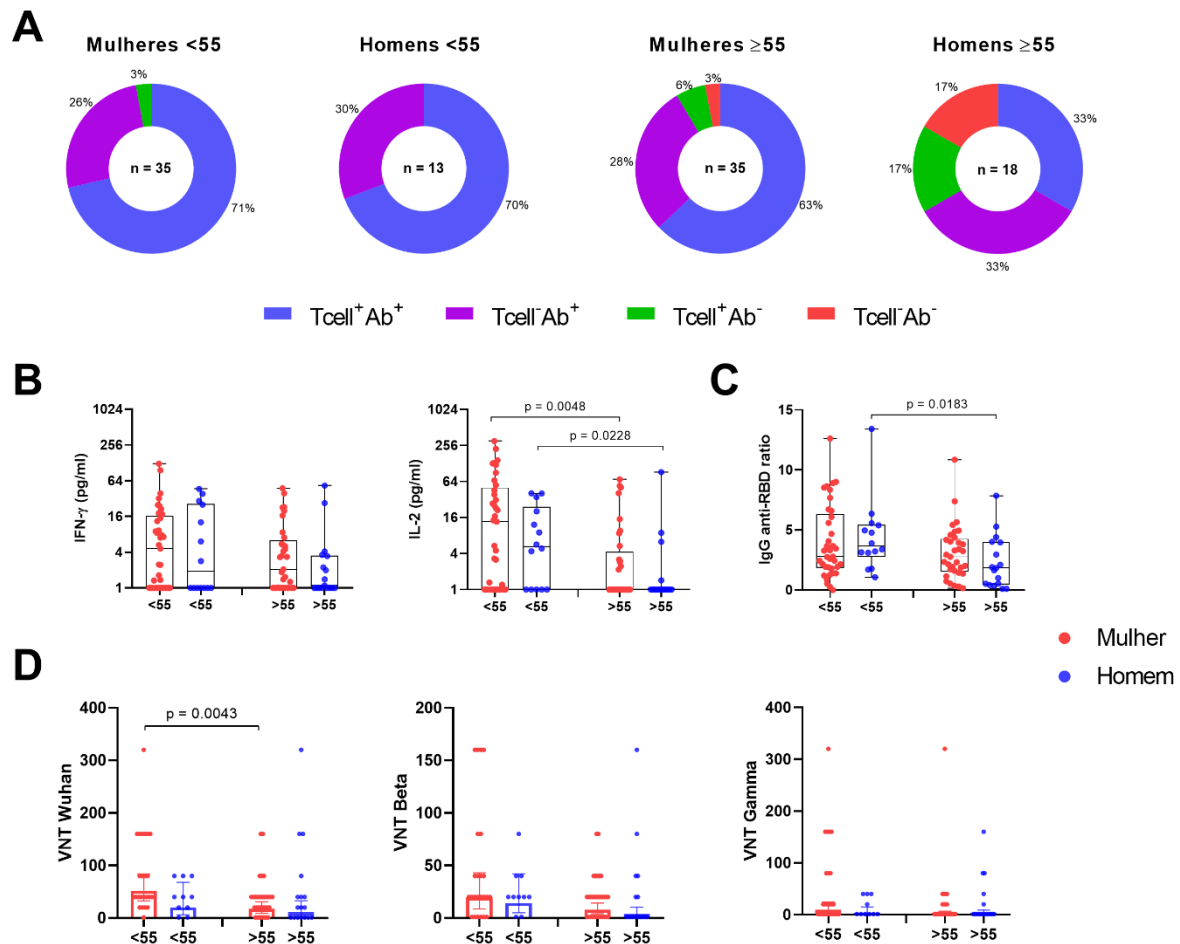
Figura 5. Produção de citocinas e anticorpos em indivíduos vacinados com 2 doses de CoronaVac, agrupados por sexo e idade. (A) Perfil da produção de citocinas e anticorpos em vacinados com 2 de CoronaVac, agrupados por idade e sexo. (B) Produção de IFN-γ e IL-2 após estímulo de sangue total com peptídeos específicos de SARS-CoV-2 em indivíduos acima e abaixo de 55 anos vacinados com 2 doses de CoronaVac. (C) Produção de IgG anti-RBD de SARS-CoV-2 em indivíduos acima e abaixo de 55 anos vacinados com 2 doses de CoronaVac. (D) Títulos de neutralização viral contra as linhagens Wuhan, Delta e Gamma, respectivamente, em indivíduos acima e abaixo de 55 anos vacinados com 2 doses de CoronaVac. Box plots mostram mediana e IIQ, barras de erro mostram valores min e max; Para VNT, barras mostram média geométrica e barras de erros indicam IC 95%. VNT abaixo de 1:20 foi considerado 1 nos gráficos. Tcell+/-: produção de citocinas acima ou abaixo do cutoff; Ab+/-: produção de IgG anti-RBD acima ou abaixo do cutoff e título de NAb ≥ ou < 80. Mann-Whitney test.

Quando comparando a resposta celular após 2 doses de CoronaVac e 2 CoronaVac + 1 BNT162b2, não foi observada diferença significativa na produção de IFN-γ e IL-2 entre os dois regimes vacinais (Fig. 6A). Entretanto, a produção de IgG foi significativamente aumentada com a dose adicional BNT162b2 (Fig. 6B), bem como os títulos de anticorpos neutralizantes contra linhagem Wuhan (Fig. 6C).
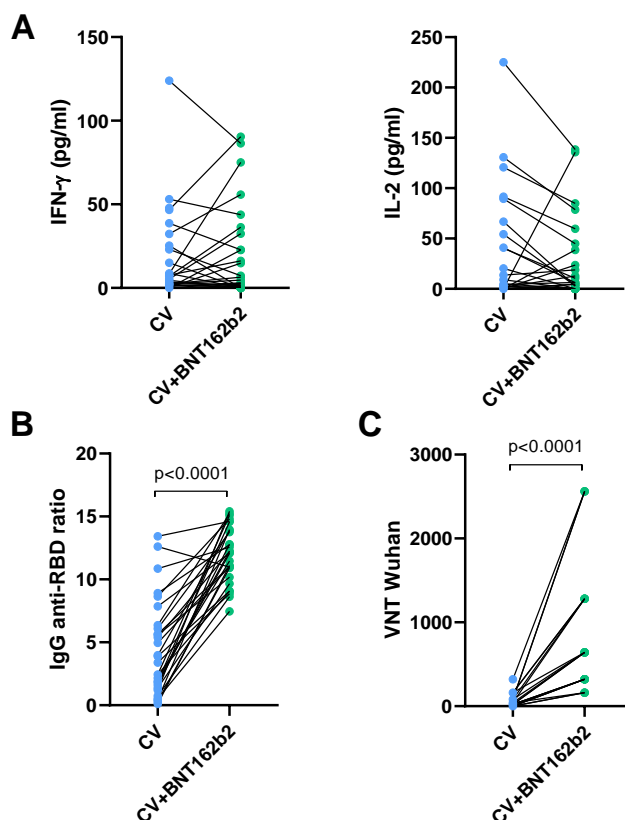
Figura 6. Comparação da produção de citocinas e anticorpos entre 2 doses CV (CV) e após reforço com BNT162b2 (CV+BNT162b2). (A) Produção de IFN-g e IL-2 após estímulo de sangue total em indivíduos vacinados com 2 doses CV ou 2CV+BNT162b2. (B) Produção de IgG anti-RBD em indivíduos vacinados com 2 doses CV ou 2CV+BNT162b2. (C) Títulos de neutralização viral contra linhagem Wuhan de SARS-CoV-2 em indivíduos vacinados com 2 doses CV ou 2CV+BNT162b2. Mann-Whitney test.

Assim como o regime de 2 doses, na terceira dose também não foi observada correlação no tempo entre coleta e vacinação (Fig. 7). Não foram observadas correlações significativas entre a produção de citocinas e anticorpos e a idade dos

indivíduos após a 3ª dose (Fig. 8A-C), porém podemos observar uma queda na produção de IFN-γ e NAbs com o aumento da idade dos participantes (Fig. 8A e C).
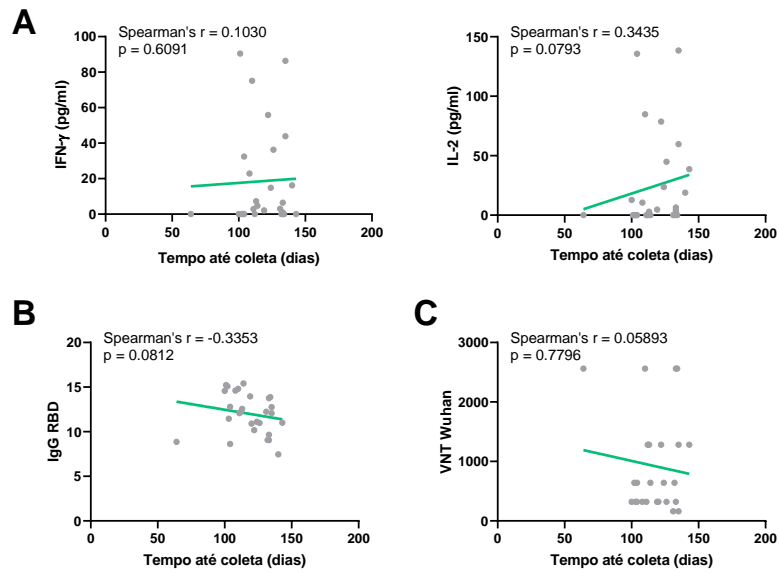
Figura 7. Correlação entre tempo até coleta e parâmetros imunológicos em indivíduos vacinados com 3 doses (CV+BNT162b2). (A) Correlação entre a produção de IFN-γ e IL-2 e o tempo até 3ª dose (CV+BNT162b2). (B) Correlação entre a produção de IgG anti-RBD e o tempo até 3ª dose (CV+BNT162b2). (C). Correlação entre títulos de anticorpos neutralizantes e o tempo até 3ª dose (CV+BNT162b2). Teste de correlação de Spearman.
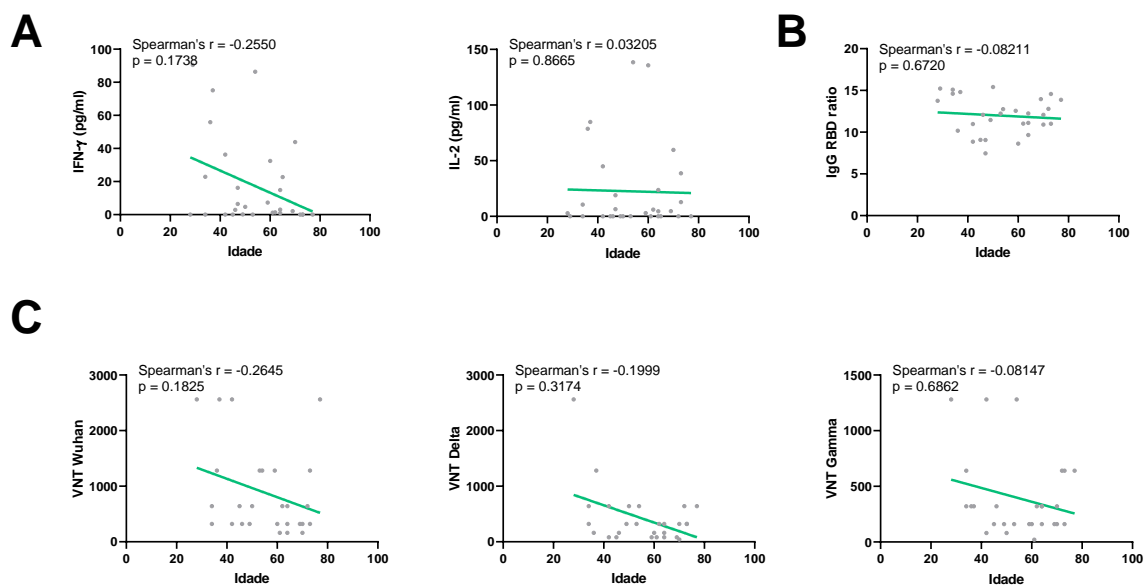
Figura 8. Correlação entre idade e parâmetros imunológicos em indivíduos vacinados com 3 doses (2 CV+BNT162b2). (A) Correlação entre idade e a produção de IFN-γ e IL-2 após estímulo do sangue total em indivíduos vacinados com 3 doses. (C-D) Correlação entre idade e a produção de IgG anti-RBD em indivíduos vacinados com 3 doses. (C) Correlação entre idade e títulos de neutralização viral contra linhagens Wuhan, Beta e Gamma, respectivamente em indivíduos vacinados com 3 doses. Teste de correlação de Spearman.

Considerando o menor número amostral após a 3ª dose (N=30), não foi possível realizar a análise agrupada em sexo e idade. Porém, avaliando resultados agrupados somente por idade, observamos um aumento da produção de IL-2 em indivíduos >55 anos em relação aos mais jovens (Fig. 9A). Anticorpos específicos e neutralizantes aumentaram significativamente com o reforço vacinal e não foi observada diferença entre adultos e idosos após 3ªdose (Fig. 9C).
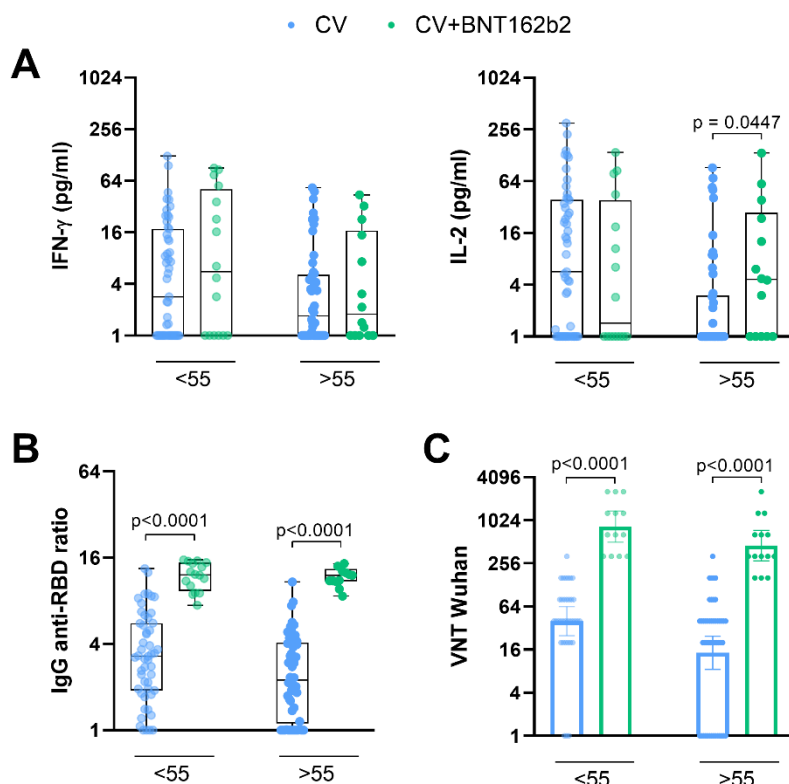
Figura 9. Comparação da produção de citocinas e anticorpos em indivíduos vacinados com 2 e ou 3 doses (CV+BNT162b2), agrupados por idade. (A) Produção de IFN-γ e IL-2 após estímulo de sangue total com peptídeos específicos de SARS-CoV-2 em indivíduos acima e abaixo de 55 anos vacinados com 2 ou 3 doses (CV+BNT162b2). (B) Produção de IgG anti-RBD de SARS-CoV-2 em indivíduos acima e abaixo de 55 anos vacinados com 2 ou 3 doses

(CV+BNT162b2). (C) Títulos de neutralização viral contra as linhagens Wuhan, Delta e Gamma, respectivamente, em indivíduos acima e abaixo de 55 anos vacinados com 2 ou 3 doses (CV+BNT162b2). Box plots mostram mediana e IIQ, barras de erro mostram valores min e max; Para VNT, barras mostram média geométrica e barras de erros indicam IC 95%. VNT abaixo de 1:20 foi considerado 1 nos gráficos. Mann-Whitney test.

4.2.   Imunodeficiência comum variável

No total, 26 pacientes ICV foram incluídos. As características dos pacientes encontram-se na Tabela 1. Indivíduos com ICV frequentemente têm diversas comorbidades, devido à disfunção imune. Na presente coorte, a comorbidade mais incidente foi doença pulmonar (88%); 65% apresentavam linfoproliferação benigna (57% esplenomegalia), 33% têm alguma doença autoimune, como psoríase e colite ulcerativa, 15% têm diarreia crônica (Fig.10). Comorbidades não apresentaram correlação com produção de citocinas e anticorpos pós vacinação (dados não mostrados).

Tabela 3. Características dos participantes

	2 doses		3 doses	Controles saudáveis	
	CoronaVac	ChAdOx1	2 CV + BNT162b2	2 doses CV	2 CV + BNT162b2
N	15	9	14	60	16
Idade, média (intervalo)	48 (25-77)	37.2 (24-52)	43.2 (20-77)	42.8 (23-60)	43.7 (28-60)
Sexo (%)					
Mulheres	9 (60)	3 (33.3)	9 (64)	43 (71.6)	12 (75)
Homens	6 (40)	6 (66.6)	5 (36)	17 (28.4)	4 (25)
Intervalo entre vacinação e coleta, média (intervalo)	66d (43-111)	48d (14-79)	33d (14-56)	45 (20-81)	113.6 (64-135)
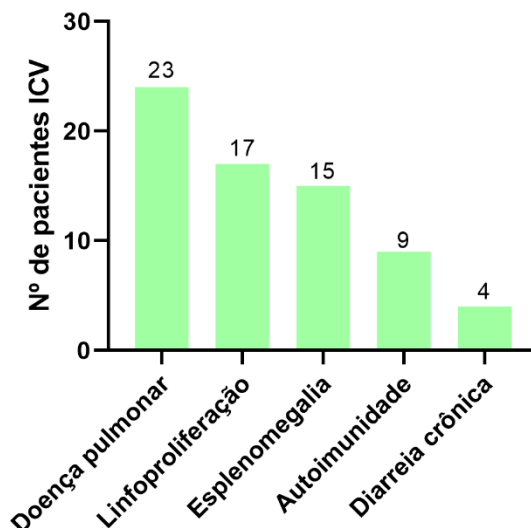
Figura 10. Comorbidades dos pacientes ICV participantes da coorte.

Considerando que foram incluídos indivíduos vacinados com diferentes plataformas vacinais, nós avaliamos a resposta imune elicitada por cada vacina separadamente. Nós observamos que indivíduos vacinados com ChAdOx1 apresentavam aumento nos anticorpos específicos anti-RBD e anti-S quando comparados com vacinados com CoronaVac (Fig.11A). Não foram observadas diferentes na resposta celular entre vacinados com ChAdOx1 e CoronaVac (Fig. 11B). Apenas indivíduos vacinados com ChAdOx1 possuíam anticorpos neutralizantes contra as linhagens avaliadas (Wuhan, Delta e Gamma; Fig. 11C-E).
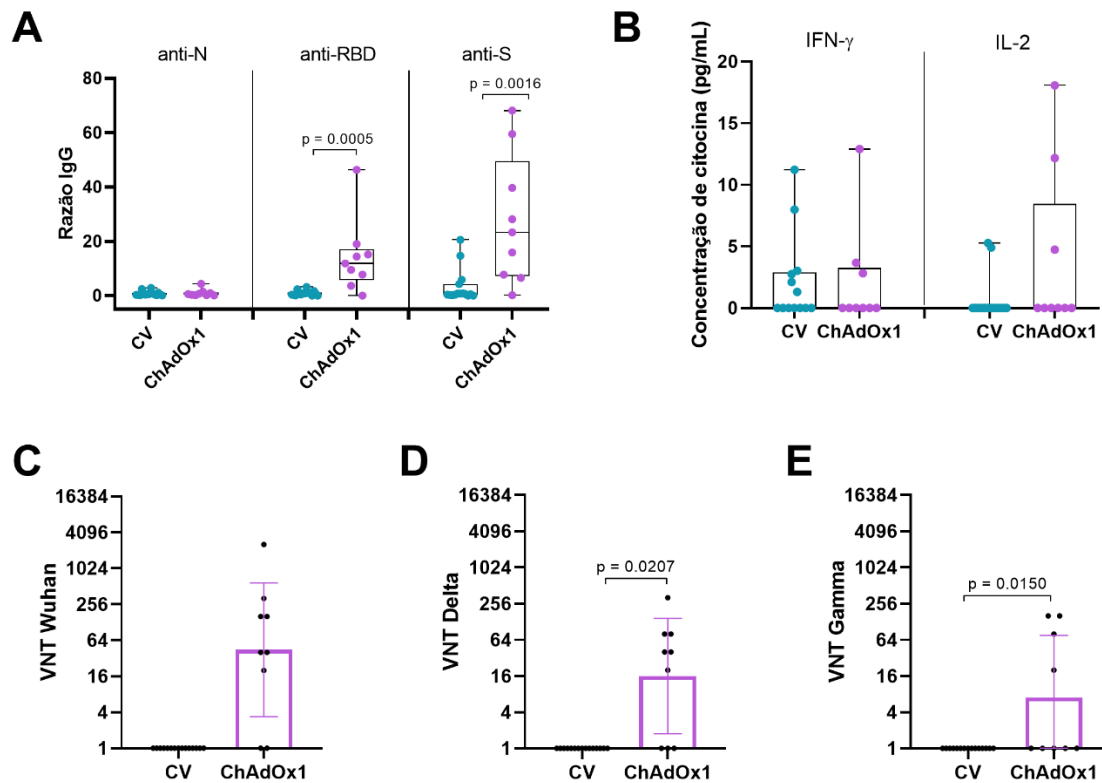
Figura 11. Comparação da resposta imune após 2 doses em pacientes ICV. (B) Produção de IFN-g e IL-2 SARS-CoV-2-específico produzidos mediante estímulo de sangue total com peptídeos de SARS-CoV-2. (C-E) Títulos de neutralização viral contra linhagens Wuhan, Delta e Gamma, respectivamente. VNT abaixo de 1:20 foi considerado 1 nos gráficos; barras mostram títulos da média geométrica e barras de erros indicam IC 95%. Análise estatística: Kruskal–Wallis com post hoc test Dunn; Mann-Whitney test.

Quando avaliando a resposta à dose adicional, observamos que o reforço com BNT162b2 em indivíduos previamente vacinados com CoronaVac aumentou IgG SARS-CoV-2-específico e produção de IL-2 (Fig. 12A-B), mas falhou em induzir a produção de anticorpos neutralizantes em 12 de 14 pacientes ICV (Fig. 12C).
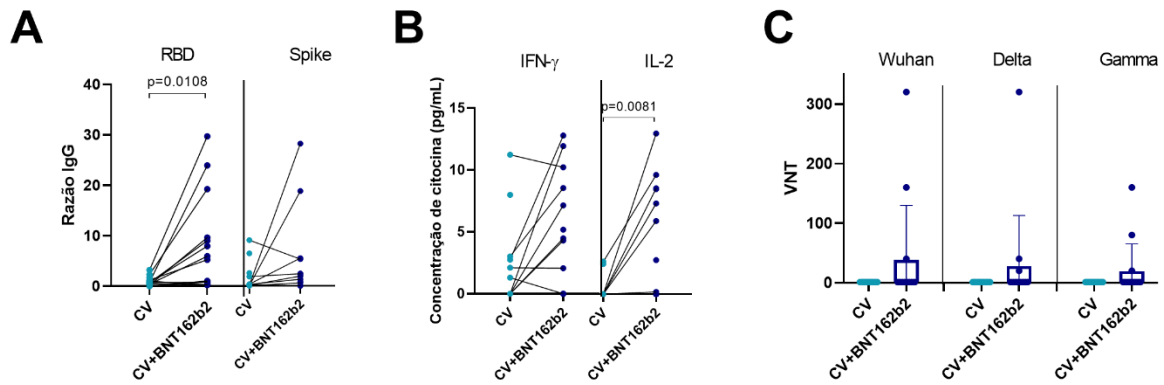
Figura 12. Comparação da resposta imune após 2ª dose e pós reforço com BNT162b2. (A) Reatividade de IgG anti-RBD e Spike. (B) Produção de IFN-g e IL-2 SARS-CoV-2-específico produzidos mediante estímulo de sangue total com peptídeos de SARS-CoV-2. (C-E) Títulos de neutralização viral contra linhagens Wuhan, Delta e Gamma, respectivamente. VNT abaixo de 1:20 foi considerado 1 nos gráficos; barras mostram títulos da média geométrica e barras de erros indicam IC 95%. Análise estatística: Kruskal–Wallis com post hoc test Dunn; Mann-Whitney test.

Para melhor avaliar a resposta da dose adicional, comparamos o regime de 3 doses (2 CV + BNT162b2) com as duas doses de ChAdOx1 e um grupo controle saudável, vacinado com 2 doses de CoronaVac (HC CV) ou após reforço com BNT162b2 (HC CV+BNT162b2). Em indivíduos saudáveis, reforço com BNT162b2 induziu maior produção de anticorpos neutralizantes e não-neutralizantes em comparação com 2 doses (Fig. 13A e C-E). Em pacientes ICV, vacinados com ChAdOx1 apresentaram mais anticorpos neutralizantes do que aqueles vacinados com CV + BNT162b2 para as linhagens Wuhan e Delta, porém apresentaram resposta menor quando comparado à indivíduos saudáveis (Fig. 13A-E).
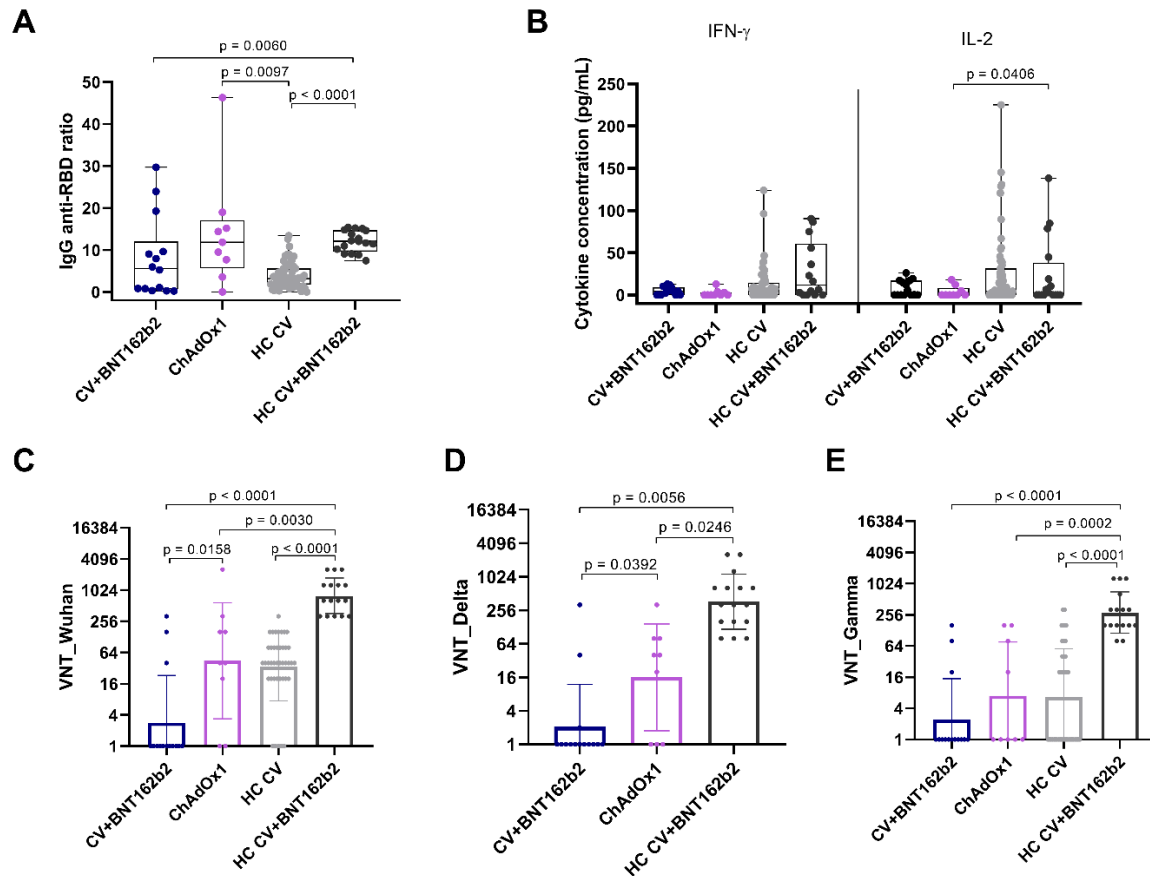
Figura 13. Comparação de pacientes ICV vacinados com 2 doses ChAdOx1 (N=9) e 2 doses de CV seguida por reforço com BNT162b2 (N=14) e controles saudáveis vacinados com 2 doses de CV (N=60) ou após reforço com BNT162b2 (N=16). (A) Reatividade de IgG anti-RBD, -N e -Spike. (B) Produção de IFN-g e IL-2 SARS-CoV-2-específico produzidos mediante estímulo de sangue total com peptídeos de SARS-CoV-2. (C-E) Títulos de neutralização viral contra linhagens Wuhan, Delta e Gamma, respectivamente. Boxplots mostram mediana e IIQ, barras de erro indicam valores máximo e mínimo. VNT abaixo de 1:20 foi considerado 1 nos gráficos; barras mostram títulos da média geométrica e barras de erros indicam IC 95%. Análise estatística: Kruskal–Wallis com post hoc test Dunn.

5. Discussão

A CoronaVac foi a primeira vacina a ficar disponível para vacinação em massa no Brasil, sendo priorizada a imunização de profissionais da saúde, imunocomprometidos e idosos. Na primeira parte deste trabalho, objetivamos avaliar a resposta após a vacinação com CoronaVac, estratificando-a por sexo e idade, quando possível. Neste estudo, a maioria do indivíduos vacinados desenvolveram algum tipo de resposta após 2 doses de vacina. Entretanto, observamos uma correlação negativa com a idade e a produção de citocinas e anticorpos, sugerindo uma menor imunogenicidade em idosos. Ao estratificar os resultados, observamos que a menor imunogenicidade foi encontrada em homens acima de 55 anos, sugerindo que este grupo pode não estar protegido contra futuras infecções e complicações advindas da doença. Ainda, homens idosos apresentaram a menor produção de IL-2, o que é particularmente preocupante, uma vez que esta citocina está relacionada ao desenvolvimento de linfócitos T de memória (ANSARI *et al.*, 2021; DHUME; MCKINSTRY, 2018).

Homens foram desproporcionalmente impactados pela COVID-19, com número de mortes e hospitalizações foram significativamente maiores neste grupo (PECKHAM *et al.*, 2020). As razões dessa discrepância não são completamente esclarecidas, porém evidências sugerem que mulheres montam melhor resposta de anticorpos (FISH, 2008), que está diretamente associado à proteção contra infecção.

Por outro lado, a associação negativa entre idade e resposta imunológica é bem estabelecida (revisado em CROOKE *et al.*, 2019) e impacta diretamente na resposta vacinal. No caso de vacinas inativadas, como a da Influenza, idosos apresentam proteção reduzida, variando entre 17 e 51% comparado com 90% observado em mais jovens (GOODWIN; VIBOUD; SIMONSEN, 2006). Ao contrário do observado na nossa coorte vacinada com CoronaVac, idosos vacinados com 2 doses de ChAdOx1 não apresentaram diferenças significativas na produção de IgG vírus-específico, NAbs e IFN-g e IL-2 quando comparado a adultos entre 18-55 (RAMASAMY *et al.*, 2020; SWANSON *et al.*, 2020). Resultados similares foram observados em estudo com idosos vacinados com mRNA-1273, que ainda apresentaram produção de anticorpos e citocinas acima daquela de indivíduos convalescentes (ANDERSON *et al.*, 2020; JACKSON *et al.*, 2020). Para indivíduos ≥80 anos vacinados com BNT162b2, foi observada uma redução da produção de IFN-γ e IL-2 frente estímulo

com peptídeos de SARS-CoV-2 em relação à indivíduos mais jovens (COLLIER *et al.*, 2021). Quando comparada com 2 doses de BNT162b2 e ChAdOx1, a CoronaVac apresentou menores títulos de anticorpos específicos 1, 3 e 6 meses após a vacinação (BARIN *et al.*, 2022). Em idosos, a soropositividade da CoronaVac foi 40-30% menor em relação às outras duas tecnologias e a queda da resposta foi mais rápida (BARIN *et al.*, 2022).

Doses adicionais foram recomendadas pelas autoridades de Saúde devido à queda gradual, mas acentuada da resposta vacinal, principalmente devido ao surgimento de variantes virais. Diversos regimes vacinais foram adotados, variando de acordo com as combinações de imunizantes disponíveis em cada país. Neste trabalho, avaliamos a resposta ao reforço com vacina de mRNA BN162b2 após imunização inicial com 2 CoronaVac. Na coorte estudada, não foram observadas diferenças na resposta celular e produção de anticorpos específicos e neutralizantes em adultos em relação aos idosos, sugerindo que a 3ª dose heteróloga foi eficiente em mitigar a diferença de resposta entre indivíduos mais jovens e mais velhos. A duração desta resposta deve ser avaliada para que se possa garantir proteção. Um estudo epidemiológico incluindo mais de 2 milhões de brasileiros vacinados com 3 doses (2 CoronaVac + 1 BNT162b2) demonstrou uma eficácia de 84% contra doença grave, 120 dias pós 3ª dose em indivíduos até 79 anos; não foi observada proteção contra infecção leve (CERQUEIRA-SILVA *et al.*, 2022). Além da eficácia da vacina, diversos estudos demonstram o efeito positivo do reforço vacinal na resposta humoral, porém estudos avaliando a resposta celular à CoronaVac ainda são escassos. Adultos e idosos vacinados com CoronaVac+BNT162b2 apresentaram um aumento significativo da resposta humoral em relação ao reforço homólogo (BARIN *et al.*, 2022). Em concordância, um estudo clínico de fase IV com 1240 participantes, reportou um aumento de 8-22 vezes maior nos títulos de neutralização às VOCs Delta e Ômicron após reforço heterólogo (Ad.26-COV-S e BNT162b2) em relação ao regime homólogo em adultos e idosos (≥61 anos) (COSTA CLEMENS *et al.*, 2022), corroborando a escolha de reforço heterólogo para este grupos de risco. Com relação à resposta celular, Schultz e col. relataram um aumento significativo na produção de IFN-g e frequência de linfócitos T CD4+ em adultos com até 59 anos vacinados com CoronaVac + BNT162b2 e manutenção dos níveis naqueles acima de 60 (SCHULTZ *et al.*, 2022). Importantemente, indivíduos vacinados com CoronaVac + BNT162b2 apresentaram produção similar de IFN-γ frente estímulo com peptídeos das linhagens

Wuhan e Ômicron, sugerindo uma reatividade cruzada desses linfócitos (GAO *et al.*, 2022; MOK *et al.*, 2022).

Apesar dos importantes achados deste estudo, destacam-se algumas limitações. O número amostral foi limitado, principalmente em relação à terceira dose. Comorbidades não foram consideradas na avaliação dos resultados, não foram inclusos peptídeos específicos das variantes em circulação no estímulo do sangue e os indivíduos vacinados foram incluídos como "sem infecção prévia" com base somente no relato de ausência de sintomas.

Na segunda parte deste trabalho, mostramos que a ChAdOx1 induziu uma maior resposta imune do que a CoronaVac após 2 doses e, surpreendentemente, também quando comparado à dose reforço com BNT162b2 após 2 CoronaVac em pacientes ICV. Em concordância com estudos maiores, a resposta de pacientes ICV à vacina foi menor que a de indivíduos saudáveis (FEIKIN *et al.*, 2022; LEEUWEN; GEURTSVANKESSEL; ELLERBROEK, 2022; SHROTRI *et al.*, 2021). Até onde sabemos, este é o primeiro trabalho que avaliou a imunogenicidade do regime heterólogo CoronaVac+BNT162b2 em pacientes ICV.

A vacina de vírus inativado elicitou uma resposta humoral menor do que a vacina de adenovírus e do grupo controle. Outras vacinas inativadas, como a da influenza, induzem resposta humoral em pacientes ICV, mas consistentemente menor que do a de controles saudáveis (HANITSCH *et al.*, 2016). Todos os regimes vacinais avaliados induziram resposta celular, similar àquela de indivíduos saudáveis, o que é encorajador, considerando a importância da resposta de linfócitos T para proteção contra COVID-19 grave e variantes virais (BAROUCH, 2022).

Ausência de incremento da resposta celular foi reportada por Leung et al após dose homóloga em uma coorte de pacientes imunocomprometidos, após a qual a frequência de linfócitos T CD4 e CD8 SARS-CoV-2 específicos não aumentou após 3ª dose de CoronaVac em comparação com a 2ª (LEUNG *et al.*, 2022), reiterando que um regime heterólogo também parece ser a estratégia ótima para este grupo de pacientes.

IgG vírus-específico foi detectado na maioria dos pacientes, assim como observado em diversos estudos (ABO-HELO *et al.*, 2021; GODA *et al.*, 2022; PHAM *et al.*, 2022), mas apenas 2 de 14 pacientes possuíam anticorpos neutralizantes (VNT>80) após a 3ª dose, o que sugere que pacientes ICV não apresentaram resposta humoral funcional mesmo após reforço. Falha na resposta neutralizante também foi reportada

por Arroyo-Sanchez et al em uma coorte de 18 pacientes ICV vacinados com vacina de mRNA (ARROYO-SÁNCHEZ *et al.*, 2022). Pham et al. mostraram que, apesar de 48% pacientes IEI produziram RBD vírus-específica, apenas 12% (2 em 16) apresentaram atividade neutralizante após vacina de mRNA (PHAM *et al.*, 2022). Por outro lado, 80% dos pacientes ICV vacinados com ChAdOx1 com reforço BNT162b2 tiveram produção de NAbs detectável (GODA *et al.*, 2022), destacando a importância de doses adicionais. No geral, ChAdOx1 induziu os maiores níveis de anticorpos neutralizantes, mas estudos longitudinais são necessários com coortes maiores são necessários para elucidar a longevidade dessa resposta.

Apesar dos achados interessantes, nosso trabalho também teve limitações. Não temos resultado deRT-qPCR para confirmar que os pacientes não estavam infectados no momento da coleta da amostra; não avaliamos a resposta contra a variante Ômicron, uma vez que todos os ensaios foram realizados durante a circulação da Delta no Brasil.

6. Conclusões

Como conclusão da avaliação da resposta vacinal em idosos, observamos que o regime de duas doses de CoronaVac apresentou baixa imunogenicidade, principalmente em indivíduos acima de 55 anos. A terceira dose de BNT162b2 levou a um aumento na resposta imune, sugerindo eficácia do reforço heterólogo em idosos. Entretanto, é necessária avaliação contínua da imunogenicidade das vacinas para que as autoridades de saúde possam tomar as providências adequadas para garantir a proteção da população e, especialmente, dos idosos.

Quanto à avaliação da resposta vacinal de imunocomprometidos, nossos resultados mostram que, apesar de pacientes ICV apresentaram um incremento na produção de anticorpos e citocinas após reforço heterólogo, a maioria falha em produzir anticorpos neutralizantes, sugerindo que vacinas inativadas podem não ser a melhor opção de imunizante para elicitar resposta nesse grupo de pacientes.

Referências

ABO-HELO, Nizar; MUHAMMAD, Emad; GHABEN-AMARA, Sondus; PANASOFF, Josef; COHEN, Shai. Specific antibody response of patients with common variable immunodeficiency to BNT162b2 coronavirus disease 2019 vaccination. **Annals of Allergy, Asthma and Immunology**, vol. 127, no. 4, p. 501–503, 2021. DOI 10.1016/j.anai.2021.07.021. Available at: https://doi.org/10.1016/j.anai.2021.07.021.

AGRAWAL, Anshu; AGRAWAL, Sudhanshu; CAO, Jia-Ning; SU, Houfen; OSANN, Kathryn; GUPTA, Sudhir. Altered Innate Immune Functioning of Dendritic Cells in Elderly Humans: A Role of Phosphoinositide 3-Kinase-Signaling Pathway. **The Journal of Immunology**, vol. 178, no. 11, p. 6912–6922, 2007. https://doi.org/10.4049/jimmunol.178.11.6912.

ALLEN, Jessica; TOAPANTA, Franklin R; CHEN, Wilbur; TENNANT, Sharon M. Understanding immunosenescence and its impact on vaccination of older adults. **Vaccine**, vol. 38, no. 52, p. 8264–8272, 2020. https://doi.org/10.1016/j.vaccine.2020.11.002.Understanding.

AMERATUNGA, Rohan; LONGHURST, Hilary; LEHNERT, Klaus. Comman Variable Immunodeficiency Disorders, T-Cell respose to SARS-CoV-2 Vaccines, and the risk of chronic COVID-19. **Journal of Allergy and Clinical Immunology Practice**, vol. 9, no. 10, p. 3575–3583, 2021. https://doi.org/https://doi.org/10.1016/j.jaip.2021.06.019.

ANDERSON, Evan J.; ROUPHAEL, Nadine G.; WIDGE, Alicia T.; JACKSON, Lisa A.; ROBERTS, Paul C.; MAKHENE, Mamodikoe; CHAPPELL, James D.; DENISON, Mark R.; STEVENS, Laura J.; PRUIJSSERS, Andrea J.; MCDERMOTT, Adrian B.; FLACH, Britta; LIN, Bob C.; DORIA-ROSE, Nicole A.; O'DELL, Sijy; SCHMIDT, Stephen D.; CORBETT, Kizzmekia S.; SWANSON, Phillip A.; PADILLA, Marcelino; … BEIGEL, John H. Safety and Immunogenicity of SARS-CoV-2 mRNA-1273 Vaccine in Older Adults. **New England Journal of Medicine**, vol. 383, no. 25, p. 2427–2438, 2020. https://doi.org/10.1056/nejmoa2028436.

ANSARI, Asgar; ARYA, Rakesh; SACHAN, Shilpa; JHA, Someshwar Nath; KALIA,

Anurag; LALL, Anupam; SETTE, Alessandro; GRIFONI, Alba; WEISKOPF, Daniela; COSHIC, Poonam; SHARMA, Ashok; GUPTA, Nimesh. Immune Memory in Mild COVID-19 Patients and Unexposed Donors Reveals Persistent T Cell Responses After SARS-CoV-2 Infection. **Frontiers in Immunology**, vol. 12, no. March, p. 1–11, 2021. https://doi.org/10.3389/fimmu.2021.636768.

ARAUJO, Danielle Bastos; MACHADO, Rafael Rahal Guaragna; AMGARTEN, Deyvid Emanuel; MALTA, Fernanda de Mello; DE ARAUJO, Gabriel Guarany; MONTEIRO, Cairo Oliveira; CANDIDO, Erika Donizetti; SOARES, Camila Pereira; DE MENEZES, Fernando Gatti; PIRES, Ana Carolina Cornachioni; SANTANA, Rúbia Anita Ferraz; VIANA, Amanda de Oliveira; DORLASS, Erick; THOMAZELLI, Luciano; FERREIRA, Luis Carlos de Sousa; BOTOSSO, Viviane Fongaro; CARVALHO, Cristiane Rodrigues Guzzo; OLIVEIRA, Danielle Bruna Leal; PINHO, João Renato Rebello; DURIGON, Edison Luiz. SARS-CoV-2 isolation from the first reported patients in brazil and establishment of a coordinated task network. **Memorias do Instituto Oswaldo Cruz**, vol. 115, no. 12, p. 1–8, 2020. https://doi.org/10.1590/0074-02760200342.

ARROYO-SÁNCHEZ, Daniel; CABRERA-MARANTE, Oscar; LAGUNA-GOYA, Rocío; ALMENDRO-VÁZQUEZ, Patricia; CARRETERO, Octavio; GIL-ETAYO, Francisco Javier; SUÀREZ-FERNÁNDEZ, Patricia; PÉREZ-ROMERO, Pilar; RODRÍGUEZ DE FRÍAS, Edgard; SERRANO, Antonio; ALLENDE, Luis M.; PLEGUEZUELO, Daniel; PAZ-ARTAL, Estela. Immunogenicity of Anti-SARS-CoV-2 Vaccines in Common Variable Immunodeficiency. **Journal of Clinical Immunology**, vol. 42, no. 2, p. 240–252, 2022. DOI 10.1007/s10875-021-01174-5. Available at: https://doi.org/10.1007/s10875-021-01174-5.

ATYEO, Caroline; FISCHINGER, Stephanie; ZOHAR, Tomer; SLEIN, Matthew D.; BURKE, John; LOOS, Carolin; MCCULLOCH, Denise J.; NEWMAN, Kira L.; WOLF, Caitlin; YU, Jingyou; SHUEY, Kiel; FELDMAN, Jared; HAUSER, Blake Marie; CARADONNA, Tim; SCHMIDT, Aaron G.; SUSCOVICH, Todd J.; LINDE, Caitlyn; CAI, Yongfei; BAROUCH, Dan; … ALTER, Galit. Distinct Early Serological Signatures Track with SARS-CoV-2 Survival. **Immunity**, vol. 53, no. 3, p. 524-532.e4, 2020. DOI 10.1016/j.immuni.2020.07.020. Available at: https://doi.org/10.1016/j.immuni.2020.07.020.

BARIN, Burc; KASAP, Ulus; SELÇUK, Ferda; VOLKAN, Ender; ULUÇKAN, Özge. Comparison of SARS-CoV-2 anti-spike receptor binding domain IgG antibody responses after CoronaVac, BNT162b2, ChAdOx1 COVID-19 vaccines, and a single booster dose: a prospective, longitudinal population-based study. **The Lancet Microbe**, vol. 3, no. 4, p. e274–e283, 2022. https://doi.org/10.1016/S2666-5247(21)00305-0.

BAROUCH, Dan H. Covid-19 Vaccines — Immunity, Variants, Boosters. **New England Journal of Medicine**, vol. 387, no. 11, p. 1011–1020, 2022. https://doi.org/10.1056/nejmra2206573.

BEKTAS, Arsun; SCHURMAN, Shepherd H.; SEN, Ranjan; FERRUCCI, Luigi. Human T cell immunosenescence and inflammation in aging. **Journal of Leukocyte Biology**, vol. 102, no. 4, p. 977–988, 2017. https://doi.org/10.1189/jlb.3ri0716-335r.

CHANDRASHEKAR, Abishek; LIU, Jinyan; MARTINO, Amanda J.; MCMAHAN, Katherine; MERCAD, Noe B.; PETER, Lauren; TOSTANOSK, Lisa H.; YU, Jingyou; MALIGA, Zoltan; NEKORCHUK, Michael; BUSMAN-SAHAY, Kathleen; TERRY, Margaret; WRIJI, Linda M.; DUCAT, Sarah; MARTINE, David R.; ATYEO, Caroline; FISCHINGER, Stephanie; BURK, John S.; SLEI, Matthew D.; … BAROU, Dan H. SARS-CoV-2 infection protects against rechallenge in rhesus macaques. **Science**, vol. 369, no. 6505, p. 812–817, 2020. https://doi.org/10.1126/science.abc4776.

CHODICK, Gabriel; TENE, Lilac; ROTEM, Ran S; PATALON, Tal; GAZIT, Sivan; BEN-TOV, Amir; WEIL, Clara; GOLDSHTEIN, Inbal; TWIG, Gilad; COHEN, Dani; MUHSEN, Khitam. The effectiveness of the TWO-DOSE BNT162b2 vaccine: analysis of real-world data. **Clin Infect Dis.**, vol. 74, no. 3, p. 472–478, 2021. https://doi.org/doi:10.1093/cid/ciab438.

COHEN, Kristen W.; LINDERMAN, Susanne L.; MOODIE, Zoe; CZARTOSKI, Julie; LAI, Lilin; MANTUS, Grace; NORWOOD, Carson; NYHOFF, Lindsay E.; EDARA, Venkata Viswanadh; FLOYD, Katharine; DE ROSA, Stephen C.; AHMED, Hasan; WHALEY, Rachael; PATEL, Shivan N.; PRIGMORE, Brittany; LEMOS, Maria P.;

DAVIS, Carl W.; FURTH, Sarah; O'KEEFE, James B.; … MCELRATH, M. Juliana. Longitudinal analysis shows durable and broad immune memory after SARS-CoV-2 infection with persisting antibody responses and memory B and T cells. **Cell Reports Medicine**, vol. 2, no. 7, p. 100354, 2021. DOI 10.1016/j.xcrm.2021.100354. Available at: https://doi.org/10.1016/j.xcrm.2021.100354.

COLLIER, Dami A; FERREIRA, Isabella A T M; KOTAGIRI, Prasanti; DATIR, Rawlings; LIM, Eleanor; TOUIZER, Emma; MENG, Bo; ABDULLAHI, Adam; CITIID-NIHR BIORESOURCE COVID-19 COLLABORATION; ELMER, Anne; KINGSTON, Nathalie; GRAVES, Barbara; LE GRESLEY, Emma; CAPUTO, Daniela; BERGAMASCHI, Laura; SMITH, Kenneth G C; BRADLEY, John R; CERON-GUTIERREZ, Lourdes; CORTES-ACEVEDO, Paulina; … GUPTA, Ravindra K. Age-related immune response heterogeneity to SARS-CoV-2 vaccine BNT162b2. **Nature**, vol. 596, p. 417–422, 2021. DOI 10.1038/s41586-021-03739-1. Available at: http://www.ncbi.nlm.nih.gov/pubmed/34192737.

COSTA CLEMENS, Sue Ann; WECKX, Lily; CLEMENS, Ralf; ALMEIDA MENDES, Ana Verena; RAMOS SOUZA, Alessandra; SILVEIRA, Mariana B.V.; DA GUARDA, Suzete Nascimento Farias; DE NOBREGA, Maristela Miyamoto; DE MORAES PINTO, Maria Isabel; GONZALEZ, Isabela G.S.; SALVADOR, Natalia; FRANCO, Marilia Miranda; DE AVILA MENDONÇA, Renata Navis; QUEIROZ OLIVEIRA, Isabelle Silva; DE FREITAS SOUZA, Bruno Solano; FRAGA, Mayara; ALEY, Parvinder; BIBI, Sagida; CANTRELL, Liberty; … DE ARRUDA CORDEIRO MATOS, Laiana Januse. Heterologous versus homologous COVID-19 booster vaccination in previous recipients of two doses of CoronaVac COVID-19 vaccine in Brazil (RHH-001): a phase 4, non-inferiority, single blind, randomised study. **The Lancet**, vol. 399, no. 10324, p. 521–529, 2022. https://doi.org/10.1016/S0140-6736(22)00094-0.

CROOKE, Stephen N.; OVSYANNIKOVA, Inna G.; POLAND, Gregory A.; KENNEDY, Richard B. Immunosenescence and human vaccine immune responses. **Immunity & Ageing**, vol. 16, no. 1, p. 1–16, 2019. https://doi.org/10.1186/s12979-019-0164-9.

CUNNINGHAM-RUNDLES, Charlotte. Common variable immune deficiency: Dissection of the variable. **Immunological Reviews**, vol. 287, no. 1, p. 145–161,

2019. https://doi.org/10.1111/imr.12728.

DAN, Jennifer M.; MATEUS, Jose; KATO, Yu; HASTIE, Kathryn M.; YU, Esther Dawen; FALITI, Caterina E.; GRIFONI, Alba; RAMIREZ, Sydney I.; HAUPT, Sonya; FRAZIER, April; NAKAO, Catherine; RAYAPROLU, Vamseedhar; RAWLINGS, Stephen A.; PETERS, Bjoern; KRAMMER, Florian; SIMON, Viviana; SAPHIRE, Erica Ollmann; SMITH, Davey M.; WEISKOPF, Daniela; … CROTTY, Shane. Immunological memory to SARS-CoV-2 assessed for up to 8 months after infection. **Science**, vol. 371, no. 6529, 2021. https://doi.org/10.1126/science.abf4063.

DELAVARI, Samaneh; ABOLHASSANI, Hassan; ABOLNEZHADIAN, Farhad; BABAHA, Fateme; YAZDANI, Reza; AGHAMOHAMAMDI, Asghar. Impact of SARS-CoV-2 Pandemic on Patients with Primary Immunodeficiency. **Journal of Clinical Immunology**, vol. 41, no. 11, p. 345–355, 2021. https://doi.org/https://doi.org/10.1007/s10875-020-00928-x ORIGINAL.

DHUME, Kunal; MCKINSTRY, Karl Kai. Early programming and late-acting checkpoints governing the development of CD4 T-cell memory. **Immunology**, vol. 155, no. 1, p. 53–62, 2018. https://doi.org/10.1111/imm.12942.

DIAMOND, Michael S.; KANNEGANTI, Thirumala Devi. Innate immunity: the first line of defense against SARS-CoV-2. **Nature Immunology**, vol. 23, no. 2, p. 165–176, 2022. https://doi.org/10.1038/s41590-021-01091-0.

DURKEE-SHOCK, Jessica R.; KELLER, Michael D. Immunizing the Imperfect Immune System: COVID-19 Vaccination in Patients with Inborn Errors of Immunity. **Annals of Allergy, Asthma & Immunology**, vol. 000, p. 1–10, 2022. https://doi.org/10.1016/j.anai.2022.06.009.

ELSNER, Rebecca A.; SHLOMCHIK, Mark J. Germinal Center and Extrafollicular B Cell Responses in Vaccination, Immunity, and Autoimmunity. **Immunity**, vol. 53, no. 6, p. 1136–1150, 2020. DOI 10.1016/j.immuni.2020.11.006. Available at: https://doi.org/10.1016/j.immuni.2020.11.006.

FEHR, Anthony R.; PERLMAN, Stanley. Coronaviruses: An Overview of Their

Replication and Pathogenesis. **Coronaviruses: Methods and Protocols**. [*S. l.: s. n.*], 2015. vol. 1282, p. 1–282. https://doi.org/10.1007/978-1-4939-2438-7.

FEIKIN, Daniel R.; HIGDON, Melissa M.; ABU-RADDAD, Laith J.; ANDREWS, Nick; ARAOS, Rafael; GOLDBERG, Yair; GROOME, Michelle J.; HUPPERT, Amit; O'BRIEN, Katherine L.; SMITH, Peter G.; WILDER-SMITH, Annelies; ZEGER, Scott; DELORIA KNOLL, Maria; PATEL, Minal K. Duration of effectiveness of vaccines against SARS-CoV-2 infection and COVID-19 disease: results of a systematic review and meta-regression. **The Lancet**, vol. 399, no. 10328, p. 924–944, 2022. DOI 10.1016/S0140-6736(22)00152-0. Available at: http://dx.doi.org/10.1016/S0140-6736(22)00152-0.

FISH, Eleanor N. The X-files in immunity: sex-based differences predispose immune responses. **Nature Reviews Immunology**, vol. 8, p. 737–744, 2008. https://doi.org/doi:10.1038/nri2394.

FRANCESCHI, Claudio; GARAGNANI, Paolo; PARINI, Paolo; GIULIANI, Cristina; SANTORO, Aurelia. Inflammaging: a new immune–metabolic viewpoint for age-related diseases. **Nature Reviews Endocrinology**, vol. 14, no. 10, p. 576–590, 2018. DOI 10.1038/s41574-018-0059-4. Available at: http://dx.doi.org/10.1038/s41574-018-0059-4.

FRASCA, Daniela; BLOMBERG, Bonnie B. Aging induces B cell defects and decreased antibody responses to influenza infection and vaccination. **Immunity and Ageing**, vol. 17, no. 1, p. 1–10, 2020. https://doi.org/10.1186/s12979-020-00210-z.

GAO, Yu; CAI, Curtis; GRIFONI, Alba; MÜLLER, Thomas R.; NIESSL, Julia; OLOFSSON, Anna; HUMBERT, Marion; HANSSON, Lotta; ÖSTERBORG, Anders; BERGMAN, Peter; CHEN, Puran; OLSSON, Annika; SANDBERG, Johan K.; WEISKOPF, Daniela; PRICE, David A.; LJUNGGREN, Hans Gustaf; KARLSSON, Annika C.; SETTE, Alessandro; ALEMAN, Soo; BUGGERT, Marcus. Ancestral SARS-CoV-2-specific T cells cross-recognize the Omicron variant. **Nature Medicine**, vol. 28, no. 3, p. 472–476, 2022. https://doi.org/10.1038/s41591-022-01700-x.

GATHMANN, Benjamin; MAHLAOUI, Nizar; GÉRARD, Laurence; OKSENHENDLER, Eric; WARNATZ, Klaus; SCHULZE, Ilka; KINDLE, Gerhard; KUIJPERS, Taco W.; VAN BEEM, Rachel T.; GUZMAN, David; WORKMAN, Sarita; SOLER-PALACÍN, Pere; DE GRACIA, Javier; WITTE, Torsten; SCHMIDT, Reinhold E.; LITZMAN, Jiri; HLAVACKOVA, Eva; THON, Vojtech; BORTE, Michael; … GRIMBACHER, Bodo. Clinical picture and treatment of 2212 patients with common variable immunodeficiency. **Journal of Allergy and Clinical Immunology**, vol. 134, no. 1, 2014. https://doi.org/10.1016/j.jaci.2013.12.1077.

GODA, Vera; KRIVÁN, Gergely; KULCSÁR, Andrea; GÖNCZI, Márton; TASNÁDY, Szabolcs; MATULA, Zsolt; NAGY, Ginette; BEKŐ, Gabriella; HORVÁTH, Máté; UHER, Ferenc; SZEKANECZ, Zoltán; VÁLYI-NAGY, István. Specific Antibody and the T-Cell Response Elicited by BNT162b2 Boosting After Two ChAdOx1 nCoV-19 in Common Variable Immunodeficiency. **Frontiers in Immunology**, vol. 13, no. June, p. 1–10, 2022. https://doi.org/10.3389/fimmu.2022.907125.

GOODWIN, Katherine; VIBOUD, Cécile; SIMONSEN, Lone. Antibody response to influenza vaccination in the elderly: A quantitative review. **Vaccine**, vol. 24, no. 8, p. 1159–1169, 2006. https://doi.org/10.1016/j.vaccine.2005.08.105.

GRIFONI, Alba; WEISKOPF, Daniela; RAMIREZ, Sydney I.; MATEUS, Jose; DAN, Jennifer M.; MODERBACHER, Carolyn Rydyznski; RAWLINGS, Stephen A.; SUTHERLAND, Aaron; PREMKUMAR, Lakshmanane; JADI, Ramesh S.; MARRAMA, Daniel; DE SILVA, Aravinda M.; FRAZIER, April; CARLIN, Aaron F.; GREENBAUM, Jason A.; PETERS, Bjoern; KRAMMER, Florian; SMITH, Davey M.; CROTTY, Shane; SETTE, Alessandro. Targets of T Cell Responses to SARS-CoV-2 Coronavirus in Humans with COVID-19 Disease and Unexposed Individuals. **Cell**, no. January, 2020. https://doi.org/10.1016/j.cell.2020.05.015.

GUO, Li; WANG, Geng; WANG, Yeming; ZHANG, Qiao; REN, Lili; GU, Xiaoying; HUANG, Tingxuan; ZHONG, Jingchuan; WANG, Ying; WANG, Xinming; HUANG, Lixue; XU, Liuhui; WANG, Conghui; CHEN, Lan; XIAO, Xia; PENG, Yanchun; KNIGHT, Julian C.; DONG, Tao; CAO, Bin; WANG, Jianwei. SARS-CoV-2-specific antibody and T-cell responses 1 year after infection in people recovered from COVID-

19: a longitudinal cohort study. **The Lancet Microbe**, vol. 3, no. 5, p. e348–e356, 2022. DOI 10.1016/S2666-5247(22)00036-2. Available at: http://dx.doi.org/10.1016/S2666-5247(22)00036-2.

HAAS, Eric J.; ANGULO, Frederick J.; MCLAUGHLIN, John M.; ANIS, Emilia; SINGER, Shepherd R.; KHAN, Farid; BROOKS, Nati; SMAJA, Meir; MIRCUS, Gabriel; PAN, Kaijie; SOUTHERN, Jo; SWERDLOW, David L.; JODAR, Luis; LEVY, Yeheskel; ALROY-PREIS, Sharon. Impact and effectiveness of mRNA BNT162b2 vaccine against SARS-CoV-2 infections and COVID-19 cases, hospitalisations, and deaths following a nationwide vaccination campaign in Israel: an observational study using national surveillance data. **The Lancet**, vol. 397, no. 10287, p. 1819–1829, 2021. DOI 10.1016/S0140-6736(21)00947-8. Available at: http://dx.doi.org/10.1016/S0140-6736(21)00947-8.

HANITSCH, Leif G.; LÖBEL, Madlen; MIEVES, Jan Florian; BAUER, Sandra; BABEL, Nina; SCHWEIGER, Brunhilde; WITTKE, Kirsten; GRABOWSKI, Patricia; VOLK, Hans Dieter; SCHEIBENBOGEN, Carmen. Cellular and humoral influenza-specific immune response upon vaccination in patients with common variable immunodeficiency and unclassified antibody deficiency. **Vaccine**, vol. 34, no. 21, p. 2417–2423, 2016. DOI 10.1016/j.vaccine.2016.03.091. Available at: http://dx.doi.org/10.1016/j.vaccine.2016.03.091.

HAUSER, Anthony; COUNOTTE, Michel J.; MARGOSSIAN, Charles C.; KONSTANTINOUDIS, Garyfallos; LOW, Nicola; ALTHAUS, Christian L.; RIOU, Julien. Estimation of SARS-CoV-2 mortality during the early stages of an epidemic: A modeling study in Hubei, China, and six regions in Europe. **PLoS Medicine**, vol. 17, no. 7, p. 1–17, 2020. DOI 10.1371/journal.pmed.1003189. Available at: http://dx.doi.org/10.1371/journal.pmed.1003189.

HERRERO, Carmen; MARQUÉS, Laura; LLOBERAS, Jorge; CELADA, Antonio. IFN-gamma dependent transcription of MHCII is impaired in aged mice. vol. 107, no. 4, p. 485–493, 2001.

HITCHINGS, Matt D.T.; RANZANI, Otavio T.; TORRES, Mario Sergio Scaramuzzini;

DE OLIVEIRA, Silvano Barbosa; ALMIRON, Maria; SAID, Rodrigo; BORG, Ryan; SCHULZ, Wade L.; DE OLIVEIRA, Roberto Dias; DA SILVA, Patricia Vieira; DE CASTRO, Daniel Barros; SAMPAIO, Vanderson de Souza; DE ALBUQUERQUE, Bernardino Cláudio; RAMOS, Tatyana Costa Amorim; FRAXE, Shadia Hussami Hauache; DA COSTA, Cristiano Fernandes; NAVECA, Felipe Gomes; SIQUEIRA, Andre M.; DE ARAÚJO, Wildo Navegantes; … CRODA, Julio. Effectiveness of CoronaVac among healthcare workers in the setting of high SARS-CoV-2 Gamma variant transmission in Manaus, Brazil: A test-negative case-control study. **The Lancet Regional Health - Americas**, vol. 1, p. 100025, 2021. DOI 10.1016/j.lana.2021.100025. Available at: https://doi.org/10.1016/j.lana.2021.100025.

ISHO, Baweleta; ABE, Kento T.; ZUO, Michelle; JAMAL, Alainna J.; RATHOD, Bhavisha; WANG, Jenny H.; LI, Zhijie; CHAO, Gary; ROJAS, Olga L.; BANG, Yeo Myong; PU, Annie; CHRISTIE-HOLMES, Natasha; GERVAIS, Christian; CECCARELLI, Derek; SAMAVARCHI-TEHRANI, Payman; GUVENC, Furkan; BUDYLOWSKI, Patrick; LI, Angel; PATERSON, Aimee; … GINGRAS, Anne Claude. Persistence of serum and saliva antibody responses to SARS-CoV-2 spike antigens in COVID-19 patients. **Science Immunology**, vol. 5, no. 52, p. 1–21, 2020. https://doi.org/10.1126/sciimmunol.abe5511.

J. A. HARTIGAN AND M. A. WONG. Algorithm AS 136 A K-Means Clustering Algorithm. **Journal of the Royal Statistical Society. Series C (Applied Statistics)**, vol. 28, no. 1, p. 100–108, 1979. https://doi.org/http://dx.doi.org/10.2307/2346830.

JACKAMAN, Connie; RADLEY-CRABB, Hannah G.; SOFFE, Zoe; SHAVLAKADZE, Tea; GROUNDS, Miranda D.; NELSON, Delia J. Targeting macrophages rescues age-related immune deficiencies in C57BL/6J geriatric mice. **Aging Cell**, vol. 12, no. 3, p. 345–357, 2013. https://doi.org/10.1111/acel.12062.

JACKSON, Lisa A.; ANDERSON, Evan J.; ROUPHAEL, Nadine G.; ROBERTS, Paul C.; MAKHENE, Mamodikoe; COLER, Rhea N.; MCCULLOUGH, Michele P.; CHAPPELL, James D.; DENISON, Mark R.; STEVENS, Laura J.; PRUIJSSERS, Andrea J.; MCDERMOTT, Adrian; FLACH, Britta; DORIA-ROSE, Nicole A.; CORBETT, Kizzmekia S.; MORABITO, Kaitlyn M.; O'DELL, Sijy; SCHMIDT, Stephen

D.; SWANSON, Phillip A.; … BEIGEL, John H. An mRNA Vaccine against SARS-CoV-2 — Preliminary Report. **New England Journal of Medicine**, vol. 383, no. 20, p. 1920–1931, 2020. https://doi.org/10.1056/nejmoa2022483.

JARA, Alejandro; UNDURRAGA, Eduardo A.; GONZÁLEZ, Cecilia; PAREDES, Fabio; FONTECILLA, Tomás; JARA, Gonzalo; PIZARRO, Alejandra; ACEVEDO, Johanna; LEO, Katherinne; LEON, Francisco; SANS, Carlos; LEIGHTON, Paulina; SUÁREZ, Pamela; GARCÍA-ESCORZA, Heriberto; ARAOS, Rafael. Effectiveness of an Inactivated SARS-CoV-2 Vaccine in Chile. **New England Journal of Medicine**, vol. 385, no. 10, p. 875–884, 2021. https://doi.org/10.1056/nejmoa2107715.

KATZENSTEIN, Terese L.; RASMUSSEN, Line D.; DRABE, Camilla Helberg; LARSEN, Carsten Schade; HANSEN, Ann Brit Eg; STÆRKIND, Mette; KNUDSEN, Lene Surland; HANSEN, Christian Holm; OBEL, Niels. Outcome of SARS-CoV-2 infection among patients with common variable immunodeficiency and a matched control group: A Danish nationwide cohort study. **Frontiers in Immunology**, vol. 13, no. September, p. 1–10, 2022. https://doi.org/10.3389/fimmu.2022.994253.

KELLY, Jennifer; KHAN, Aslam Ali; YIN, Jiyi; FERGUSON, Thomas A.; APTE, Rajendra S. Senescence regulates macrophage activation and angiogenic fate at sites of tissue injury in mice. **Journal of Clinical Investigation**, vol. 117, no. 11, p. 3421–3426, 2007. https://doi.org/10.1172/JCI32430.

KUNG, Yu-An; LEE, Kuo-Ming; CHIANG, Huan-Jung; HUANG, Shen-Yu; WE, Chung-Wung; SHISH, Shin-Ru. Molecular Virology of SARS-CoV-2 and Related Coronaviruses. **Microbiology and Molecular Biology Reviews**, vol. 86, no. 2, p. 1–21, 2022.

KYOIZUMI, Seishi; KUBO, Yoshiko; KAJIMURA, Junko; YOSHIDA, Kengo; IMAI, Kazue; HAYASHI, Tomonori; NAKACHI, Kei; YOUNG, Lauren F.; MOORE, Malcolm A.; VAN DEN BRINK, Marcel R. M.; KUSUNOKI, Yoichiro. Age-Associated Changes in the Differentiation Potentials of Human Circulating Hematopoietic Progenitors to T- or NK-Lineage Cells. **The Journal of Immunology**, vol. 190, no. 12, p. 6164–6172, 2013. https://doi.org/10.4049/jimmunol.1203189.

LAM, Jonathan H.; SMITH, Fauna L.; BAUMGARTH, Nicole. B Cell Activation and Response Regulation during Viral Infections. **Viral Immunology**, vol. 33, no. 4, p. 294–306, 2020. https://doi.org/10.1089/vim.2019.0207.

LE BERT, Nina; TAN, Anthony T.; KUNASEGARAN, Kamini; THAM, Christine Y.L.; HAFEZI, Morteza; CHIA, Adeline; CHNG, Melissa Hui Yen; LIN, Meiyin; TAN, Nicole; LINSTER, Martin; CHIA, Wan Ni; CHEN, Mark I.Cheng; WANG, Lin Fa; OOI, Eng Eong; KALIMUDDIN, Shirin; TAMBYAH, Paul Anantharajah; LOW, Jenny Guek Hong; TAN, Yee Joo; BERTOLETTI, Antonio. SARS-CoV-2-specific T cell immunity in cases of COVID-19 and SARS, and uninfected controls. **Nature**, vol. 584, no. 7821, p. 457–462, 2020. DOI 10.1038/s41586-020-2550-z. Available at: http://dx.doi.org/10.1038/s41586-020-2550-z.

LEE, William T.; GIRARDIN, Roxanne C.; DUPUIS, Alan P.; KULAS, Karen E.; PAYNE, Anne F.; WONG, Susan J.; ARINSBURG, Suzanne; NGUYEN, Freddy T.; MENDU, Damodara Rao; FIRPO-BETANCOURT, Adolfo; JHANG, Jeffrey; WAJNBERG, Ania; KRAMMER, Florian; CORDON-CARDO, Carlos; AMLER, Sherlita; MONTECALVO, Marisa; HUTTON, Brad; TAYLOR, Jill; MCDONOUGH, Kathleen A. Neutralizing Antibody Responses in COVID-19 Convalescent Sera. **Journal of Infectious Diseases**, vol. 223, no. 1, p. 47–55, 2021. https://doi.org/10.1093/infdis/jiaa673.

LEEUWEN, Leanne P M Van; GEURTSVANKESSEL, Corine H; ELLERBROEK, Pauline M. Immunogenicity of the mRNA-1273 COVID-19 vaccine in adult patients with inborn errors of immunity. **Journal of Allergy and Clinical Immunology**, vol. 149, no. 6, p. 1949–1957, 2022. https://doi.org/https://doi.org/10.1016/j.jaci.2022.04.002.

LEUNG, Daniel; MU, Xiaofeng; DUQUE, Jaime S.Rosa; CHENG, Samuel M.S.; WANG, Manni; ZHANG, Wenyue; ZHANG, Yanmei; TAM, Issan Y.S.; LEE, Toby S.S.; LAM, Jennifer H.Y.; CHAN, Sau Man; CHEANG, Cheuk Hei; CHUNG, Yuet; WONG, Howard H.W.; LEE, Amos M.T.; LI, Wing Yan; CHAOTHAI, Sara; TSANG, Leo C.H.; CHUA, Gilbert T.; … LAU, Yu Lung. Safety and immunogenicity of 3 doses of

BNT162b2 and CoronaVac in children and adults with inborn errors of immunity. **Frontiers in Immunology**, vol. 13, no. September, 2022. https://doi.org/10.3389/fimmu.2022.982155.

LEVIN, Einav G.; LUSTIG, Yaniv; COHEN, Carmit; FLUSS, Ronen; INDENBAUM, Victoria; AMIT, Sharon; DOOLMAN, Ram; ASRAF, Keren; MENDELSON, Ella; ZIV, Arnona; RUBIN, Carmit; FREEDMAN, Laurence; KREISS, Yitshak; REGEV-YOCHAY, Gili. Waning Immune Humoral Response to BNT162b2 Covid-19 Vaccine over 6 Months. **New England Journal of Medicine**, vol. 385, no. 24, p. e84, 2021. https://doi.org/10.1056/nejmoa2114583.

LOTFI, Melika; HAMBLIN, Michael R; REZAEI, Nima. COVID-19: Transmission, prevention, and potential therapeutic opportunities. **Clinica Chimica Acta**, vol. 508, no. January, p. 254–266, 2020. DOI https://doi.org/10.1016/j.cca.2020.05.044 R. Available at: www.elsevier.com/locate/cca Review.

LU, Lu; MOK, Bobo Wing-Yee; CHEN, Lin-Lei; CHAN, Jacky Man-Chun; TSANG, Owen Tak-Yin; LAM, Bosco Hoi-Shiu; CHUANG, Vivien Wai-Man; CHU, Allen Wing-Ho; CHAN, Wan-Mui; IP, Jonathan Daniel; CHAN, Brian Pui-Chun; ZHANG, Ruiqi; YIP, Cyril Chik-Yan; CHENG, Vincent Chi-Chung; CHAN, Kwok-Hung; JIN, Dong-Yan; HUNG, Ivan Fan-Ngai; YUEN, Kwok-Yung; CHEN, Honglin; TO, Kelvin Kai-Wang. Neutralization of Severe Acute Respiratory Syndrome Coronavirus 2 Omicron Variant by Sera From BNT162b2 or CoronaVac Vaccine Recipients. **Clinical Infectious Diseases**, , p. 1–16, 16 Dec. 2021. DOI 10.1093/cid/ciab1041. Available at: https://academic.oup.com/cid/advance-article/doi/10.1093/cid/ciab1041/6463504.

LUSTIG, Yaniv; SAPIR, Einav; REGEV-YOCHAY, Gili; COHEN, Carmit; FLUSS, Ronen; OLMER, Liraz; INDENBAUM, Victoria; MANDELBOIM, Michal; DOOLMAN, Ram; AMIT, Sharon; MENDELSON, Ella; ZIV, Arnona; HUPPERT, Amit; RUBIN, Carmit; FREEDMAN, Laurence; KREISS, Yitshak. BNT162b2 COVID-19 vaccine and correlates of humoral immune responses and dynamics: a prospective, single-centre, longitudinal cohort study in health-care workers. **The Lancet Respiratory Medicine**, vol. 9, no. 9, p. 999–1009, 2021. DOI 10.1016/S2213-2600(21)00220-4. Available at: http://dx.doi.org/10.1016/S2213-2600(21)00220-4.

MANIAN, Deepti V.; JENSEN, Chelsee; THEEL, Elitza S.; MILLS, John R.; JOSHI, Avni. Non-neutralizing antibodies and limitations of serologic testing for severe acute respiratory syndrome coronavirus 2 in patients receiving immunoglobulin replacement products. **Ann Allergy Asthma Immunol.**, vol. 126, no. 207, p. 7, 2021. .

MECKIFF, Benjamin J.; RAMÍREZ-SUÁSTEGUI, Ciro; FAJARDO, Vicente; CHEE, Serena J.; KUSNADI, Anthony; SIMON, Hayley; ESCHWEILER, Simon; GRIFONI, Alba; PELOSI, Emanuela; WEISKOPF, Daniela; SETTE, Alessandro; AY, Ferhat; SEUMOIS, Grégory; OTTENSMEIER, Christian H.; VIJAYANAND, Pandurangan. Imbalance of Regulatory and Cytotoxic SARS-CoV-2-Reactive CD4+ T Cells in COVID-19. **Cell**, vol. 183, no. 5, p. 1340-1353.e16, 2020. https://doi.org/10.1016/j.cell.2020.10.001.

MERINO, Ana; BUENDIA, Paula; MARTIN-MALO, Alejandro; ALJAMA, Pedro; RAMIREZ, Rafael; CARRACEDO, Julia. Senescent CD14+CD16+ Monocytes Exhibit Proinflammatory and Proatherosclerotic Activity. **The Journal of Immunology**, vol. 186, no. 3, p. 1809–1815, 2011. https://doi.org/10.4049/jimmunol.1001866.

MEYTS, Isabelle; BUCCIOL, Giorgia; QUINTI, Isabella; NEVEN, Bénédicte; FISCHER, Alain; SEOANE, Elena; LOPEZ-GRANADOS, Eduardo; GIANELLI, Carla; ROBLES-MARHUE, Angel; TANGYE, Stuart G. Coronavirus disease 2019 in patients with inborn errors of immunity: An international study. **J Allergy Clin Immunol.**, vol. 147, no. 2, p. 520–531, 2021. https://doi.org/10.1016/j.jaci.2020.09.010.

MOK, Chris Ka Pun; COHEN, Carolyn A.; CHENG, Samuel M.S.; CHEN, Chunke; KWOK, Kin On; YIU, Karen; CHAN, Tat On; BULL, Maireid; LING, Kwun Cheung; DAI, Zixi; NG, Susanna S.; LUI, Grace Chung Yan; WU, Chao; AMARASINGHE, Gaya K.; LEUNG, Daisy W.; WONG, Samuel Yeung Shan; VALKENBURG, Sophie A.; PEIRIS, Malik; HUI, David S. Comparison of the immunogenicity of BNT162b2 and CoronaVac COVID-19 vaccines in Hong Kong. **Respirology**, vol. 27, no. 4, p. 301–310, 2022. https://doi.org/10.1111/resp.14191.

MOSS, Paul. The T cell immune response against SARS-CoV-2. **Nature**

Immunology, vol. 23, no. 2, p. 186–193, 2022. https://doi.org/10.1038/s41590-021-01122-w.

NAQVI, A.A.T.; FATIMA, K.; MOHAMMAD, T.; FATIMA, U.; SINGH, I.K.; SINGH, A.; ATIF, S.M.; HARIPRASAD, G.; HASAN, G.M.; HASSAN, Md.I. Insights into SARS-CoV-2 genome, structure, evolution, pathogenesis and therapies: Structural genomics approach. **BBA - Molecular Basis of Disease**, vol. 1866, no. January, p. 1–17, 2020. .

PECKHAM, Hannah; DE GRUIJTER, Nina M.; RAINE, Charles; RADZISZEWSKA, Anna; CIURTIN, Coziana; WEDDERBURN, Lucy R.; ROSSER, Elizabeth C.; WEBB, Kate; DEAKIN, Claire T. Male sex identified by global COVID-19 meta-analysis as a risk factor for death and ITU admission. **Nature Communications**, vol. 11, no. 1, p. 1–10, 2020. DOI 10.1038/s41467-020-19741-6. Available at: http://dx.doi.org/10.1038/s41467-020-19741-6.

PENCE, Brandt D. Fanning the Flames of Inflammaging: Impact of Monocyte Metabolic Reprogramming. **Immunometabolism.**, vol. 2, no. 3, p. 1–6, 2020. https://doi.org/doi:10.20900/immunometab20200025.

PENG, Qiaoli; ZHOU, Runhong; WANG, Yuewen; ZHAO, Meiqing; LIU, Na; LI, Shuang; HUANG, Haode; YANG, Dawei; AU, Ka Kit; WANG, Hui; MAN, Kwan; YUEN, Kwok Yung; CHEN, Zhiwei. Waning immune responses against SARS-CoV-2 variants of concern among vaccinees in Hong Kong. **eBioMedicine**, vol. 77, p. 103904, 2022. DOI 10.1016/j.ebiom.2022.103904. Available at: https://doi.org/10.1016/j.ebiom.2022.103904.

PHAM, Michele N; MURUGESAN, Kanagavel; BANAEI, Niaz; PINSKY, Benjamin A. Immunogenicity and tolerability of COVID-19 messenger RNA vaccines in primary immunodeficiency patients with functional B-cell defects. **Journal of Allergy and Clinical Immunology**, vol. 149, no. 3, p. 908–911, 2022. https://doi.org/https://doi.org/10.1016/j.jaci.2021.11.022 907.

PICCOLI, Luca; PARK, Young Jun; TORTORICI, M. Alejandra; CZUDNOCHOWSKI,

Nadine; WALLS, Alexandra C.; BELTRAMELLO, Martina; SILACCI-FREGNI, Chiara; PINTO, Dora; ROSEN, Laura E.; BOWEN, John E.; ACTON, Oliver J.; JACONI, Stefano; GUARINO, Barbara; MINOLA, Andrea; ZATTA, Fabrizia; SPRUGASCI, Nicole; BASSI, Jessica; PETER, Alessia; DE MARCO, Anna; … VEESLER, David. Mapping Neutralizing and Immunodominant Sites on the SARS-CoV-2 Spike Receptor-Binding Domain by Structure-Guided High-Resolution Serology. **Cell**, vol. 183, no. 4, p. 1024-1042.e21, 2020. DOI 10.1016/j.cell.2020.09.037. Available at: https://doi.org/10.1016/j.cell.2020.09.037.

PLUNKETT, Fiona J.; FRANZESE, Ornella; FINNEY, Helene M.; FLETCHER, Jean M.; BELARAMANI, Lavina L.; SALMON, Mike; DOKAL, Inderjeet; WEBSTER, David; LAWSON, Alastair D. G.; AKBAR, Arne N. The Loss of Telomerase Activity in Highly Differentiated CD8+CD28−CD27− T Cells Is Associated with Decreased Akt (Ser473) Phosphorylation. **The Journal of Immunology**, vol. 178, no. 12, p. 7710–7719, 2007. https://doi.org/10.4049/jimmunol.178.12.7710.

PRITZ, Theresa; LAIR, Julian; BAN, Michael; KELLER, Michael; WEINBERGER, Birgit; KRISMER, Martin; GRUBECK-LOEBENSTEIN, Beatrix. Plasma cell numbers decrease in bone marrow of old patients. **European Journal of Immunology**, vol. 45, no. 3, p. 738–746, 2015. https://doi.org/10.1002/eji.201444878.

QI, Hai; LIU, Bo; WANG, Xinquan; ZHANG, Linqi. The humoral response and antibodies against SARS-CoV-2 infection. **Nature Immunology**, 2022. https://doi.org/10.1038/s41590-022-01248-5.

QING, Enya; GALLAGHER, Tom. SARS Coronavirus Redux. **Trends in Immunology**, vol. 41, no. 4, p. 269–271, 2020. https://doi.org/https://doi.org/10.1016/j.it.2020.02.007.

RAMASAMY, Maheshi N.; MINASSIAN, Angela M.; EWER, Katie J.; FLAXMAN, Amy L.; FOLEGATTI, Pedro M.; OWENS, Daniel R.; VOYSEY, Merryn; ALEY, Parvinder K.; ANGUS, Brian; BABBAGE, Gavin; BELIJ-RAMMERSTORFER, Sandra; BERRY, Lisa; BIBI, Sagida; BITTAYE, Mustapha; CATHIE, Katrina; CHAPPELL, Harry; CHARLTON, Sue; CICCONI, Paola; CLUTTERBUCK, Elizabeth A.; … ZIZI, Dalila.

Safety and immunogenicity of ChAdOx1 nCoV-19 vaccine administered in a prime-boost regimen in young and old adults (COV002): a single-blind, randomised, controlled, phase 2/3 trial. **The Lancet**, vol. 396, no. 10267, p. 1979–1993, 2020. https://doi.org/10.1016/S0140-6736(20)32466-1.

RAMESH, Manish; HAMM, David; SIMCHONI, Noa; CUNNINGHAM-RUNDLES, Charlotte. Clonal and constricted T cell repertoire in Common Variable Immune Deficiency. **Clin Immunol.**, vol. 178, no. May, p. 1–9, 2017. https://doi.org/10.1016/j.clim.2015.01.002.

ROBBIANI, Davide F.; GAEBLER, Christian; MUECKSCH, Frauke; LORENZI, Julio C.C.; WANG, Zijun; CHO, Alice; AGUDELO, Marianna; BARNES, Christopher O.; GAZUMYAN, Anna; FINKIN, Shlomo; HÄGGLÖF, Thomas; OLIVEIRA, Thiago Y.; VIANT, Charlotte; HURLEY, Arlene; HOFFMANN, Hans Heinrich; MILLARD, Katrina G.; KOST, Rhonda G.; CIPOLLA, Melissa; GORDON, Kristie; … NUSSENZWEIG, Michel C. Convergent antibody responses to SARS-CoV-2 in convalescent individuals. **Nature**, vol. 584, no. 7821, p. 437–442, 2020. DOI 10.1038/s41586-020-2456-9. Available at: http://dx.doi.org/10.1038/s41586-020-2456-9.

RYDYZNSKI MODERBACHER, Carolyn; RAMIREZ, Sydney I.; DAN, Jennifer M.; GRIFONI, Alba; HASTIE, Kathryn M.; WEISKOPF, Daniela; BELANGER, Simon; ABBOTT, Robert K.; KIM, Christina; CHOI, Jinyong; KATO, Yu; CROTTY, Eleanor G.; KIM, Cheryl; RAWLINGS, Stephen A.; MATEUS, Jose; TSE, Long Ping Victor; FRAZIER, April; BARIC, Ralph; PETERS, Bjoern; … CROTTY, Shane. Antigen-Specific Adaptive Immunity to SARS-CoV-2 in Acute COVID-19 and Associations with Age and Disease Severity. **Cell**, vol. 183, no. 4, p. 996-1012.e19, 2020. DOI 10.1016/j.cell.2020.09.038. Available at: https://doi.org/10.1016/j.cell.2020.09.038.

SADARANGANI, Manish; MARCHANT, Arnaud; KOLLMANN, Tobias R. Immunological mechanisms of vaccine-induced protection against COVID-19 in humans. **Nature Reviews Immunology**, vol. 21, no. 8, p. 475–484, 2021. DOI 10.1038/s41577-021-00578-z. Available at: http://dx.doi.org/10.1038/s41577-021-00578-z.

SAHIN, Ugur; MUIK, Alexander; VOGLER, Isabel; DERHOVANESSIAN, Evelyna; KRANZ, Lena M.; VORMEHR, Mathias; QUANDT, Jasmin; BIDMON, Nicole; ULGES, Alexander; BAUM, Alina; PASCAL, Kristen E.; MAURUS, Daniel; BRACHTENDORF, Sebastian; LÖRKS, Verena; SIKORSKI, Julian; KOCH, Peter; HILKER, Rolf; BECKER, Dirk; ELLER, Ann Kathrin; … TÜRECI, Özlem. BNT162b2 vaccine induces neutralizing antibodies and poly-specific T cells in humans. **Nature**, vol. 595, no. 7868, p. 572–577, 2021. DOI 10.1038/s41586-021-03653-6. Available at: http://dx.doi.org/10.1038/s41586-021-03653-6.

SASAKI, Sanae; SULLIVAN, Meghan; NARVAEZ, Carlos F.; HOLMES, Tyson H.; FURMAN, David; ZHENG, Nai Ying; NISHTALA, Madhuri; WRAMMERT, Jens; SMITH, Kenneth; JAMES, Judith A.; DEKKER, Cornelia L.; DAVIS, Mark M.; WILSON, Patrick C.; GREENBERG, Harry B.; HE, Xiao Song. Limited efficacy of inactivated influenza vaccine in elderly individuals is associated with decreased production of vaccine-specific antibodies. **Journal of Clinical Investigation**, vol. 121, no. 8, p. 3109–3119, 2011. https://doi.org/10.1172/JCI57834.

SCHULIEN, Isabel; KEMMING, Janine; OBERHARDT, Valerie; WILD, Katharina; SEIDEL, Lea M.; KILLMER, Saskia; SAGAR; DAUL, Franziska; SALVAT LAGO, Marilyn; DECKER, Annegrit; LUXENBURGER, Hendrik; BINDER, Benedikt; BETTINGER, Dominik; SOGUKPINAR, Oezlem; RIEG, Siegbert; PANNING, Marcus; HUZLY, Daniela; SCHWEMMLE, Martin; KOCHS, Georg; … NEUMANN-HAEFELIN, Christoph. Characterization of pre-existing and induced SARS-CoV-2-specific CD8+ T cells. **Nature Medicine**, vol. 27, no. 1, p. 78–85, 2021. DOI 10.1038/s41591-020-01143-2. Available at: http://dx.doi.org/10.1038/s41591-020-01143-2.

SCHULTZ, Bárbara M.; MELO-GONZÁLEZ, Felipe; DUARTE, Luisa F.; GÁLVEZ, Nicolás M.S.; PACHECO, Gaspar A.; SOTO, Jorge A.; BERRÍOS-ROJAS, Roslye V.; GONZÁLEZ, Liliana A.; MORENO-TAPIA, Daniela; RIVERA-PÉREZ, Daniela; RÍOS, Mariana; VÁZQUEZ, Yaneisi; HOPPE-ELSHOLZ, Guillermo; ANDRADE-PARRA, Catalina A.; VALLEJOS, Omar P.; PIÑA-ITURBE, Alejandro; ITURRIAGA, Carolina; URZUA, Marcela; NAVARRETE, María S.; … BUENO, Susan M. A Booster Dose of CoronaVac Increases Neutralizing Antibodies and T Cells that Recognize Delta and Omicron Variants of Concern. **mBio**, vol. 13, no. 4, 2022.

https://doi.org/10.1128/mbio.01423-22.

SEIDEL, Markus G.; KINDLE, Gerhard; GATHMANN, Benjamin; QUINTI, Isabella; BUCKLAND, Matthew; VAN MONTFRANS, J.; SCHEIBLE, Raphael; RUSCH, Stephan; GASTEIGER, Lukas M.; GRIMBACHER, Bodo; MAHLAOUI, N.; EHL, Stephan; ABINUN, M.; ALBERT, Michael; COHEN, Sarah Beaussant; BUSTAMANTE, Jacinta; CANT, Andrew; CASANOVA, Jean Laurent; CHAPEL, H.; … ZHANG, Shen Yin. The European Society for Immunodeficiencies (ESID) Registry Working Definitions for the Clinical Diagnosis of Inborn Errors of Immunity. **Journal of Allergy and Clinical Immunology: In Practice**, vol. 7, no. 6, p. 1763–1770, 2019. https://doi.org/10.1016/j.jaip.2019.02.004.

SEKINE, Takuya; PEREZ-POTTI, André; RIVERA-BALLESTEROS, Olga; STRÅLIN, Kristoffer; GORIN, Jean Baptiste; OLSSON, Annika; LLEWELLYN-LACEY, Sian; KAMAL, Habiba; BOGDANOVIC, Gordana; MUSCHIOL, Sandra; WULLIMANN, David J.; KAMMANN, Tobias; EMGÅRD, Johanna; PARROT, Tiphaine; FOLKESSON, Elin; AKBER, Mira; BERGLIN, Lena; BERGSTEN, Helena; BRIGHENTI, Susanna; … BUGGERT, Marcus. Robust T Cell Immunity in Convalescent Individuals with Asymptomatic or Mild COVID-19. **Cell**, vol. 183, no. 1, p. 158-168.e14, 2020. https://doi.org/10.1016/j.cell.2020.08.017.

SEOW, Jeffrey; GRAHAM, Carl; MERRICK, Blair; ACORS, Sam; PICKERING, Suzanne; STEEL, Kathryn J.A.; HEMMINGS, Oliver; O'BYRNE, Aoife; KOUPHOU, Neophytos; GALAO, Rui Pedro; BETANCOR, Gilberto; WILSON, Harry D.; SIGNELL, Adrian W.; WINSTONE, Helena; KERRIDGE, Claire; HUETTNER, Isabella; JIMENEZ-GUARDEÑO, Jose M.; LISTA, Maria Jose; TEMPERTON, Nigel; … DOORES, Katie J. Longitudinal observation and decline of neutralizing antibody responses in the three months following SARS-CoV-2 infection in humans. **Nature Microbiology**, vol. 5, no. 12, p. 1598–1607, 2020. DOI 10.1038/s41564-020-00813-8. Available at: http://dx.doi.org/10.1038/s41564-020-00813-8.

SETTE, Alessandro; CROTTY, Shane. Adaptive immunity to SARS-CoV-2 and COVID-19. **Cell**, no. January, p. 19–21, 2020. https://doi.org/https://doi.org/10.1016/j.cell.2021.01.007.

SHAH, Vibhuti Kumar; FIRMAL, Priyanka; ALAM, Aftab; GANGULY, Dipyaman; CHATTOPADHYAY, Samit. Overview of Immune Response During SARS-CoV-2 Infection: Lessons From the Past. **Frontiers in Immunology**, vol. 11, no. August, p. 1–17, 2020. https://doi.org/10.3389/fimmu.2020.01949.

SHAW, Albert C.; GOLDSTEIN, Daniel R.; MONTGOMERY, Ruth R. Age-dependent dysregulation of innate immunity. **Nature Reviews Immunology**, vol. 13, no. 12, p. 875–887, 2013. https://doi.org/10.1038/nri3547.

SHROTRI, Madhumita; VAN SCHALKWYK, May C.I.; POST, Nathan; EDDY, Danielle; HUNTLEY, Catherine; LEEMAN, David; RIGBY, Samuel; WILLIAMS, Sarah V.; BERMINGHAM, William H.; KELLAM, Paul; MAHER, John; SHIELDS, Adrian M.; AMIRTHALINGAM, Gayatri; PEACOCK, Sharon J.; ISMAIL, Sharif A. T cell response to SARS-cov-2 infection in humans: A systematic review. **PLoS ONE**, vol. 16, no. 1 January, p. 1–21, 2021. DOI 10.1371/journal.pone.0245532. Available at: http://dx.doi.org/10.1371/journal.pone.0245532.

SONG, Jin Wen; ZHANG, Chao; FAN, Xing; MENG, Fan Ping; XU, Zhe; XIA, Peng; CAO, Wen Jing; YANG, Tao; DAI, Xiao Peng; WANG, Si Yu; XU, Ruo Nan; JIANG, Tian Jun; LI, Wen Gang; ZHANG, Da Wei; ZHAO, Peng; SHI, Ming; AGRATI, Chiara; IPPOLITO, Giuseppe; MAEURER, Markus; … ZHANG, Ji Yuan. Immunological and inflammatory profiles in mild and severe cases of COVID-19. **Nature Communications**, vol. 11, no. 1, 2020. https://doi.org/10.1038/s41467-020-17240-2.

SWADLING, Leo; DINIZ, Mariana O.; SCHMIDT, Nathalie M.; AMIN, Oliver E.; CHANDRAN, Aneesh; SHAW, Emily; PADE, Corinna; GIBBONS, Joseph M.; LE BERT, Nina; TAN, Anthony T.; JEFFERY-SMITH, Anna; TAN, Cedric C. S.; THAM, Christine Y. L.; KUCYKOWICZ, Stephanie; AIDOO-MICAH, Gloryanne; ROSENHEIM, Joshua; DAVIES, Jessica; JOHNSON, Marina; JENSEN, Melanie P.; … MAINI, Mala K. Pre-existing polymerase-specific T cells expand in abortive seronegative SARS-CoV-2. **Nature**, vol. 601, no. October, p. 110–117, 2021. https://doi.org/10.1038/s41586-021-04186-8.

SWANSON, Phillip A.; PADILLA, Marcelino; HOYLAND, Wesley; MCGLINCHEY,

Kelly; FIELDS, Paul. A; BIBI, Sagida; FAUST, Saul N.; MCDERMOTT, Adrian B.; LAMBE, Teresa; POLLARD, Andrew J.; DURHAM, Nicholas M.; KELLY, Elizabeth J. T-cell mediated immunity after AZD1222 vaccination: A polyfunctional spike-specific Th1 response with a diverse TCR repertoire. **medRxiv**, no. 165, p. 1–13, 2020.

TANG, Fang; QUAN, Yan; XIN, Zhong-Tao; WRAMMERT, Jens; MA, Mai-Juan; LV, Hui; WANG, Tian-Bao; YANG, Hong; RICHARDUS, Jan H.; LIU, Wei; CAO, Wu-Chun. Lack of Peripheral Memory B Cell Responses in Recovered Patients with Severe Acute Respiratory Syndrome: A Six-Year Follow-Up Study. **The Journal of Immunology**, vol. 186, no. 12, p. 7264–7268, 2011. https://doi.org/10.4049/jimmunol.0903490.

TANRIOVER, Mine Durusu; DOGANAY, Hamdi Levent; AKOVA, Murat; GUNER, Hatice Rahmet; AZAP, Alpay; AKHAN, Sila; KÖSE, Sükran; ERDINÇ, Fatma Sebnem; GÜR, Hazal; UNAL, Serhat. Efficacy and safety of an inactivated whole-virion SARS-CoV-2 vaccine (CoronaVac): interim results of a double-blind, randomised, placebo-controlled, phase 3 trial in Turkey. **The Lancet**, vol. 398, no. July, p. 213–222, 2021. https://doi.org/https://doi.org/10.1016/ S0140-6736(21)01429-X.

TAY, Matthew Zirui; POH, Chek Meng; RÉNIA, Laurent; MACARY, Paul A.; NG, Lisa F.P. The trinity of COVID-19: immunity, inflammation and intervention. **Nature Reviews Immunology**, vol. 20, no. 6, p. 363–374, 2020. DOI 10.1038/s41577-020-0311-8. Available at: http://dx.doi.org/10.1038/s41577-020-0311-8.

TREGONING, John S.; FLIGHT, Katie E.; HIGHAM, Sophie L.; WANG, Ziyin; PIERCE, Benjamin F. Progress of the COVID-19 vaccine effort: viruses, vaccines and variants versus efficacy, effectiveness and escape. **Nature Reviews Immunology**, vol. 21, no. 10, p. 626–636, 2021. DOI 10.1038/s41577-021-00592-1. Available at: http://dx.doi.org/10.1038/s41577-021-00592-1.

WALLS, Alexandra C.; PARK, Young Jun; TORTORICI, M. Alejandra; WALL, Abigail; MCGUIRE, Andrew T.; VEESLER, David. Structure, Function, and Antigenicity of the SARS-CoV-2 Spike Glycoprotein. **Cell**, vol. 181, no. 2, p. 281-292.e6, 2020. DOI 10.1016/j.cell.2020.02.058. Available at: http://dx.doi.org/10.1016/j.cell.2020.02.058.

WAN, Yushun; SHANG, Jian; GRAHAM, Rachel; BARIC, Ralph S.; LI, Fang. Receptor Recognition by the Novel Coronavirus from Wuhan: an Analysis Based on Decade-Long Structural Studies of SARS Coronavirus. **Journal of Virology**, vol. 94, no. 7, p. 1–9, 2020. .

WANG, Mei Yue; ZHAO, Rong; GAO, Li Juan; GAO, Xue Fei; WANG, De Ping; CAO, Ji Min. SARS-CoV-2: Structure, Biology, and Structure-Based Therapeutics Development. **Frontiers in Cellular and Infection Microbiology**, vol. 10, no. November, p. 1–17, 2020. https://doi.org/10.3389/fcimb.2020.587269.

WEIFENBACH, Niels; JUNG, Alisha; LÖTTERS, Stefan. COVID-19 infection in CVID patients: What we know so far. **Immunity, Inflammation and Disease**, vol. 9, no. 3, p. 632–634, 2021. https://doi.org/10.1002/iid3.450.

WHEATLEY, Adam K.; JUNO, Jennifer A.; WANG, Jing J.; SELVA, Kevin J.; REYNALDI, Arnold; TAN, Hyon Xhi; LEE, Wen Shi; WRAGG, Kathleen M.; KELLY, Hannah G.; ESTERBAUER, Robyn; DAVIS, Samantha K.; KENT, Helen E.; MORDANT, Francesca L.; SCHLUB, Timothy E.; GORDON, David L.; KHOURY, David S.; SUBBARAO, Kanta; CROMER, Deborah; GORDON, Tom P.; … KENT, Stephen J. Evolution of immune responses to SARS-CoV-2 in mild-moderate COVID-19. **Nature Communications**, vol. 12, no. 1, p. 1–11, 2021. DOI 10.1038/s41467-021-21444-5. Available at: http://dx.doi.org/10.1038/s41467-021-21444-5.

WRAY, Susan; ARROWSMITH, Sarah. The Physiological Mechanisms of the Sex-Based Difference in Outcomes of COVID19 Infection. **Frontiers in Physiology**, vol. 12, no. February, p. 1–12, 2021. https://doi.org/10.3389/fphys.2021.627260.

WU, Fan; ZHAO, Su; YU, Bin; CHEN, Yan Mei; WANG, Wen; SONG, Zhi Gang; HU, Yi; TAO, Zhao Wu; TIAN, Jun Hua; PEI, Yuan Yuan; YUAN, Ming Li; ZHANG, Yu Ling; DAI, Fa Hui; LIU, Yi; WANG, Qi Min; ZHENG, Jiao Jiao; XU, Lin; HOLMES, Edward C.; ZHANG, Yong Zhen. A new coronavirus associated with human respiratory disease in China. **Nature**, vol. 579, no. 7798, p. 265–269, 2020. https://doi.org/10.1038/s41586-020-2008-3.

WU, Zhiwei; HU, Yaling; XU, Miao; CHEN, Zhen; YANG, Wanqi; JIANG, Zhiwei; LI, Minjie; JIN, Hui; CUI, Guoliang; CHEN, Panpan; WANG, Lei; ZHAO, Guoqing; DING, Yuzhu; ZHAO, Yuliang; YIN, Weidong. Safety, tolerability, and immunogenicity of an inactivated SARS-CoV-2 vaccine (CoronaVac) in healthy adults aged 60 years and older: a randomised, double-blind, placebo-controlled, phase 1/2 clinical trial. **The Lancet Infectious Diseases**, vol. 21, no. 6, p. 803–812, 2021. DOI 10.1016/S1473-3099(20)30987-7. Available at: http://dx.doi.org/10.1016/S1473-3099(20)30987-7.

YALÇIN, Tuğba Y.; TOPÇU, Deniz; DOĞAN, Özlem; AYDIN, Saliha; SARI, Nuran; EROL, Çiğdem; KULOĞLU, Zeynep E.; AZAP, Özlem K.; CAN, Füsun; ARSLAN, Hande. Immunogenicity after two doses of inactivated virus vaccine in healthcare workers with and without previous COVID-19 infection: Prospective observational study. **Journal of Medical Virology**, vol. 94, no. 1, p. 279–286, 2022. https://doi.org/10.1002/jmv.27316.

YANG, Haitao; RAO, Zihe. Structural biology of SARS-CoV-2 and implications for therapeutic development. **Nature Reviews Microbiology**, vol. 19, no. 11, p. 685–700, 2021. DOI 10.1038/s41579-021-00630-8. Available at: http://dx.doi.org/10.1038/s41579-021-00630-8.

ZHANG, Yanjun; ZENG, Gang; PAN, Hongxing; LI, Changgui; HU, Yaling; CHU, Kai; HAN, Weixiao; CHEN, Zhen; TANG, Rong; YIN, Weidong; CHEN, Xin; HU, Yuansheng; LIU, Xiaoyong; JIANG, Congbing; LI, Jingxin; YANG, Minnan; SONG, Yan; WANG, Xiangxi; GAO, Qiang; ZHU, Fengcai. Safety, tolerability, and immunogenicity of an inactivated SARS-CoV-2 vaccine in healthy adults aged 18–59 years: a randomised, double-blind, placebo-controlled, phase 1/2 clinical trial. **The Lancet Infectious Diseases**, vol. 21, no. 2, p. 181–192, 2021. DOI 10.1016/S1473-3099(20)30843-4. Available at: http://dx.doi.org/10.1016/S1473-3099(20)30843-4.

ZHOU, Yunjiao; LIU, Zezhong; LI, Shibo; XU, Wei; ZHANG, Qianqian; SILVA, Israel T.; LI, Cheng; WU, Yanling; JIANG, Qingling; LIU, Zhenmi; WANG, Qiujing; GUO, Yu; WU, Jianbo; GU, Chengjian; CAI, Xia; QU, Di; MAYER, Christian T.; WANG, Xiangxi; JIANG, Shibo; … WANG, Qiao. Enhancement versus neutralization by SARS-CoV-2 antibodies from a convalescent donor associates with distinct epitopes on the RBD. **Cell Reports**, vol. 34, no. 5, 2021. https://doi.org/10.1016/j.celrep.2021.108699.

Reduced T Cell and Antibody Responses to Inactivated Coronavirus Vaccine Among Individuals Above 55 Years Old

Giuliana X. Medeiros[1,2‡], Greyce Luri Sasahara[2‡], Jhosiene Y. Magawa[1,2‡], João Paulo S. Nunes[1,2], Fernanda R. Bruno[2], Andreia C. Kuramoto[1,2], Rafael R. Almeida[2], Marcelo A. Ferreira[3], Guilherme P. Scagion[4], Érika D. Candido[4], Fabyano B. Leal[4], Danielle B. L. Oliveira[4,5], Edison L. Durigon[4,6], Roberto Carlos V. Silva Jr.[2], Daniela S. Rosa[7,9], Silvia B. Boscardin[8,9], Verônica Coelho[1,2,9], Jorge Kalil[1,2,9], Keity S. Santos[1,2,9*†] and Edecio Cunha-Neto[1,2,9*†]

[1] Faculdade de Medicina da Universidade de São Paulo, Departamento de Clínica Médica, Disciplina de Alergia e Imunologia Clínica, São Paulo, Brazil, [2] Laboratório de Imunologia, Instituto do Coração (InCor), Hospital das Clínicas da Faculdade de Medicina da Universidade de São Paulo (HCFMUSP), São Paulo, Brazil, [3] Laboratório de Biologia Celular, LIM59, Departamento de Patologia da Faculdade de Medicina, Universidade de São Paulo, São Paulo, Brazil, [4] Departamento de Microbiologia, Instituto de Ciências Biomédicas, Universidade de São Paulo, São Paulo, Brazil, [5] Instituto Israelita de Ensino e Pesquisa Albert Einstein, Hospital Israelita Albert Einstein, São Paulo, Brazil, [6] Laboratório de Virologia, Plataforma Científica Pasteur da Universidade de São Paulo, São Paulo, Brazil, [7] Departamento de Microbiologia, Imunologia e Parasitologia, Universidade Federal de São Paulo (UNIFESP-EPM), São Paulo, Brazil, [8] Departamento de Parasitologia, Instituto de Ciências Biomédicas, Universidade de São Paulo, São Paulo, Brazil, [9] Instituto de Investigação em Imunologia (iii), Instituto Nacional de Ciências e Tecnologia (INCT), São Paulo, Brazil

CoronaVac is an inactivated SARS-CoV-2 vaccine that has been rolled out in several low and middle-income countries including Brazil, where it was the mainstay of the first wave of immunization of healthcare workers and the elderly population. We aimed to assess the T cell and antibody responses of vaccinated individuals as compared to convalescent patients. We detected IgG against SARS-CoV-2 antigens, neutralizing antibodies against the reference Wuhan SARS-CoV-2 strain and used SARS-CoV-2 peptides to detect IFN-g and IL-2 specific T cell responses in a group of CoronaVac vaccinated individuals (N = 101) and convalescent (N = 72) individuals. The frequency among vaccinated individuals, of whom 96% displayed T cell and/or antibody responses to SARS-CoV-2, is comparable to 98.5% responses of convalescent individuals. We observed that among vaccinated individuals, men and individuals 55 years or older developed significantly lower anti-RBD, anti-NP and neutralization titers against the Wuhan strain and antigen-induced IL-2 production by T cells. Neutralizing antibody responses for Gamma variant were even lower than for the Wuhan strain. Even though some studies indicated CoronaVac helped reduce mortality among elderly people, considering the appearance of novel variants of concern, CoronaVac vaccinated individuals above 55 years old are likely to benefit from a heterologous third dose/booster vaccine to increase immune response and likely protection.

Keywords: COVID-19, vaccine, CoronaVac, T cell responses, antibody, neutralizing antibody, age

INTRODUCTION

Terminating the COVID-19 pandemic is dependent on global vaccination. CoronaVac (Sinovac, China) is a vaccine based on inactivated SARS-CoV-2 that has been deployed in China, Brazil, Indonesia, Thailand, Turkey, and Chile among other countries. It has been shown that CoronaVac's immunogenicity is lower than natural infection (1). In Brazil, CoronaVac was the mainstay of the first wave of immunization of healthcare workers and the elderly population. Despite the finding of reduced COVID-19 mortality in Brazil among people above 70 or 75 years of age when CoronaVac was the most used vaccine, indicating protection for this group, immunogenicity of this vaccine in elderly individuals is still poorly known (2–4). Some studies reported seroconversion for up to 98% of vaccinated individuals, but anti-Spike antibody titers were significantly lower among those aged ≥60 years (5, 6). Also, the immunogenicity of inactivated vaccines such as Influenza have already been shown to be more limited among the elderly (7).

mRNA-based vaccines that protect more than 90% of the vaccinated individuals from severe COVID-19 were shown to induce T cell response (8, 9). Although an immunogenicity study in Chile has evaluated cellular immunity to CoronaVac, few patients were above 60 years of age (10). In order to assess the effect of age and sex in the vaccine response of adults and elderly people, we studied the anti-SARS-CoV-2 responses of a group of 101 vaccinated individuals (namely, 42 patients above 60). In this paper, we assessed T cell immune responses with an antigen-induced cytokine release assay (CRA) on whole blood and both binding antibody responses (against Spike, RBD and NP) and neutralizing antibodies against the original Wuhan strain.

MATERIALS AND METHODS

Study Design and Participants

A cross-sectional study was performed with CoronaVac vaccinated health care workers, who reported no previous infection with SARS-CoV-2 (n = 101; median age = 55 IQR = 39–67); these subjects received two doses of 3 µg vaccine/shot, 3 weeks apart. The study was conducted at the Instituto do Coração in São Paulo, Brazil. Venous blood was collected at least 21 days (median = 37, IQR = 22–62) after the second immunization (**Table 1**). Convalescent individuals (confirmed by a previous positive SARS-CoV-2 RT-PCR result) with mild disease (11) (n = 72; median age = 40, IQR = 32–47) with at least 150 days since the onset of the infectious episode were included as positive controls. Seronegative samples with no T cell response specific for SARS-CoV-2, obtained during the pandemic (n = 36; median age = 36 IQR = 30–47), were also included as negative controls. All volunteers signed written informed consent and the study was approved by the Ethics Committee of the Hospital das Clínicas da Universidade de São Paulo (CAPPesq CAAE30155220.3.0000.0068).

Antibody ELISA

Enzyme-linked immunosorbent assay (ELISA) was performed using 96-well high- binding half-area polystyrene plates coated overnight at 4°C with 4 µg/ml of Spike protein, 2 µg/ml Nucleocapsid protein (NP) (Kindly provided by Dr. Ricardo Gazzinelli, UFMG, Brazil) or 0.8 µg/ml of the RBD domain from SARS-CoV-2 were all expressed in HEK293T cells (12). In short, 50 µl of diluted sera (1:100) were incubated at 37°C for 45 min. Peroxidase-conjugated goat anti-human IgG (BD Pharmingen, USA), anti-human IgA (KPL, USA) or anti-human IgM (Sigma, USA) secondary antibody conjugates were diluted 1:10,000, and incubated at 37°C for 30 min. The optical density (OD) at 492 nm was measured with a microplate reader (Epoch, BioTek, USA). Values were determined as OD minus blank and cutoff was determined as the average OD of 12 samples pre-pandemics + 3× standard deviation. Results are given as the ratio of OD sample/ cutoff. An antibody ratio of ≥1.2 was considered positive.

Virus Neutralization Assay

SARS-CoV-2 (GenBank: MT MT350282) was used to conduct a cytopathic effect (CPE)-based virus neutralization test (VNT) as previously described (13). The virus strain properties were previously described on Araujo et al. (14). We used 96-well plates containing 5×10^4 cells/ml of Vero cells (ATCC CCL-81). A series of dilutions (1:20 to 1:2,560) was prepared for the assay. Serum dilutions were mixed at equal volumes with the virus (100 tissue culture infectious doses, 100% endpoint per well—VNT100) and pre-incubated for virus neutralization for 1 h at 37°C. The mixtures containing serum and virus were transferred onto the confluent cell monolayer and incubated at 5% CO_2 for three days at 37°C, all the procedures were conducted in a Biosafety laboratory level three (BSL3). After 72 h, plates were analyzed by light microscopy. Gross CPE was observed on Vero cells, distinguishing the presence/absence of CPE-VNT against the Wuhan reference strain or the Gamma variant, which was prevalent in Brazil by the time of the sampling. To determine neutralizing antibody titers, the highest serum dilution that was able to neutralize virus growth was considered. As positive control, a reference serum from an RT-qPCR positive individual and a plaque reduction in the neutralization test >640 was used in each assay.

Antigen-Induced T Cell Cytokine Release Assay

Antigen-induced T cell cytokine release assays (CRA) were performed by incubating 250 µl/well of heparinized peripheral blood onto round-bottom 96-well plates for 48 h at a humidified 37°C, 5% CO2 environment in the presence of 20 pooled CD4+ T cell epitopes (**Supplementary Table 1**). Twenty CD4+ T cell epitopes used as antigen-specific T cell stimulus were bioinformatically identified and synthesized by scanning the whole proteome in SARS-CoV-2 reference genome (RefSeq: NC_045512.2) using the promiscuous HLA-DR binding peptide approach (15). Plates were centrifuged, and plasma supernatant was harvested and stored at −80°C until use. IFN-γ and IL-2 levels in cell-free culture supernatants were evaluated by ELISA, according to manufacturer's instructions (R&D Systems, Minneapolis, MN). The cutoff values for IFN and IL-2 were obtained by a Receiver Operator Curve analysis with diagnostics as reference groups and IFN or IL-2 values as predictors. Cytokine values were subtracted from the

TABLE 1 | Characteristics of study participants.

	Vaccinated	Convalescent	Seronegative control		P value
n	101	72	36	Test A	p=4.37 x 10^{-10}
				B	C vs SC p=0.94
Age, mean ± sd (range)	54 ± 16.3 (23-90)	40.5 ± 10.5 (24-68)	39 ± 12.3 (22-44)		C vs V p<0.0001 SC vs V p<0.0001
Sex, n (%)					
Female	70 (71)	54 (75)	26 (72)	E	p=0.7129
Male	30 (29)	18 (25)	10 (28)		
Interval between sampling and 2nd dose or symptoms onset, median (range)	37 (21-80)	207 (159-240)	NA		
Antibody levels, median ratio (IQR)					
IgG RBD	2.94 (3.04)	1.46 (1.00)	0.13 (0.09)	C D	p=1.85 x 10^{-20} C vs SC p<0.0001 C vs V p=0.000147 SC vs V p<0.0001
IgG NP	1.17 (2.69)	1.31 (1.34)	0.12 (0.14)	C D	p=2.97 x 10^{-15} C vs SC p<0.0001 C vs V p=0.682 SC vs V p<0.0001
IgG Spike	1.43 (3.03)	3.76 (2.28)	0.12 (0.11)	C D	p=6.45 x 10^{-18} C vs SC p<0.0001 C vs V p<0.0001 SC vs V p<0.0001
Cytokine levels (pg/mL), median (IQR)					
IFN-γ	2.06 (9.00)	3.51 (8.48)	0 (0.37)	C D	p=1.18 x 10^{-7} C vs SC p<0.0001 C vs V p=1 SC vs V p<0.0001
IL-2	1.21 (16.8)	2.72 (22.0)	0 (0.00)	C D	p =2.7 x 10^{-9} C vs SC p<0.0001 C vs V p=0.326 SC vs V p<0.0001
Neutralization assay					
n	83	31	36		
Neutralization titer (VNT100), GMT (CI 95%)	1:40 22.2 (15.2 - 32.4)	0.0972222 82.0 (56.7 - 118.6)	0 0	F	p = 0.0097

Tests: A, ANOVA; B, Post-hoc Tukey HSD; C, Kruskal-Wallis; D, Post-hoc Dunn; E, Chi square test.
F, Wilcoxon-Mann-Whitney.
Comparisons: V, vaccinated; C, convalescent; SC, seronegative control.
NA, Not applicable.

DMSO control. The quantification limit of the IFN-γ test was 1.17 pg/ml and 0.98 pg/ml for IL-2.

Statistical Analysis

Statistical analyses were performed using GraphPad Prism version 9 and R platform for statistical analysis version 4.0.3. Continuous variables were analyzed using Shapiro–Wilk test to assess the normality of their distribution. Comparison of continuous variables was carried out using Kruskal–Wallis test with Dunn's *post-hoc* test for several groups or Mann–Whitney test when only two groups were compared. Pearson's chi squared test was used to assess categorical data association. Correlation was evaluated by the Spearman's coefficient. The age limit value to characterize groups of immune response was established after a two-step process. A K-means cluster analysis based on five continuous variables (ratios of IgG from NP, RBD, Spike and levels of IFN-γ and IL-2) was used to identify two groups of different immune responses, according to the algorithm of

Hartigan and Wong (16). The age threshold that could distinguish the two resulting clusters with the highest accuracy was obtained by a Receiver Operator Characteristic curve analysis with the clusters as reference and the age variable as predictor (**Supplementary Figure 1**). A p-value <0.05 was considered statistically significant for all analyses.
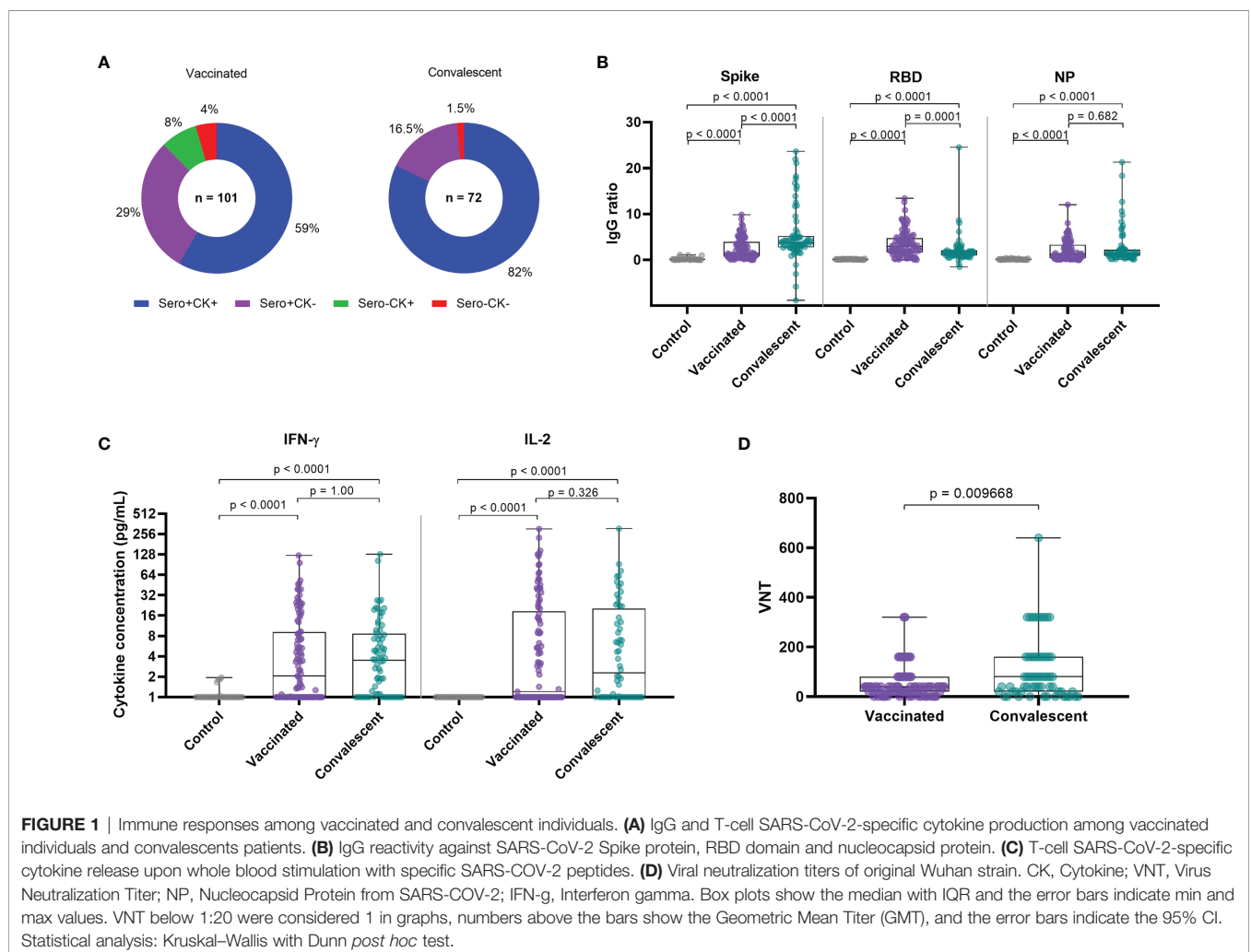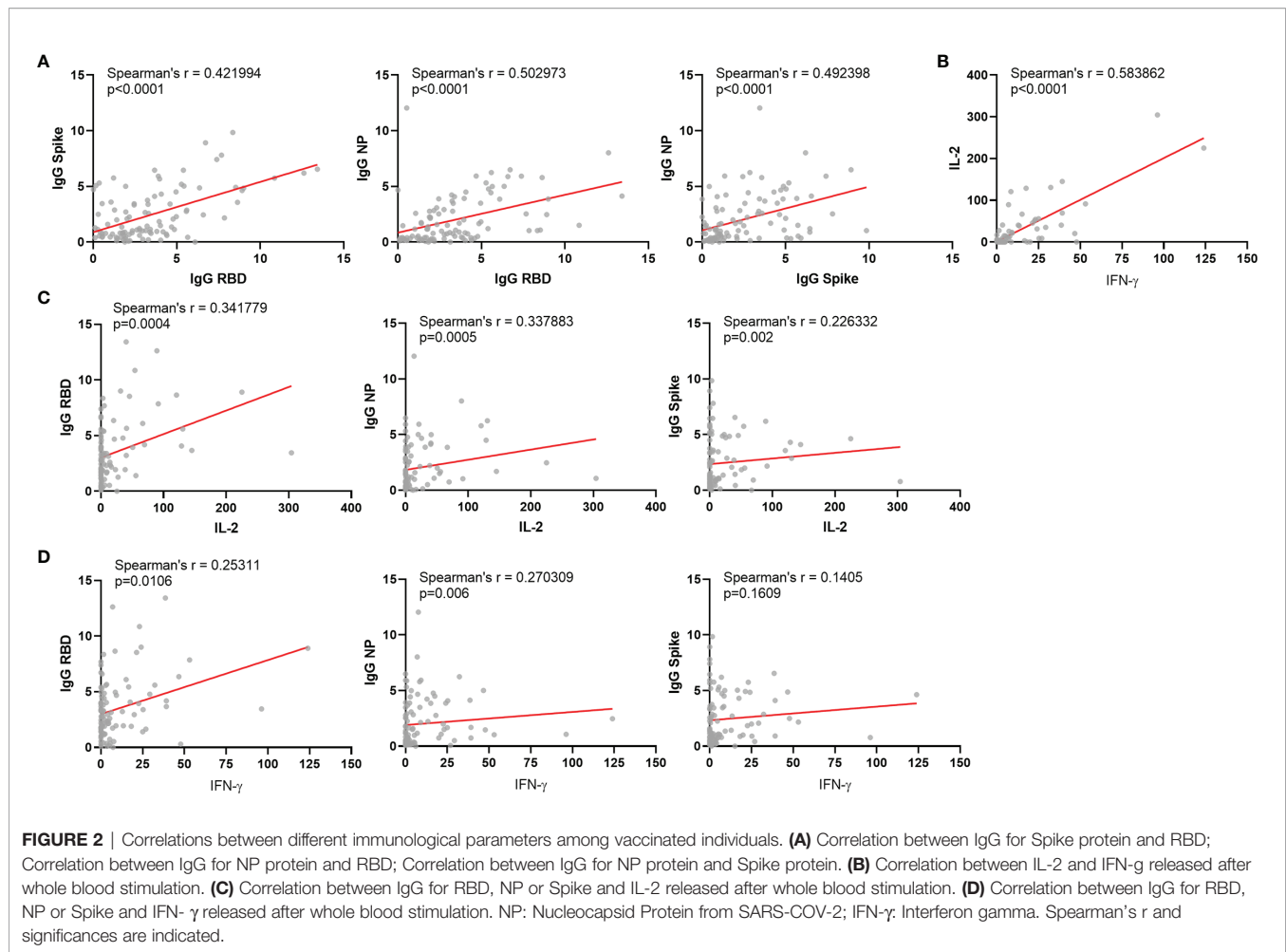
RESULTS

Demographical data and assays for each group are described in **Table 1**. Among vaccinated individuals, 96% displayed antigen-induced cellular cytokine and/or antibody responses to at least one antigen tested, and 98.5% of convalescents displayed cellular and/or antibody responses. Of interest, both cellular and humoral responses were displayed by 59 and 82% of vaccinated and convalescent individuals, respectively (**Figure 1A**). Vaccinated and convalescent individuals displayed significantly higher antibody and T cell responses than seronegative controls. Vaccinated individuals displayed significantly lower IgG responses against Spike protein, but higher responses against the RBD domain as compared to convalescent patients, while responses to NP were similar between those two groups (**Figure 1B**).

Regarding T cell responses as measured by cytokine release after peptide stimulation, we observed that IL-2 and IFN-γ levels were similarly increased among vaccinated individuals and convalescents in comparison to the seronegative control group (**Figure 1C**). Geometric mean titers (GMT) of neutralization titers for the vaccinated group were 4 times lower as compared to convalescent patients, even though time since infection was much longer than time after vaccination (**Figure 1D**). Of interest, time of sampling since vaccination or infection did not correlate with higher or lower immune responses (**Supplementary Figures 2**, **3**).

Most immune response levels were positively correlated among each other, as previously reported (**Figure 2**) (17). Neutralization titers positively correlated with IgG levels for the three antigens tested and also with IFN-γ and IL-2 production upon whole blood stimulation (**Figure 3**). Among vaccinated individuals, we observed significant negative correlations between age and IL-2 cytokine release, but not for

FIGURE 1 | Immune responses among vaccinated and convalescent individuals. **(A)** IgG and T-cell SARS-CoV-2-specific cytokine production among vaccinated individuals and convalescents patients. **(B)** IgG reactivity against SARS-CoV-2 Spike protein, RBD domain and nucleocapsid protein. **(C)** T-cell SARS-CoV-2-specific cytokine release upon whole blood stimulation with specific SARS-COV-2 peptides. **(D)** Viral neutralization titers of original Wuhan strain. CK, Cytokine; VNT, Virus Neutralization Titer; NP, Nucleocapsid Protein from SARS-COV-2; IFN-g, Interferon gamma. Box plots show the median with IQR and the error bars indicate min and max values. VNT below 1:20 were considered 1 in graphs, numbers above the bars show the Geometric Mean Titer (GMT), and the error bars indicate the 95% CI. Statistical analysis: Kruskal–Wallis with Dunn *post hoc* test.

FIGURE 2 | Correlations between different immunological parameters among vaccinated individuals. **(A)** Correlation between IgG for Spike protein and RBD; Correlation between IgG for NP protein and RBD; Correlation between IgG for NP protein and Spike protein. **(B)** Correlation between IL-2 and IFN-g released after whole blood stimulation. **(C)** Correlation between IgG for RBD, NP or Spike and IL-2 released after whole blood stimulation. **(D)** Correlation between IgG for RBD, NP or Spike and IFN- γ released after whole blood stimulation. NP: Nucleocapsid Protein from SARS-COV-2; IFN-γ: Interferon gamma. Spearman's r and significances are indicated.
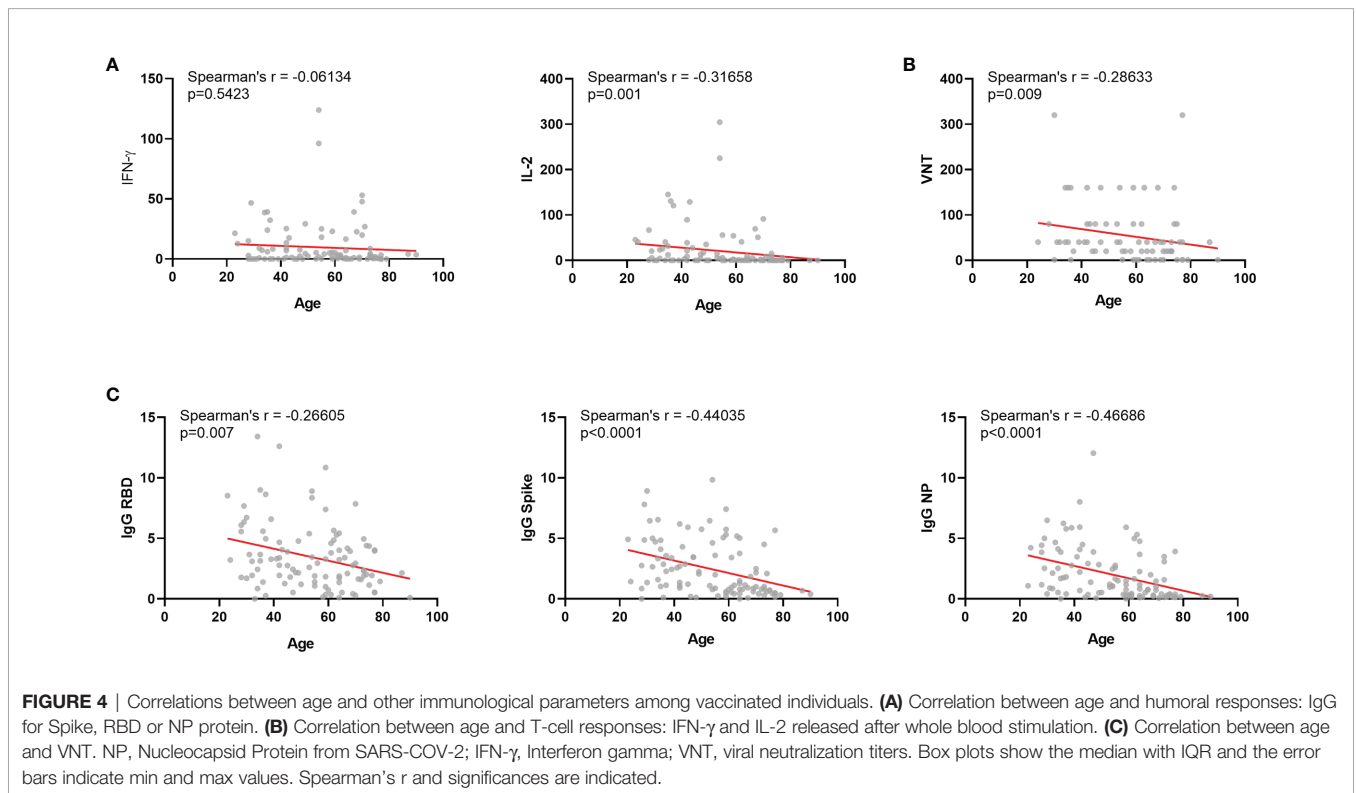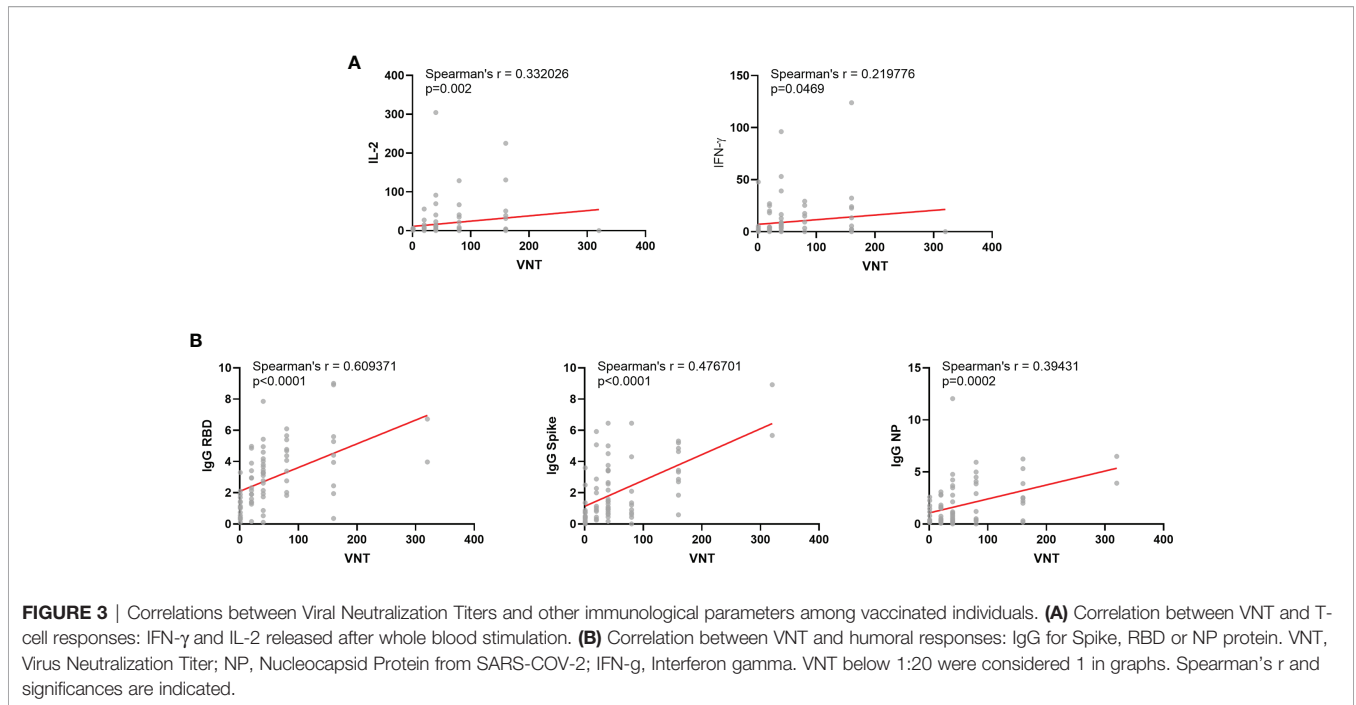
I IFN-γ (**Figure 4A**). We also observed a negative correlation between age and neutralization titers (**Figure 4B**), and also age and IgG antibody levels against Spike, RBD and NP (**Figure 4C**).

The identification of clusters from the numerical variables allowed us to identify the age of ~55 years as the best divisor. Therefore, we compared the two age groups considering under 55 and 55 or older. Among vaccinated, while 97% of the women ≥55 displayed antibody and/or T cell responses, 83% of men from the same age group displayed detectable responses (**Figure 5A**). Moreover, while 63% of women ≥55 displayed antibody and T cell responses simultaneously, only 33% of men in the same age group presented both types of response (**Figure 5A**). Antibody responses alone were observed in 33% vs 29% of men and women vaccinated individuals ≥55, respectively, and cellular responses in the absence of detectable IgG were found among 17% male and 6% female vaccinated individuals ≥55 years old (**Figure 5A**). Antibody responses for male vaccinated individuals ≥55 years old displayed the lowest levels of anti- Spike, anti-RBD and anti-NP IgG and IL-2 release (**Figures 5B, C**). Female vaccinated individuals ≥55 years old also showed lower anti-NP and anti-Spike IgG and IL-2 release than younger females (**Figures 5B, C**).

Similar results were observed when we assessed neutralizing antibody and T cell cytokine production (**Figure 6A**). Older vaccinated men displaying both VNT and cytokine production corresponded to only 28% as compared to younger males presenting 67%, while among women, 70% of the younger and 55% of the older women presented both responses. Neutralization of Wuhan reference strain presented lower GMT for women >55 years old as compared with the younger group (**Figure 6B**). Lastly, we aimed to verify VNT capacity against the Gamma VOC, besides Wuhan strain, after vaccination. The overall VNT for the tested variant were lower than for Wuhan strain among vaccinated (**Figure 6C**). The dataset used for all analysis is available in **Supplementary Table 2**.
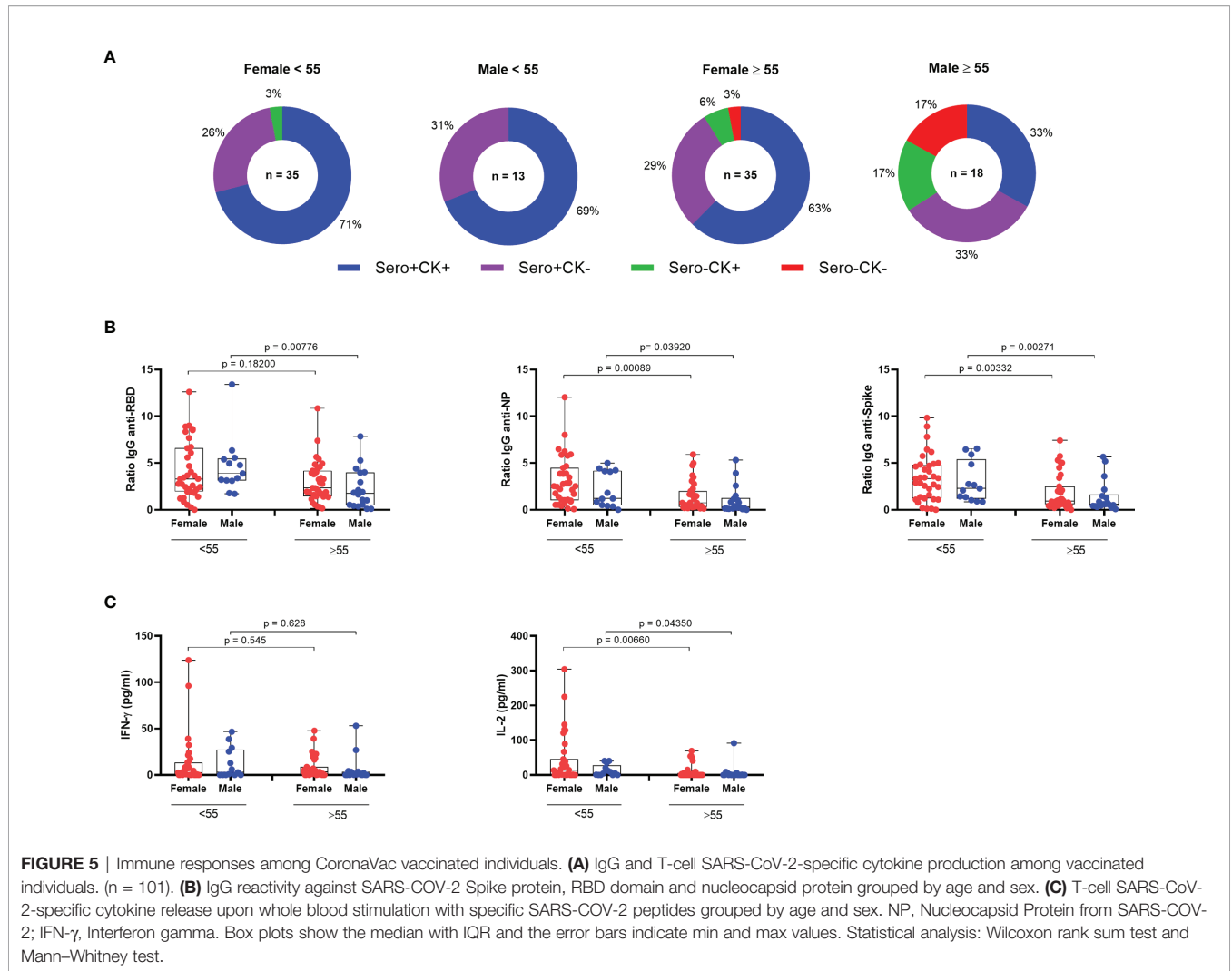
DISCUSSION

CoronaVac was the first anti-COVID vaccine available for mass immunization in Brazil, where it followed schedules targeting first the healthcare workers and the elderly population. We aimed to evaluate humoral and cellular responses after vaccination and stratify considering sex and age. In our

FIGURE 3 | Correlations between Viral Neutralization Titers and other immunological parameters among vaccinated individuals. (A) Correlation between VNT and T-cell responses: IFN-γ and IL-2 released after whole blood stimulation. (B) Correlation between VNT and humoral responses: IgG for Spike, RBD or NP protein. VNT, Virus Neutralization Titer; NP, Nucleocapsid Protein from SARS-COV-2; IFN-g, Interferon gamma. VNT below 1:20 were considered 1 in graphs. Spearman's r and significances are indicated.

FIGURE 4 | Correlations between age and other immunological parameters among vaccinated individuals. (A) Correlation between age and humoral responses: IgG for Spike, RBD or NP protein. (B) Correlation between age and T-cell responses: IFN-γ and IL-2 released after whole blood stimulation. (C) Correlation between age and VNT. NP, Nucleocapsid Protein from SARS-COV-2; IFN-γ, Interferon gamma; VNT, viral neutralization titers. Box plots show the median with IQR and the error bars indicate min and max values. Spearman's r and significances are indicated.

study, the majority of vaccinated individuals developed some kind of immune response to the vaccine and the magnitude of most of the immune response measures positively correlated with each other. However, we observed a negative correlation between age and SARS-CoV-2-peptide epitopes antigen-induced IL-2 release and antibody responses to Spike, RBD and NP, suggesting a lower immunogenicity in older individuals. Upon stratification by age and sex, we observed that most of this reduced immunogenicity was among the ≥55 years male population. The proportion of individuals who
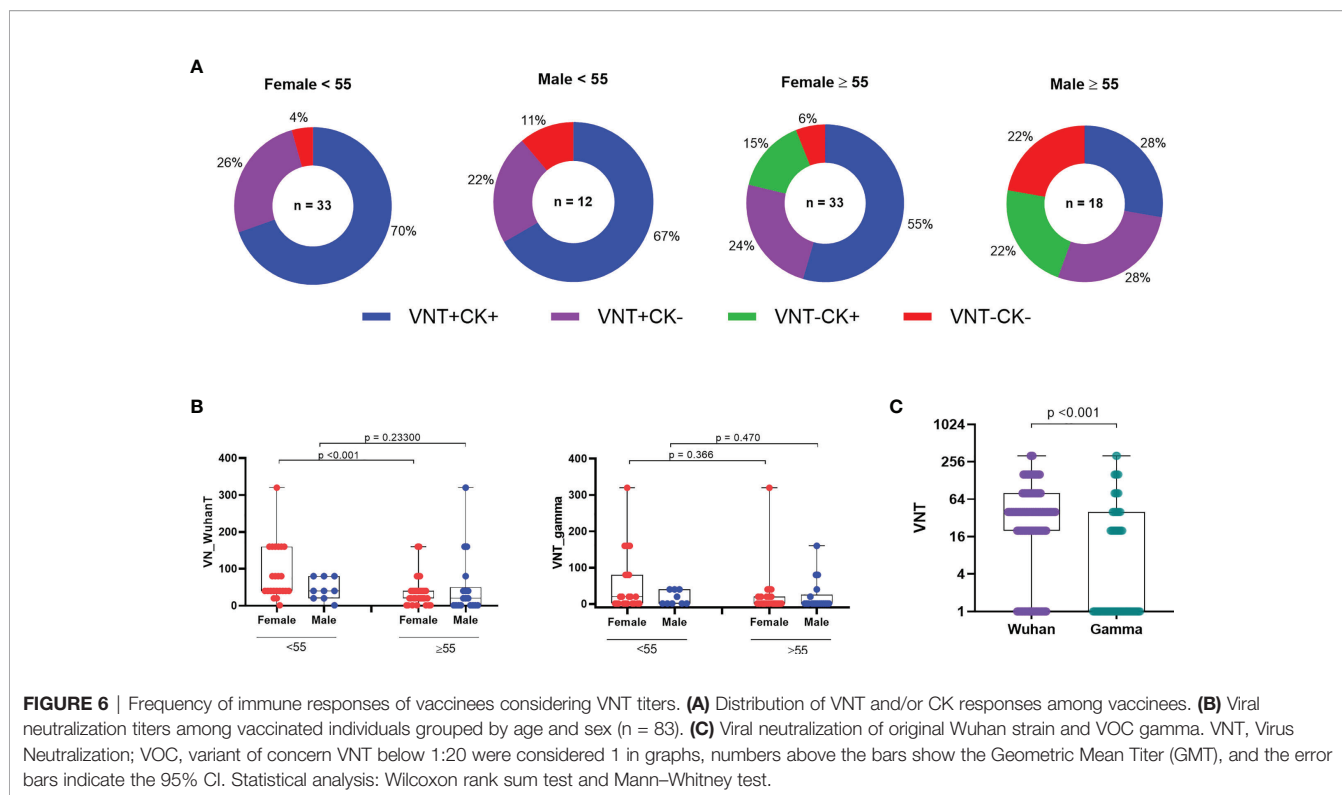
FIGURE 5 | Immune responses among CoronaVac vaccinated individuals. **(A)** IgG and T-cell SARS-CoV-2-specific cytokine production among vaccinated individuals. (n = 101). **(B)** IgG reactivity against SARS-COV-2 Spike protein, RBD domain and nucleocapsid protein grouped by age and sex. **(C)** T-cell SARS-CoV-2-specific cytokine release upon whole blood stimulation with specific SARS-COV-2 peptides grouped by age and sex. NP, Nucleocapsid Protein from SARS-COV-2; IFN-γ, Interferon gamma. Box plots show the median with IQR and the error bars indicate min and max values. Statistical analysis: Wilcoxon rank sum test and Mann–Whitney test.

displayed any response to the vaccine varied from 100% among younger women (<55 years old) to 83% among men 55 or older. Significantly, the simultaneous detection of antibody and cellular immune responses varied from 71% among women younger than 55 years old to only 33% among men 55 or older. This suggests that the immunogenicity of the vaccine regimen is less pronounced in this age and sex group. Also, the finding of reduced IL-2 in older male vaccinees is of particular concern, considering that interleukin-2 is essential for the development of memory T cells (18, 19).

Men are disproportionately affected by COVID-19 compared to their female counterparts. World death and hospitalization data during COVID-19 pandemic show a clear male bias (20). The mechanisms for such bias have not been elucidated, but it is fair to assume that differential immune responses play an important role. It has been hypothesized that this discrepancy is due to the fact that men generate a worse innate immune response than women. In regard to adaptive immunity, there is convincing evidence suggesting that women mount higher

antibody responses (21), which is directly associated with a better vaccine response (22).

It is well reported that aging is associated with a decline in immune function [reviewed in (23)]. This process, known as immunosenescence, often leads to impaired response to vaccines in older adults. In the case of inactivated vaccines, such as influenza, elderly individuals have a significantly lower protection, with efficacy ranging from 17 to 51%, as compared to up to 90% for younger individuals (24).

COVID-19 immunogenicity across young and elderly individuals has been studied for other vaccines. For ChadOx1, no differences were found following the second dose either for anti-Spike IgG and neutralizing antibodies or for IFN-γ and IL-2 Th1 T cell responses among the 18–55, 55–69 and ≥70 year old groups (25, 26). A study between mRNA-1273 vaccine recipient groups of 56–70 or ≥71 years of age revealed that binding, neutralizing-antibody and IFN-γ and IL-2 responses were similar to those reported among vaccine recipients between the ages of 18 and 55 years and were

FIGURE 6 | Frequency of immune responses of vaccinees considering VNT titers. **(A)** Distribution of VNT and/or CK responses among vaccinees. **(B)** Viral neutralization titers among vaccinated individuals grouped by age and sex (n = 83). **(C)** Viral neutralization of original Wuhan strain and VOC gamma. VNT, Virus Neutralization; VOC, variant of concern VNT below 1:20 were considered 1 in graphs, numbers above the bars show the Geometric Mean Titer (GMT), and the error bars indicate the 95% CI. Statistical analysis: Wilcoxon rank sum test and Mann–Whitney test.

above the median of a panel of controls who had donated convalescent serum (8, 27). As for the Pfizer BNT162b2 mRNA vaccine, one of the few studies comprising older adults (≥80 years old) showed a suboptimal neutralizing antibody response and reduced T cell count following the first dose (28). A second study reported that BNT162b2 elicited relatively lower antibody levels in adults over 50 years old vs younger adults (29). Lastly, responses among Chinese patients aged 18–55 and 65–85 showed similar IgG and somewhat lower neutralizing antibody and a more variable T cell response than younger individuals (30). T cell and antibody immune responses of the elderly groups after mRNA or adenovirus vector vaccines were thus found to be largely similar to those of younger individuals, which is in contrast with observations in our group of inactivated virus based CoronaVac vaccinated individuals. To our knowledge. this is the first report showing T-cell responses after vaccination with Coronavac with a significant group of older individuals. In our study, we used a whole blood IFN-γ and IL-2 release assay, while the cited studies used ELISPOT and flow cytometry analysis. Although ELISPOT could be considered more sensitive than the whole blood-based cytokine release assay used here, CRA has been shown to accurately assess cellular immunity to SARS-CoV-2 and vaccination (31–34). Of note, Tan et al. (35) performed a direct comparison between ELISPOT and CRA and found the sensitivity of the two methods are comparable with a strong positive correlation with each other. In addition, IgG antibody and VNT assays were similar to those used in the previous studies, and our results showed lower percentages among

elderly individuals—especially in the male sex. This is especially relevant given the finding that CoronaVac vaccinated individuals were also shown to have significantly reduced neutralizing capacity against VOCs alpha, beta, and delta (1). The main VOCs circulating in Brazil at the time of sampling were gamma and alpha (36).

Our cluster analysis showed a difference in immune responses between older and younger of 55 years of age, which is not a common cutoff of age for comparison used in other studies. It shows that lower immune responses were detectable for people younger than 60 years and indicates that waning immunity could be just a matter of time after vaccination for these people. A nationwide evaluation of vaccine effectiveness comprising 25,752,013 Brazilians vaccinated with CoronaVac showed a reduced protection against hospitalization, ICU admission and death in individuals older than 79 years of age (67.2%), decreasing to 33.6% in individuals above 90 years ≥14 days after the 2nd dose. Sixty days after vaccination, there was an increase in the hospitalization rate in individuals >80 years old, indicating waning immunity and an eventual need for a booster dose for the elderly population (37).

Despite the important insight on the immunogenicity of CoronaVac, our study had limitations. The sample sizes were limited, and comorbidities were not considered for analysis in any group. Only 82% of participants had serum samples available for viral neutralization assay. Vaccinated individuals were included based on self-reporting no previous infection, but no basal antibody levels or SARS-CoV-2 RT-PCR were performed upon inclusion.

In summary, our results show a lower overall immune response for people older than 55 years after two-dose immunization with inactivated vaccine CoronaVac. In general, vaccinated subjects presented VNTs lower than convalescents for Wuhan strain and vaccination conferred lower VNTs against gamma VOC compared to Wuhan strain. Given the finding that mixing vaccines with different platforms may elicit stronger immunogenicity (38), our results corroborate the recommendation of the Brazilian Ministry of Health for a heterologous third dose/booster vaccine for elderly individuals vaccinated with CoronaVac.

DATA AVAILABILITY STATEMENT

The datasets presented in this study can be found in online repositories. The names of the repository/repositories and accession number(s) can be found in the article/**Supplementary Material**.

ETHICS STATEMENT

The studies involving human participants were reviewed and approved by the Ethics Committee of the Hospital das Clínicas da Universidade de São Paulo (CAPPesq 79 CAAE30155220.3.0000.0068). The patients/participants provided their written informed consent to participate in this study.

AUTHOR CONTRIBUTIONS

Study design, data analysis, and critical review: SBB, VC, JK, KSS, and ECN. Data analysis and critical review: MAF. Data collection, data analysis, and critical review: GXM, GLS, JYM, FRB, JPSN, RRA, GPS, EDC, FBL, DBLO, ELD, RCVS, DSR. All authors listed have made a substantial, direct, and intellectual contribution to the work and approved it for publication.

SUPPLEMENTARY MATERIAL

The Supplementary Material for this article can be found online at: https://www.frontiersin.org/articles/10.3389/fimmu.2022.812126/full#supplementary-material

Supplementary Figure 1 | Receiver Operator Characteristic (ROC) curve used to establish the age threshold that could distinguish the two resulting clusters with the highest accuracy.

Supplementary Figure 2 | Correlations between time post symptom onset and immunological parameters among convalescent individuals. **(A)** Correlation between time post symptom onset and T-cell responses: IFN-γ and IL-2 released after whole blood stimulation. **(B)** Correlation between time post symptom onset and humoral responses: IgG for Spike, RBD or NP protein.

Supplementary Figure 3 | Correlations between time post 2nd dose of CoronaVac and immunological parameters among vaccinated individuals. **(A)** Correlation between time post symptom onset and T-cell responses: IFN-γ and IL-2 released after whole blood stimulation. **(B)** Correlation between time post symptom onset and viral neutralization of original Wuhan strain. **(C)** Correlation between time post symptom onset and humoral responses: IgG for RBD, Spike or NP protein.

REFERENCES

1. Vacharathit V, Aiewsakun P, Manopwisedjaroen S, Srisaowakarn C, Laopanupong T, Ludowyke N, et al. CoronaVac Induces Lower Neutralising Activity Against Variants of Concern Than Natural Infection. *Lancet Infect Dis* (2021) 21(10):1352–4. doi: 10.1016/S1473-3099(21)00568-5. Elsevier Ltd.

2. Victora PC, Castro PMC, Gurzenda S, Medeiros AC, França GVA, Barros PAJD. Estimating the Early Impact of Vaccination Against COVID-19 on Deaths Among Elderly People in Brazil: Analyses of Routinely-Collected Data on Vaccine Coverage and Mortality. *EClinicalMedicine* (2021) 38:1–6. doi: 10.1016/j.eclinm.2021.101036

3. Alencar CH, de G Cavalcanti LP, de Almeida MM, Barbosa PPL, de S Cavalcante KK, de Melo DN, et al. High Effectiveness of SARS-CoV-2 Vaccines in Reducing COVID-19-Related Deaths in Over 75-Year-Olds, Ceará State, Brazil. *Trop Med Infect Dis* (2021) 6(3):129. doi: 10.3390/tropicalmed6030129

4. Ranzani OT, Hitchings M, Dorion Nieto M, D'Agostini TL, De Paula RC, De Paula OFP, et al. Effectiveness of the CoronaVac Vaccine in the Elderly Population During a P.1 Variant-Associated Epidemic of COVID-19 in Brazil: A Test-Negative Case-Control Study. *BMJ* (2021) 374(2015):1–12. doi: 10.1136/bmj.n2015

5. Bajaj V, Gadi N, Spihlman AP, Wu SC, Choi CH, Moulton VR. Aging, Immunity, and COVID-19: How Age Influences the Host Immune Response to Coronavirus Infections? *Front Physiol* (2021) 11:1–23. doi: 10.3389/fphys.2020.571416

6. Seyahi E, Bakhdiyarli G, Oztas M, Kuskucu MA, Tok Y, Sun N, et al. Antibody Response to Inactivated COVID-19 Vaccine (CoronaVac) in Immune-Mediated Diseases: A Controlled Study Among Hospital Workers and Elderly. *Rheumatol Int* (2021) 41(8):1429–40. doi: 10.1007/s00296-021-04910-7

7. Haq K, McElhaney JE. Immunosenescence: Influenza Vaccination and the Elderly. *Curr Opin Immunol* (2014) 29(1):38–42. doi: 10.1016/j.coi.2014.03.008

8. Anderson EJ, Rouphael NG, Widge AT, Jackson LA, Roberts PC, Makhene M, et al. Safety and Immunogenicity of SARS-CoV-2 mRNA-1273 Vaccine in Older Adults. *N Engl J Med* (2020) 383(25):2427–38. doi: 10.1056/NEJMoa2028436

9. McElhaney JE, Beran J, Devaster JM, Esen M, Launay O, Leroux-Roels G, et al. AS03-Adjuvanted Versus Non-Adjuvanted Inactivated Trivalent Influenza Vaccine Against Seasonal Influenza in Elderly People: A Phase 3 Randomised Trial. *Lancet Infect Dis* (2013) 13(6):485–96. doi: 10.1016/S1473-3099(13)70046-X

10. Bueno SM, Abarca K, González PA, Gálvez NMS, Soto JA, Duarte LF, et al. Safety and Immunogenicity of an Inactivated Severe Acute Respiratory Syndrome Coronavirus 2 Vaccine in a Subgroup of Healthy Adults in Chile. *Clin Infect Dis* (2021) (Xx Xxxx):1–13.

11. Marshall JC, Murthy S, Diaz J, Adhikari N, Angus DC, Arabi YM, et al. A Minimal Common Outcome Measure Set for COVID-19 Clinical Research. *Lancet Infect Dis* (2020) 20(8):e192–7. doi: 10.1016/S1473-3099(20)30483-7

12. Oliveira JR, Machado RRG, Arcuri HA, Magawa JY, Daher IP, Urbanski AH, et al. Immunodominant B Cell Epitope in a Hotspot Mutation Site and Mechanism of Immune Escape for SARS-CoV-2. *medRxiv* (2021) 0–17. doi: 10.1101/2021.03.11.21253399

13. Wendel S, Kutner JM, Machado R, Fontão-Wendel R, Bub C, Fachini R, et al. Screening for SARS-CoV-2 Antibodies in Convalescent Plasma in Brazil: Preliminary Lessons From a Voluntary Convalescent Donor Program. *Transfusion* (2020) 60(12):2938–51. doi: 10.1111/trf.16065

14. Araujo DB, Machado RRG, Amgarten DE, Malta F de M, de Araujo GG, Monteiro CO, et al. SARS-CoV-2 Isolation From the First Reported Patients in Brazil and Establishment of a Coordinated Task Network. *Mem Inst Oswaldo Cruz* (2020) 115(12):1–8. doi: 10.1590/0074-02760200342

15. Fonseca SG, Coutinho-Silva A, Fonseca LAM, Segurado AC, Moraes SL, Rodrigues H, et al. Identification of Novel Consensus CD4 T-Cell Epitopes From Clade B HIV-1 Whole Genome That Are Frequently Recognized by HIV-1 Infected Patients. *Aids* (2006) 20(18):2263–73. doi: 10.1097/01.aids.0000253353.48331.5f

16. Hartigan JA, Wong MA. Algorithm AS 136 A K-Means Clustering Algorithm. *J R Stat Soc Ser B Methodol* (2012) 28(1):100–8.

17. Ni L, Ye F, Cheng M-L, Qin C-F, Chen F, Dong C. Detection of SARS-CoV-2-Specific Humoral and Cellular Immunity in COVID-19 Convalescent Individuals. *Immunity* (2020) 52(6):971–7. doi: 10.1016/j.immuni.2020.04.023

18. Dhume K, McKinstry KK. Early Programming and Late-Acting Checkpoints Governing the Development of CD4 T-Cell Memory. *Immunology* (2018) 155(1):53–62. doi: 10.1111/imm.12942

19. Ansari A, Arya R, Sachan S, Jha SN, Kalia A, Lall A, et al. Immune Memory in Mild COVID-19 Patients and Unexposed Donors Reveals Persistent T Cell Responses After SARS-CoV-2 Infection. *Front Immunol* (2021) 12:1–11. doi: 10.3389/fimmu.2021.636768

20. Peckham H, de Gruijter NM, Raine C, Radziszewska A, Ciurtin C, Wedderburn LR, et al. Male Sex Identified by Global COVID-19 Meta-Analysis as a Risk Factor for Death and ITU Admission. *Nat Commun* (2020) 11(1):1–10. doi: 10.1038/s41467-020-19741-6

21. Fish EN. The X-Files in Immunity: Sex-Based Differences Predispose Immune Responses. *Nat Rev Immunol* (2008) 8:737–44. doi: 10.1038/nri2394

22. Flanagan KL, Fink AL, Plebanski M, Klein SL. Sex and Gender Differences in the Outcomes of Vaccination Over the Life Course. *Annu Rev Cell Dev Biol* (2017) 33:577–99. doi: 10.1146/annurev-cellbio-100616-060718

23. Crooke SN, Ovsyannikova IG, Poland GA, Kennedy RB. Immunosenescence and Human Vaccine Immune Responses. *Immun Ageing Immun Ageing;* (2019) 16(1):1–16. doi: 10.1186/s12979-019-0164-9

24. Goodwin K, Viboud C, Simonsen L. Antibody Response to Influenza Vaccination in the Elderly: A Quantitative Review. *Vaccine* (2006) 24(8):1159–69. doi: 10.1016/j.vaccine.2005.08.105

25. Ramasamy MN, Minassian AM, Ewer KJ, Flaxman AL, Folegatti PM, Owens DR, et al. Safety and Immunogenicity of ChAdOx1 Ncov-19 Vaccine Administered in a Prime-Boost Regimen in Young and Old Adults (COV002): A Single-Blind, Randomised, Controlled, Phase 2/3 Trial. *Lancet* (2020) 396(10267):1979–93. doi: 10.1016/S0140-6736(20)32466-1

26. Swanson PA, Padilla M, Hoyland W, McGlinchey K, Fields PA, Bibi S, et al. T-Cell Mediated Immunity After AZD1222 Vaccination: A Polyfunctional Spike-Specific Th1 Response With a Diverse TCR Repertoire. *Sci Transl Med* (2021) 13(620):1–15. doi: 10.1126/scitranslmed.abj7211

27. Jackson LA, Anderson EJ, Rouphael NG, Roberts PC, Makhene M, Coler RN, et al. An mRNA Vaccine Against SARS-CoV-2 — Preliminary Report. *N Engl J Med* (2020) 383(20):1920–31. doi: 10.1056/NEJMoa2022483

28. Collier DA, Ferreira IATM, Kotagiri P, Datir R, Lim E, Touizer E, et al. Age-Related Immune Response Heterogeneity to SARS-CoV-2 Vaccine BNT162b2. *Nature* (2021) 596:417–22. doi: 10.1101/2021.02.03.21251054

29. Richards NE, Keshavarz B, Workman LJ, Nelson MR, Platts-Mills TAE, Wilson JM. Comparison of SARS-CoV-2 Antibody Response by Age Among Recipients of the BNT162b2 vs the mRNA-1273 Vaccine. *JAMA Netw Open* (2021) 4(9):8–11. doi: 10.1001/jamanetworkopen.2021.24331

30. Li J, Hui A, Zhang X, Yang Y, Tang R, Ye H, et al. Safety and Immunogenicity of the SARS-CoV-2 BNT162b1 mRNA Vaccine in Younger and Older Chinese Adults: A Randomized, Placebo-Controlled, Double-Blind Phase 1 Study. *Nat Med* (2021) 27(6):1062–70. doi: 10.1038/s41591-021-01330-9

31. Brand I, Gilberg L, Bruger J, Garí M, Wieser A, Eser TM, et al. Broad T Cell Targeting of Structural Proteins After SARS-CoV-2 Infection: High Throughput Assessment of T Cell Reactivity Using an Automated Interferon Gamma Release Assay. *Front Immunol* (2021) 12:1–10. doi: 10.3389/fimmu.2021.688436

32. Fernández-González M, Agulló V, Padilla S, García JA, García-Abellán J, Botella Á, et al. Clinical Performance of a Standardized SARS-CoV-2 Interferon-γ Release Assay for Simple Detection of T-Cell Responses After Infection or Vaccination. *Clin Infect Dis* (2021) 1–12. doi: 10.1093/cid/ciab1021

33. Murugesan K, Jagannathan P, Pham TD, Pandey S, Bonilla HF, Jacobson K, et al. Interferon-γRelease Assay for Accurate Detection of Severe Acute Respiratory Syndrome Coronavirus 2 T-Cell Response. *Clin Infect Dis* (2021) 73(9):E3130–2. doi: 10.1093/cid/ciaa1537

34. Aiello A, Naja S, Petruccioli E, Petrone L, Vanini V, Farroni C, et al. Spike Is the Most Recognized Antigen in the Whole-Blood Platform in Both Acute and Convalescent COVID-19 Patients. *Int J Infect Dis* (2021) 106:338–47. doi: 10.1016/j.ijid.2021.04.034

35. Tan AT, Lim JME, Le Bert N, Kunasegaran K, Chia A, Qui MDC, et al. Rapid Measurement of SARS-Cov-2 Spike T Cells in Whole Blood From Vaccinated and Naturally Infected Individuals. *J Clin Invest* (2021) 131(17):e152379. doi: 10.1172/JCI152379

36. Fiocruz. *GISAID: Linhagens do SARS-CoV-2 Em Circulação*. (2021). pp. 1–6. Available from: http://www.genomahcov.fiocruz.br/gisaid/.

37. Cerqueira-Silva T, Oliveira V de A, Pescarini J, Pescarini JM, Júnior JB, Machado TM, et al. Influence of Age on the Effectiveness and Duration of Protection of Vaxzevria and CoronaVac Vaccines. *Lancet Reg Health Am* (2021) 6:1–11. doi: 10.1016/j.lana.2021.100154

38. Deming ME, Lyke KE. A 'Mix and Match' Approach to SARS-CoV-2 Vaccination. *Nat Med* (2021) 27:1510–1. doi: 10.1038/s41591-021-01463-x

Follow-up of young adult monozygotic twins after simultaneous critical coronavirus disease 2019: a case report

Mateus V. de Castro[1†], Monize V. R. Silva[1†], Flávia B. Soares[1,2†], Vivian R. Cória[1], Michel S. Naslavsky[1,2], Marilia O. Scliar[1,2], Erick C. Castelli[3], Jamile R. de Oliveira[4,5], Giuliana X. de Medeiros[4,5], Greyce L. Sasahara[5], Keity S. Santos[4,5,6], Edecio Cunha-Neto[4,5,6], Jorge Kalil[4,5,6] and Mayana Zatz[1,2]*

[1]Human Genome and Stem Cell Research Center, University of São Paulo, São Paulo, Brazil, [2]Department of Genetics and Evolutionary Biology, Biosciences Institute, University of São Paulo, São Paulo, Brazil, [3]Molecular Genetics and Bioinformatics Laboratory, Experimental Research Unit (Unipex), School of Medicine, São Paulo State University (UNESP), Botucatu, Brazil, [4]Departamento de Clínica Médica, Disciplina de Alergia e Imunologia Clínica, Faculdade de Medicina da Universidade de São Paulo, São Paulo, Brazil, [5]Laboratório de Imunologia, Instituto do Coração (InCor), LIM 19, Hospital das Clínicas da Faculdade de Medicina da Universidade de São Paulo, (HCFMUSP), São Paulo, Brazil, [6]Instituto de Investigação em Imunologia—Instituto Nacional de Ciências e Tecnologia-iii-INCT, São Paulo, Brazil

Background: The influence of the host genome on coronavirus disease 2019 (COVID-19) susceptibility and severity is supported by reports on monozygotic (MZ) twins where both were infected simultaneously with similar disease outcomes, including several who died due to the SARS-CoV-2 infection within days apart. However, successive exposures to pathogens throughout life along with other environmental factors make the immune response unique for each individual, even among MZ twins.

Case presentation and methods: Here we report a case of a young adult monozygotic twin pair, who caught attention since both presented simultaneously severe COVID-19 with the need for oxygen support despite age and good health conditions. One of the twins, who spent more time hospitalized, reported symptoms of long-COVID even 7 months after infection. Immune cell profile and specific responses to SARS-CoV-2 were evaluated as well as whole exome sequencing.

Conclusion: Although the MZ twin brothers shared the same genetic mutations which may be associated with their increased risk of developing severe COVID-19, their clinical progression was different, reinforcing the

role of both immune response and genetics in the COVID-19 presentation and course. Besides, post-COVID syndrome was observed in one of them, corroborating an association between the duration of hospitalization and the occurrence of long-COVID symptoms.

Introduction

The ongoing global pandemic of coronavirus disease 2019 (COVID-19) caused by the SARS-CoV-2 virus has already affected the health of millions of people worldwide, with a significant number of deaths [1]. Although older patients and those with comorbidities who are infected are more subject to unfavorable outcomes, reports of young people without chronic diseases who died from COVID-19 support the existence of genetic and immunological risk factors [2, 3]. Also, several reports of identical twins deceased due to COVID-19 within days apart give further support to the influence of the host genome on COVID-19.

The first worldwide case of death from COVID-19, within 3 days apart, in one pair of adult unvaccinated MZ was reported in April 2020 in the United Kingdom. Aged 37, both twin sisters worked as nurses and had the same underlying health condition. Recently (2022), France's famous twin Bogdanoff's brothers died of COVID-19 6 days apart. Aged 72, the brothers had not been vaccinated against COVID-19 either.

The identification of genetic variants related to immune response, associated with higher susceptibility to the infection or severe COVID-19 has been the focus of numerous studies around the world [2, 4–8]. Currently, genome-wide association studies (GWAS) have identified some genetic variants, including rare loss-of-function variants in genes involved in type I interferon (IFN) pathways [3, 9, 10] or missense variants that affect the activity of transmembrane serine protease 2 [3, 11, 12], that contribute to susceptibility or severe COVID-19, respectively. Here, we investigated a case of simultaneous critical COVID-19 in young adult MZ brothers in 2021, before being vaccinated. We present a comprehensive assessment of their innate and adaptive immunity, genetic profiling, and systemic biomarkers.

Case presentation

In June 2021, a 31-year-old Brazilian monozygotic twin brother pair (ID 01 and ID 02) started with cough and fever on the 26th. Both tested positive for SARS-CoV-2 infection on June 29th. During the following days symptoms worsened with dyspnea. From June 30th to July 4th, azithromycin was used.

Blood oxygen saturation reached a critical level of 80% and the twin brothers were admitted directly to the intensive care unit on July 8th. They were intubated due to pulmonary involvement and were extubated after 5 days of mechanical ventilation (July 13th). The Gamma variant was the only SARS-CoV-2 variant identified in the region at the end of June 2021 [13] and it is known that this variant was associated with increased mortality risk and severity of COVID-19 cases in younger age groups, particularly in the unvaccinated population at the time [14]. The twins received the same supportive ICU measures (sedation and proning). Also, at the hospital, both twins received the same treatment: dexamethasone (from July 9th to July 19th), to inhibit inflammation in the lungs. Due to detected resistant bacterial infections in both twins after extubation, they were treated with meropenem (from July 13th to July 20th). ID 01 was discharged on the 22nd of July and ID 02 7 days later. Both required respiratory physiotherapy for at least 3 months after hospital discharge. Seven months after the COVID-19 episode, ID 02 complained of persistent muscle fatigue, commonly associated with the post-COVID syndrome. The twins lived apart but worked at the same company as realtors. They did not have any known health conditions or comorbidities. The entire timeline of main events is presented in **Figure 1**.

Blood samples from the twins were collected in February 2022 (7 months after COVID-19 diagnosis and 4 months after getting a second dose of Pfizer-BioNTech COVID-19 vaccine) at our Research Center (HUG-CELL) for global immune profiling and genetic investigation. Peripheral blood mononuclear cells (PBMCs), plasma, and serum were obtained to perform the immunological assays and DNA for whole-exome sequencing (WES). Complementary clinical laboratory analyses were also performed in whole blood samples.

Surface immunophenotyping of PBMC was performed by flow cytometry (**Table 1**). The twins displayed normal frequencies of CD3+, CD4+, and CD8+ T-cells, monocytes, NK cells, and lymphocytes B as expected in healthy donors [15]. The type I/III IFN production by PBMCs after toll-like receptor (TLR) stimulus (double-stranded RNA Poly I:C), was evaluated for 1, 4, and 8 h. Although there was heterogeneity in IFN or IFN-induced gene expression, the twins presented an early and strong (FC = 20 or higher) mRNA expression of at least two of the five types of I/III IFN analyzed. Thus, no failure in the innate IFN

FIGURE 1
Clinical timeline of the major events of the twins' case.
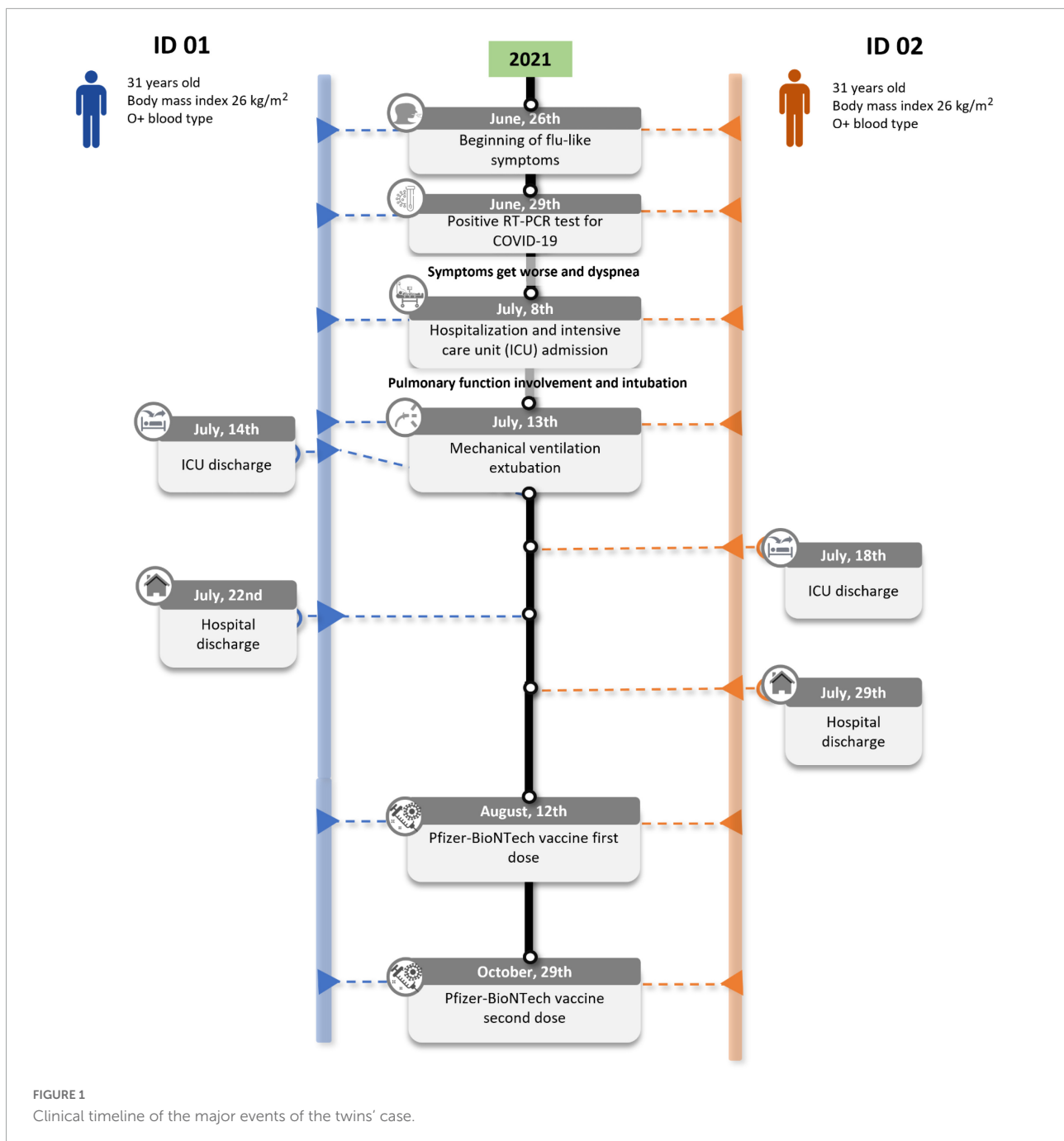
response was observed. The production of interferon-gamma (IFN-γ) and interleukin-2 (IL-2) by PBMC, after stimulation by SARS-CoV-2 peptides, was also evaluated. Similar results were observed in both twins, for CD4 + T lymphocyte responses. ELISA serological assays were performed for SARS-CoV-2 IgA, IgG, and IgM for the receptor-binding domain (RBD) and nucleocapsid protein (NP) to assess their humoral immune response. The antibody profiles of SARS-CoV-2 IgA, IgM, and IgG were virtually identical between the MZ twin brothers.

The global immune profiling of the twins is presented in Figure 2.

Hematologic and systemic parameters of the post-COVID phase (Table 2) revealed great similarity between the MZ twins, except for a very slight increase in creatine phosphokinase (an enzyme specific to muscle tissues, which may increase after muscle injuries) and ferritin (an acute phase reactant that can increase its serum concentration during inflammation), presented by ID 02. These findings might be related to the fatigue reported only by this twin. Likewise, both presented mild

TABLE 1 PBMCs immunophenotyping of the twin volunteers, 7 months after COVID-19 episode.

ID	CD3 + T-cells	CD4 + T-cells	CD8 + T-cells	Monocytes	NK cells	B-cells
01	56.2	63.5	31.1	7.7	8.9	9.3
02	57.5	57.7	35.3	8.0	8.8	7.7
Healthy*	45–70	25–60	5–30	10–30	5–10	5–15

*Reference parameters values for individuals in the same age range (15).

FIGURE 2

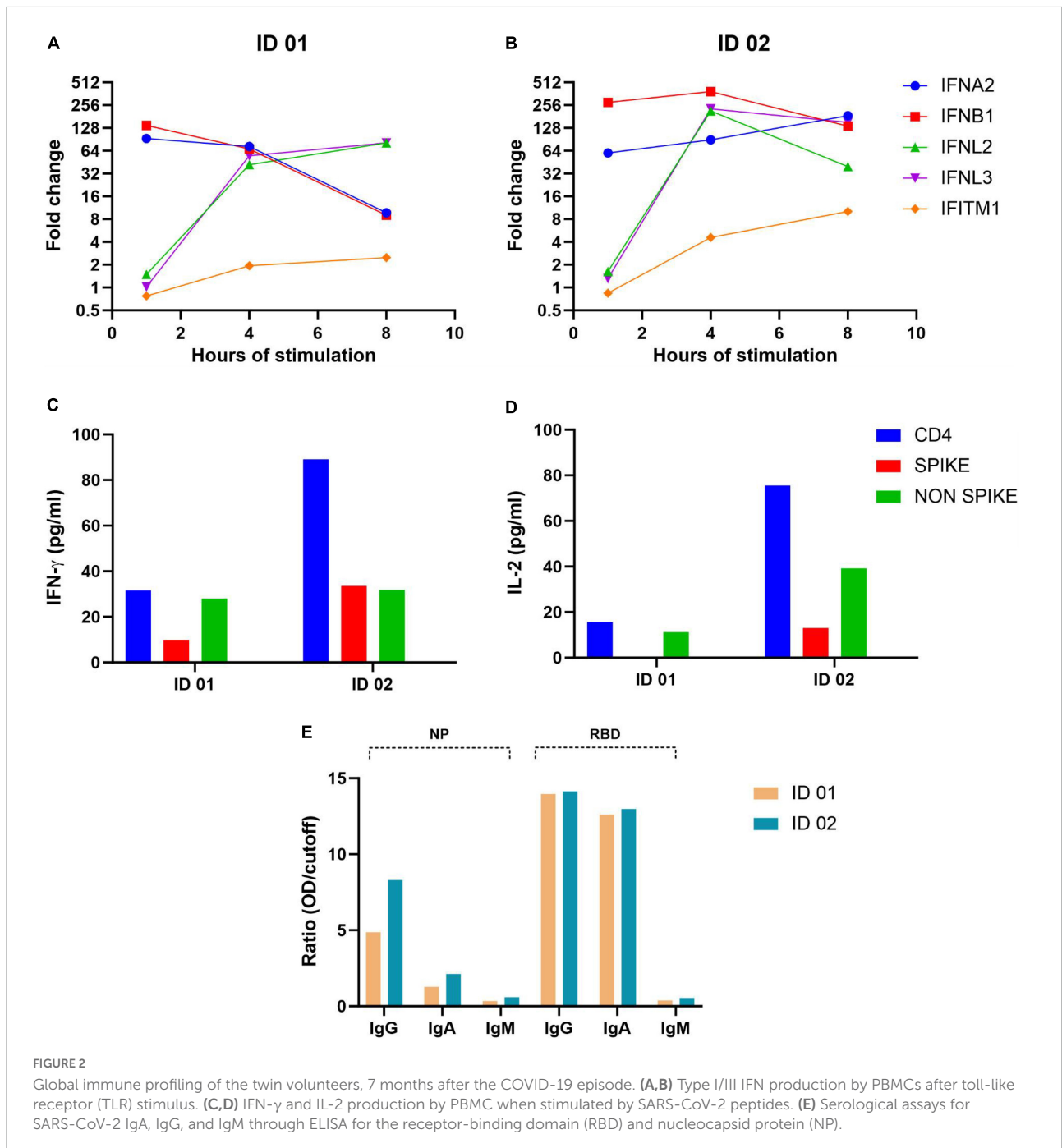Global immune profiling of the twin volunteers, 7 months after the COVID-19 episode. **(A,B)** Type I/III IFN production by PBMCs after toll-like receptor (TLR) stimulus. **(C,D)** IFN-γ and IL-2 production by PBMC when stimulated by SARS-CoV-2 peptides. **(E)** Serological assays for SARS-CoV-2 IgA, IgG, and IgM through ELISA for the receptor-binding domain (RBD) and nucleocapsid protein (NP).

TABLE 2   Blood test parameters of the volunteers, 7 months after the COVID-19 episode.

Variables	ID 01	ID 02	Reference values
Erythrogram			
Erythrocyte/red blood cell (RBC) count (millions/mm^3)	4.64	4.57	4.30–5.70
Hemoglobin concentration (g/dL)	14.8	14.1	13.5–17.5
Hematocrit (%)	42.0	42.0	39.0–50.0
Mean cell/corpuscular volume—MCV (μ^3)	90.5	91.9	81.2–95.1
Mean cell hemoglobin—MCH (%)	31.9	30.9	26.0–34.0
Mean cell hemoglobin concentration—MCHC (pg)	35.2	33.6	31.0–36.0
RBC distribution width—RDW (%)	11.6	11.3	8.0–15.5
Erythrocyte sedimentation rate—ESR (mm/1 h)	**12**	**18**	0–6
Leukogram			
Leukocyte/white blood cell (WBC) count/mm^3	4,310	4,840	3,500–10,500
Neutrophil count/mm^3	2,030.01	2,574.88	1,700.00–8,400.00
Eosinophil count/mm^3	349.11	208.12	50.00–420.00
Basophil count/mm^3	60.34	48.40	0.00–105.00
Lymphocyte count/mm^3	1,560.22	1,669.80	900.00–3,150.00
Monocyte count/mm^3	310.32	338.80	140.00–1,260.00
Coagulation parameters			
Platelet count/mm^3	311,000	304,000	140,000–400,000
Prothrombin time (s)	10.2	10.6	9.6–12.0
Activated partial thromboplastin time—APTT (s)	32.5	32.1	22.7–32.5
D dimer (μg/mL)	0.15	0.17	0–0.50
Homeostasis parameters			
C-reactive protein—CRP (mg/dL)	0.12	0.14	0–0.60
Ferritin (ng/mL)	331.0	**512.1**	25.0–400.0
Lactate dehydrogenase—LDH (U/L)	193	198	0–250
Parameters of tissues' functions			
B-type natriuretic peptide–BNP (pg/mL)	<5	<5	<100
Troponin T (ng/mL)	<0.003	0.003	0.000–0.030 (negative)
Creatine phosphokinase—CPK (U/L)	186	**211**	0–190
Glutamic-oxaloacetic transaminase—GOT (U/L)	34	28	0–50
Glutamic pyruvic transaminase—GPT (U/L)	47	33	0–50
Urea (mg/dL)	27	28	10–50
Creatinine (mg/dL)	0.8	0.9	0.7–1.2

The parameters out of the reference values were highlighted in red.

changes in erythrocyte sedimentation rate, a parameter that may be increased in different inflammatory conditions.

WES was performed in peripheral blood DNA with the Illumina NovaSeq platform at HUG-CELL facilities. The identical twins do not carry any rare variants in genes associated with inborn errors (IE) of Toll-like receptor 3 (TLR3) and IFN regulatory factor 7 (IRF7) dependent type I IFN immunity, which underlies life-threatening COVID-19 pneumonia (5, 16). Also, we did not detect any copy number variation (CNV) in IE genes. The Neanderthal-derived genetic variant rs35044562 (17) was not detected in the twins. However, we detected two rare missense variants (with a mean CADD score > 20), one in the *BTK* gene (NM_000061:exon8:c.G684A:p.M228I) carried in homozygosity and one in the *NFKB2* gene (NM_002502:exon22:c.T2531C:p.V844A) carried in the heterozygous state, which may be linked to their increased risk of developing severe COVID-19. In addition, we analyzed

the genotypes and haplotypes (Supplementary Table 1) of the HLA cluster in the MHC region by using a hla-mapper (version 4) (18) to optimize read alignment along the MHC region. Interestingly, the twins present the alleles HLA-A*02:01 and HLA-E*01:01 (both carried in the heterozygous state), which were associated with the high severity of COVID-19.

Discussion

Twin studies are important to investigate the contribution of genetics vs. the environment, in the susceptibility or resistance to infectious diseases as well as their pathomechanisms. Moreover, the study of the monozygotic ones may represent a powerful approach to further explore the immunological factors that contributed to the host defense. Beyond the host genotype, the individual immune response plays a determining role in

the success or failure against SARS-CoV-2 (15). The immune repertoire which is also somatically defined by mutations occurring at later stages of development could justify different disease courses, and/or outcomes even in monozygotic twins (19, 20).

The genetic causes responsible for the clinical variability associated with COVID-19 remain the subject of investigation. Worldwide genomic studies of large cohorts of individuals with different clinical manifestations have been published, suggesting the involvement of different genetic variants responsible for greater susceptibility or resistance to SARS-CoV-2. GWAS identified a potential effect of variants in the *SLC6A20*, *LZTFL1*, *CCR9*, *FYCO1*, *CXCR6,* and *XCR1* genes as responsible for greater susceptibility to SARS-CoV-2 (2, 19) in addition to variants in the genes *REXO2*, *C11orf71*, *NNMT,* and *CADM1*, involved in the immune response (21). Additionally, variants in many genes involved with the innate immune response seem to be involved in the susceptibility/predisposition to severe cases of COVID-19 such as those involved in the IFN and TLRs pathways, as well as the *ACE2* and *TMPRSS2* genes involved in virus entry into the cell (3, 7, 22). Variants in the genes *IL1B, IL1R1, IL1RN, IL6, IL17A, FCGR2A*, and *TNF* which encode cytokines would also have a possible relation with disease susceptibility and cytokine storm development. The Human Leukocyte Antigen (HLA) gene cluster and genes associated with the Major Histocompatibility Complex (MHC) are important candidates for the mechanisms of innate and adaptive immunity and susceptibility to COVID-19 infection and manifestation (23).

Interestingly the identified heterozygous *NFKB1* missense variant (NM_002502:exon22:c.T2531C:p.V844AI) and the hemizygous missense variant in the *BTK* gene (NM_000061:exon8:c.G684A:p.M228I) are the central hubs that connect proinflammatory signaling pathways for survival, proliferation, cytokine production, and lymphocyte development. Interestingly, variants in both genes have been reported in primary antibody immunodeficiencies (24, 25). However, since these variants were not studied at the protein or functional level, their pathogenicity is yet to be determined. Genetic variant in chromosome 3, previously associated with high severity cases of COVID-19 and inherited from Neanderthals (rs35044563), was not detected in both volunteers (17). Regarding the HLA complex, the twins present the alleles HLA-A*02:01 and HLA-E*01:01 (both carried in the heterozygous state), which were associated with high severity of COVID-19 (13).

The global immune profiling assays, after 7 months of the COVID-19 episode, revealed great similarities between the MZ twins. It is known that the failure to elicit a strong type I IFN response contributes to severe COVID-19 (14). Infections trigger massive T cell expansion, leading to the skewing of the TCR repertoire due to antigen−specific T cell expansion. A low clonotype sharing between MZ twins with

rheumatoid arthritis that were mismatched for SARS-CoV-2 infection suggests an immune repertoire reshaping might be induced after COVID-19 (26). However, clonality and alterations of T-cell receptors' repertoires were partly associated with immune activation mediated by IFN type I and III (27) and here both twins displayed early and strong I/III IFN responses. The production of cytokines IFN-γ and IL-2 by T lymphocytes, when stimulated by SARS-CoV-2 peptides, was expressive. IL-2 and IFN-γ, which play a critical role in the activation of macrophages and other immune cells related to viral clearance, were found to be specific biomarkers of SARS-CoV-2 cellular response (28). The virus-specific antibody responses showed a vigorous IgA and IgG similar response in both twins. Since these analyses were done post-vaccination, it is not clear whether it was the viral infection or the vaccines that stimulated the production of these antibodies but it is clear there is no deficient humoral response. Taken together, regarding the immune response, all parameters analyzed were practically identical among the MZ twins.

Although both twins required intensive care and mechanical ventilation for 5 days, ID 02 required longer hospitalization and presented long-term symptoms consistent with long COVID. After 7 months of follow-up, twin ID 02 reported persistent muscle weakness and fatigue, while twin ID 01 referred to a return to his usual state of health. Muscle dysfunction (intense fatigue) is among the most reported symptoms of the post-COVID syndrome (17). The laboratory values obtained at 7 months demonstrated that twin ID 02 had an elevation in ferritin and CPK but otherwise had similar hematological and functional parameters relative to twin ID 01. Importantly, the twins were not on any medications or supplements. The CK levels at admission are reported to be higher in those subjects who later experience more severe outcomes and were associated with a worse prognosis (20) while severe to critical COVID-19 patients showed higher ferritin levels compared to mild to moderate COVID-19 patients (29). Thus, the slightly abnormal ferritin and CPK from ID 02 even after 7 months post-hospitalization might play a role in the pathogenesis of post-acute sequelae of COVID-19.

Conclusion

This case study on two young-adult monozygotic twins simultaneously infected with SARS-CoV-2, both requiring ICU care but with different periods of clinical progression suggests the contribution of both immune response and the genetics in the COVID-19 presentation and course. Besides, the post-COVID syndrome was observed in one of them, corroborating an association between the duration of hospitalization and the occurrence of long-COVID symptoms.

Data availability statement

The original contributions presented in this study are included in the article/**Supplementary material**, further inquiries can be directed to the corresponding author.

Ethics statement

The studies involving human participants were reviewed and approved by CAAE 34786620.2.0000.5464. The patients/participants provided their written informed consent to participate in this study. Written informed consent was obtained from the individual(s) for the publication of any potentially identifiable images or data included in this article.

Author contributions

MC and MVRS: data curation, investigation, formal analysis, visualization, and writing—original draft. FS: data curation and investigation. VC and EC-N: writing—review and editing. MN: conceptualization, formal analysis, investigation, methodology, software, and writing—review and editing. MOS and EC: formal analysis, investigation, methodology, software, and writing—review and editing. JO and GS: methodology and writing—review and editing. KS: investigation, visualization, and writing—review and editing. JK: funding acquisition, resources, and writing—review and editing. MZ: conceptualization, funding acquisition, project administration, writing—original draft, and writing—review and editing. All authors contributed to the article and approved the submitted version.

Conflict of interest

The authors declare that the research was conducted in the absence of any commercial or financial relationships that could be construed as a potential conflict of interest.

Publisher's note

All claims expressed in this article are solely those of the authors and do not necessarily represent those of their affiliated organizations, or those of the publisher, the editors and the reviewers. Any product that may be evaluated in this article, or claim that may be made by its manufacturer, is not guaranteed or endorsed by the publisher.

Supplementary material

The Supplementary Material for this article can be found online at: https://www.frontiersin.org/articles/10.3389/fmed.2022.1008585/full#supplementary-material

References

1. World Health Organization. *WHO coronavirus (COVID-19) dashboard*. Geneva: World Health Organization (2022).

2. Fricke-Galindo I, Falfán-Valencia R. Genetics insight for COVID-19 susceptibility and severity: A review. *Front Immunol.* (2021) 12:622176. doi: 10.3389/fimmu.2021.622176

3. Velavan TP, Pallerla SR, Rüter J, Augustin Y, Kremsner PG, Krishna S, et al. Host genetic factors determining COVID-19 susceptibility and severity. *EBioMedicine.* (2021) 72:103629. doi: 10.1016/j.ebiom.2021.103629

4. Bastard P, Rosen LB, Zhang Q, Michailidis E, Hoffmann HH, Zhang Y, et al. Autoantibodies against type I IFNs in patients with life-threatening COVID-19. *Science.* (2020) 370:eabd4585.

5. Zhang Q, Bastard P, Liu Z, Le Pen J, Moncada-Velez M, Chen J, et al. Inborn errors of type I IFN immunity in patients with life-threatening COVID-19. *Science.* (2020) 370:eabd4570.

6. Asgari S, Pousaz LA. Human genetic variants identified that affect COVID susceptibility and severity. *Nature.* (2021) 600:390–1. doi: 10.1038/d41586-021-01773-7

7. SeyedAlinaghi S, Mehrtak M, MohsseniPour M, Mirzapour P, Barzegary A, Habibi P, et al. Genetic susceptibility of COVID-19: A systematic review of current evidence. *Eur J Med Res.* (2021) 26:46. doi: 10.1186/s40001-021-00516-8

8. Casanova JL, Su HC. COVID human genetic effort. A global effort to define the human genetics of protective immunity to SARS-CoV-2 infection. *Cell.* (2020) 181:1194–9.

9. Povysil G, Butler-Laporte G, Shang N, Wang C, Khan A, Alaamery M, et al. Rare loss-of-function variants in type I IFN immunity genes are not associated with severe COVID-19. *J Clin Invest.* (2021) 131:147834. doi: 10.1172/JCI152475

10. van der Made CI, Simons A, Schuurs-Hoeijmakers J, van den Heuvel G, Mantere T, Kersten S, et al. Presence of genetic variants among young men with severe COVID-19. *JAMA.* (2020) 324:663–73. doi: 10.1001/jama.2020.13719

11. Jahanafrooz Z, Chen Z, Bao J, Li H, Lipworth L, Guo X. An overview of human proteins and genes involved in SARS-CoV-2 infection. *Gene.* (2022) 808:145963. doi: 10.1016/j.gene.2021.145963

12. Monticelli M, Hay Mele B, Benetti E, Fallerini C, Baldassarri M, Furini S, et al. Protective role of a TMPRSS2 variant on severe COVID-19 outcome in young males and elderly women. *Genes.* (2021) 12:596. doi: 10.3390/genes12040596

13. Saulle I, Vicentini C, Clerici M, Biasin M. Antigen presentation in SARS-CoV-2 infection: The role of class I HLA and ERAP polymorphisms. *Hum Immunol.* (2021) 82:551–60. doi: 10.1016/j.humimm.2021.05.003

14. Setaro AC, Gaglia MM. All hands on deck: SARS-CoV-2 proteins that block early anti-viral interferon responses. *Curr Res Virol Sci.* (2021) 2:100015. doi: 10.1016/j.crviro.2021.100015

15. Kokuina E, Breff-Fonseca MC, Villegas-Valverde CA, Mora-Díaz I. Normal values of T, B and NK lymphocyte subpopulations in peripheral blood of healthy cuban adults. *MEDICC Rev.* (2019) 21:16–21. doi: 10.37757/MR2019.V21.N2-3.5

16. Zhang Q, Bastard P, Cobat A, Casanova JL. Human genetic and immunological determinants of critical COVID-19 pneumonia. *Nature.* (2022) 603:587–98.

17. Zeberg H, Pääbo S. The major genetic risk factor for severe COVID-19 is inherited from Neanderthals. *Nature.* (2020) 587:610–2. doi: 10.1038/s41586-020-2818-3

18. Castelli EC, Paz MA, Souza AS, Ramalho J, Mendes-Junior CT. Hla-mapper: An application to optimize the mapping of HLA sequences produced by massively parallel sequencing procedures. *Hum Immunol.* (2018) 1:678. doi: 10.1016/j.humimm.2018.06.010

19. Severe Covid-19 Gwas Group, Ellinghaus D, Degenhardt F, Bujanda L, Buti M, Albillos A, et al. Genomewide association study of severe covid-19 with respiratory failure. *N Engl J Med.* (2020) 383:1522–34. doi: 10.1056/NEJMoa2020283

20. Orsucci D, Trezzi M, Anichini R, Blanc P, Barontini L, Biagini C, et al. Increased creatine kinase may predict a worse COVID-19 outcome. *J Clin Med.* (2021) 10:1734. doi: 10.3390/jcm10081734

21. Li Y, Ke Y, Xia X, Wang Y, Cheng F, Liu X, et al. Genome-wide association study of COVID-19 severity among the Chinese population. *Cell Discov.* (2021) 7:1–16. doi: 10.1038/s41421-021-00318-6

22. Hou Y, Zhao J, Martin W, Kallianpur A, Chung MK, Jehi L, et al. New insights into genetic susceptibility of COVID-19: An ACE2 and TMPRSS2 polymorphism analysis. *BMC Med.* (2020) 18:216. doi: 10.1186/s12916-020-01673-z

23. Castelli EC, de Castro MV, Naslavsky MS, Scliar MO, Silva NSB, Andrade HS, et al. MHC variants associated with symptomatic versus asymptomatic SARS-CoV-2 infection in highly exposed individuals. *Front Immunol.* (2021) 12:3898. doi: 10.3389/fimmu.2021.742881

24. Shi C, Wang F, Tong A, Zhang XQ, Song HM, Liu ZY, et al. NFKB2 mutation in common variable immunodeficiency and isolated adrenocorticotropic hormone deficiency: A case report and review of literature. *Medicine.* (2016) 95:e5081. doi: 10.1097/MD.0000000000005081

25. Tsukada S, Rawlings DJ, Witte ON. Role of Bruton's tyrosine kinase in immunodeficiency. *Curr Opin Immunol.* (1994) 6:623–30. doi: 10.1016/0952-7915(94)90151-1

26. Arruda LCM, Gaballa A, Da Silva Rodrigues R, Makower B, Uhlin M. SARS-CoV-2 (COVID-19)-specific T cell and B cell responses in convalescent rheumatoid arthritis: Monozygotic twins pair case observation. *Scand J Immunol.* (2022) 95:e13151. doi: 10.1111/sji.13151

27. Schultheiß C, Paschold L, Simnica D, Mohme M, Willscher E, von Wenserski L, et al. Next-generation sequencing of T and B cell receptor repertoires from COVID-19 patients showed signatures associated with severity of disease. *Immunity.* (2020) 53:442.e–55.e. doi: 10.1016/j.immuni.2020.06.024

28. Pérez-Cabezas B, Ribeiro R, Costa I, Esteves S, Teixeira AR, Reis T, et al. IL-2 and IFN-γ are biomarkers of SARS-CoV-2 specific cellular response in whole blood stimulation assays. *medRxiv* [Preprint] (2021). doi: 10.1101/2021.01.04.20248897

29. Kaushal K, Kaur H, Sarma P, Bhattacharyya A, Sharma DJ, Prajapat M, et al. Serum ferritin as a predictive biomarker in COVID-19. A systematic review, meta-analysis and meta-regression analysis. *J Crit Care.* (2022) 67:172–81. doi: 10.1016/j.jcrc.2021.09.023

ACS Biomaterials SCIENCE & ENGINEERING

Article

Electrochemical Immunosensors Based on Zinc Oxide Nanorods for Detection of Antibodies Against SARS-CoV-2 Spike Protein in Convalescent and Vaccinated Individuals

Freddy A. Nunez, Ana C. H. Castro, Vivian L. de Oliveira, Ariane C. Lima, Jamille R. Oliveira, Giuliana X. de Medeiros, Greyce L. Sasahara, Keity S. Santos, Alexandre J. C. Lanfredi, and Wendel A. Alves*

Cite This: *ACS Biomater. Sci. Eng.* 2023, 9, 458−473

Read Online

ACCESS | Metrics & More | Article Recommendations | Supporting Information

ABSTRACT: Even after over 2 years of the COVID-19 pandemic, research on rapid, inexpensive, and accurate tests remains essential for controlling and avoiding the global spread of SARS-CoV-2 across the planet during a potential reappearance in future global waves or regional outbreaks. Assessment of serological responses for COVID-19 can be beneficial for population-level surveillance purposes, supporting the development of novel vaccines and evaluating the efficacy of different immunization programs. This can be especially relevant for broadly used inactivated whole virus vaccines, such as CoronaVac, which produced lower titers of neutralizing antibodies. and showed lower efficacy for specific groups such as the elderly and immunocompromised. We developed an impedimetric biosensor based on the immobilization of SARS-CoV-2 recombinant trimeric spike protein (S protein) on zinc oxide nanorod (ZnONR)-modified fluorine-doped tin oxide substrates for COVID-19 serology testing. Due to electrostatic interactions, the negatively charged S protein was immobilized via physical adsorption. The electrochemical response of the immunosensor was measured at each modification step and characterized by scanning electron microscopy and electrochemical techniques. We successfully evaluated the applicability of the modified ZnONR electrodes using serum samples from COVID-19 convalescent individuals, CoronaVac-vaccinated with or without positive results for SARS-CoV-2 infection, and pre-pandemic samples from healthy volunteers as controls. ELISA for IgG anti-SARS-CoV-2 spike protein was performed for comparison, and ELISA for IgG anti-RBDs of seasonal coronavirus (HCoVs) was used to test the specificity of immunosensor detection. No cross-reactivity with HCoVs was detected using the ZnONR immunosensor, and more interestingly, the sensor presented higher sensitivity when compared to negative ELISA results. The results demonstrate that the ZnONRs/spike-modified electrode displayed sensitive results for convalescents and vaccinated samples and shows excellent potential as a tool for the population's assessment and monitoring of seroconversion and seroprevalence.
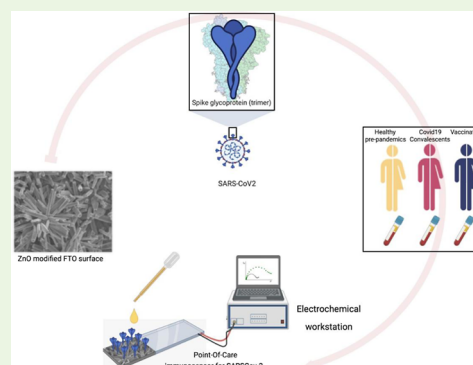
KEYWORDS: *COVID-19, SARS-CoV-2, electrochemical immunosensors, zinc oxide, serological diagnosis, immunosurveillance, CoronaVac*

INTRODUCTION

The coronavirus disease (COVID-19) pandemic has been a global health crisis for 2 years, causing over 456 million infections and more than six million deaths.[1] Several studies have been conducted to establish the seroprevalence of SARS-CoV-2 among the general population.[2−4] Vaccination against COVID-19 continues to be the most effective method of preventing severe disease, hospitalization, and death during the current pandemic, including those associated with the Omicron variant.[5,6]

Mass vaccination campaigns to prevent Covid-19 are now being conducted worldwide, with different types of vaccines, such as viral vector-based vaccines,[7] mRNA-based,[8] and inactivated virus vaccines.[9] The most widely used inactivated virus vaccine is the CoronaVac,[10,11] used especially in low- and middle-income countries.[12] Several studies reported very low vaccine-induced antibody titers in CoronaVac-vaccinated individuals.[12−15] Accurate and accessible seroprevalence detection may be of particular interest to public health activities in countries where this vaccine has been primarily used in vaccination programs.

Tests to detect seroprevalence in the general population to COVID-19 are critical to evaluate the effectiveness of vaccination programs, support the development of vaccines, and contribute to our understanding of the extent of infection among individuals who were not identified through active case finding and surveillance efforts, determining the attack rate in the population and the infection fatality rate.[16] The conventional methodology for serological determinations includes the traditional enzyme-linked immunosorbent assay (ELISA),[17] immunochromatographic Lateral flow assay (LFA),[18] and electrochemical biosensors.[19,20]

Methods based on electrochemical biosensors have been explored as promising alternatives for real-time monitoring of COVID-19.[21] Such devices feature a high level of sensitivity, specificity, operability, cost-effectiveness, miniaturization, and expeditious testing. They also decrease the need for costly equipment, specialized personnel, and extensive sample preparation. Such aspects make them useful diagnostic tools since they provide rapid and accurate results.[22,23]

One of the nanomaterials widely employed for biosensor production in recent years is zinc oxide (ZnO). This n-type semiconductive material features a broad energy gap (Eg = 3.37 eV) and a large exciton binding ability (60 meV).[24] With its unique chemical, optical, and electrical properties, added to its easy manufacturing in nanostructures of several sizes and morphologies, this metal oxide is a highly versatile material that has gained the attention of researchers not only for the development of electrochemical biosensors but also for electronic and optoelectronic devices, solar cells and supercapacitors, and biomedical applications.[25,26]

Indeed, ZnO can now be grown as bulk crystals, thin films, and nanostructures with various techniques[27] such as wet chemical method,[28] microwaves,[29] sputtering,[30] vapor deposition,[31−33] and electrodeposition.[34−36] This advancement has enabled its usage as a biosensor component, offering a high degree of reproducibility, scalability, design flexibility, and multiplexing of operational features. Some successful examples of practical device enhancement are the manufacturing of miniaturized micro−nano electrodes in glucose and urea sensors,[37−39] bacterial meningitis detection,[40] cholesterol biosensing,[41] H1N1 influenza detection,[42] legionella pneumophila diagnosis,[43] grapevine virus detection,[44] cancer diagnosis,[45,46] and many other devices employed as promising immunosensors.[47−52]

The high isoelectric point (IEP 9.5) of ZnO nanostructures makes them suitable for adsorbing materials with lower isoelectric points such as enzymes and proteins by the electrostatic interactions.[40,53] A positively charged ZnO matrix offers a receptive microenvironment for the negatively charged proteins or enzymes to maintain their activity. It significantly promotes the direct electron transport between the enzyme/protein and the electrode.[54] Several ZnO nanostructures have been prepared with shape controllers, such as urchin-like,[55] flower-like,[56] nanoplates,[57] nanorods,[58] and nanobelts.[59] The zinc oxide can occur in one-dimensional (1D), two-dimensional (2D), and three-dimensional (3D) structures.[60]

In this study, we have successfully developed ZnO nanorods functionalized with SARS-CoV-2 recombinant trimeric spike protein for electrochemical immunoassay of SARS-CoV-2 antibody detection tests. The platform distinguished in impedance measurement serum samples from naturally infected and vaccinated individuals with inactivated SARS-CoV-2 vaccine (CoronaVac) from negative control samples

and was also capable of detecting seroconversion in samples from individuals previously considered seronegative by the standard ELISA test, with high sensitivity. There was no cross-reactivity for common human coronavirus (HCoV), demonstrating excellent specificity. These hierarchical electrodes based on ZnONRs can be used as an inexpensive surface substrate or electrode for seroprevalence determination, control, and monitoring of COVID-19.

■ MATERIALS AND METHODS

Materials. Zinc nitrate hexahydrate ($Zn(NO_3)_2 \cdot 6H_2O$, reagent grade 98%), hexamethylenetetramine (HMTA, ACS reagent ≥99%), glycine (ACS reagent ≥98.5%), potassium ferricyanide (ACS reagent, ≥99%), and potassium ferrocyanide (ACS reagent 98.5%) were obtained from Sigma-Aldrich. Potassium chloride (reagent grade 99%) was purchased from Labsynth. The SARS-CoV-2 recombinant trimeric spike protein has been kindly supplied by the Cell Culture Engineering Laboratory (LECC) of COPPE/Federal University of Rio de Janeiro. The monoclonal anti-SARS coronavirus recombinant human antibody, Clone CR3022 (produced in HEK293 cells), NR-5248 was made under HHSN272201400008C and obtained through BEI Resources, NIAID, NIH.

A total of 107 human blood serum samples were analyzed, divided into four groups: Pre-pandemic ($N = 15$), convalescents ($N = 47$) with polymerase chain reaction diagnostic confirmation at least 40 days after the onset of COVID-19 symptoms, CoronaVac-vaccinated individuals (without previous positive results for COVID-19 disease) ($N = 25$), and CoronaVac-vaccinated previously infected individuals (with a previous positive result for COVID-19 disease and vaccinated after that) ($N = 20$). All vaccinated individuals received two doses of a 3 μg vaccine/shot each, 4 weeks apart. Serum from convalescent individuals and CoronaVac-vaccinated individuals was processed at the Heart Institute Immunology Laboratory—InCor/HC-FMUSP. All convalescents and CoronaVac-vaccinated volunteers signed written informed consent approved by the Ethics Committee in Research of the Clinics Hospital of the University of Sao Paulo Medical School. (CAPPesq CAAE30155220.3.0000.0068). The BCRJ cell bank supplied serum from pre-pandemic individuals through approval by the Ethics Committee of the Federal University of ABC (CAAE—43139921.2.0000.5594). The samples were classified along with the article as prepandemic, convalescents, CoronaVac-vaccinated, and CoronaVac-vaccinated previously infected and stored at −80 °C until subsequent use.

ZnONR Preparation Processes. Fluorine-doped tin oxide (FTO) glasses were used as substrates to produce ZnONR films. The 1×1.5 cm-dimensioned substrates were washed three times by sonication in ethanol, deionized water, and acetone for 15 min. A two-step methodology based on the literature has been applied to grow the films, with minor modifications.[61] First, a seed layer was prepared by dripping aqueous solutions of $Zn(NO_3)_2$ (20 μL, 0.5 mol L^{-1}) and HMT (20 μL, 0.5 mol L^{-1}) on the substrates. After 5 min of deposition, the substrates were spin-coated for 6 s at 500 rpm and then for 30 s at 3000 rpm. Finally, they were annealed at 200 °C for 15 min. In the second step, the ZnONR films were grown hydrothermally by soaking the modified substrates in a mixture of $Zn(NO_3)_2$ (0.1 mol L^{-1}) and HMT (0.1 mol L^{-1}), keeping their volume ratio at 1:1 (v/v). The hydrothermal growth was performed at 100 °C for 4 h in a sealed beaker. The final modified electrode was called FTO-ZnONRs.

Fabrication of the Electrochemical Immunosensor. The FTO-ZnONR electrode was first rinsed with a phosphate buffer solution to generate a hydrophilic surface; then, 20 μL of SARS-CoV-2 recombinant spike protein (4 μg mL^{-1}) diluted in phosphate buffer (pH 7.4) was placed onto the FTO-ZnONR surface for adsorption. The drop was in contact with the ZnONR surface for 5 h, rinsed to remove any unbound protein, and dried (FTO-ZnONRs/spike). A glycine solution (10 μmol L^{-1}) was used as a blocking solution to minimize the non-specific adsorption; 20 μL was placed on the sample and left to react for 30 min, and the device was again washed
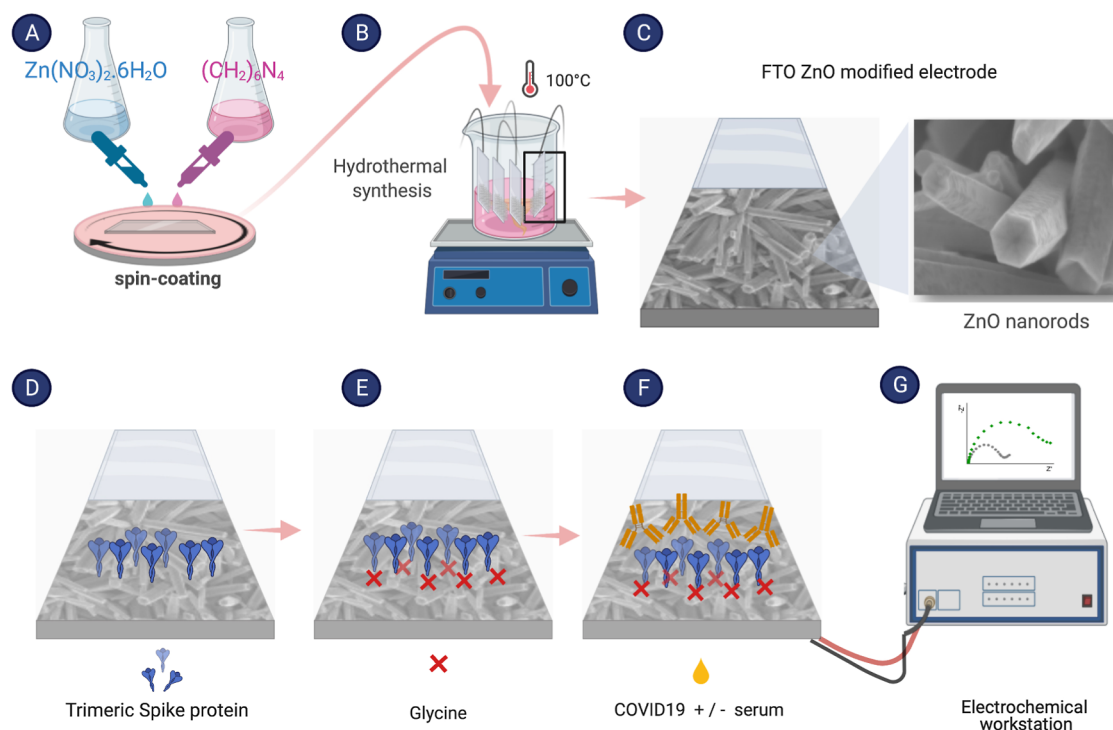
Figure 1. Schematic representation of the electrochemical ZnO immunosensor fabrication for anti-SARS-CoV-2 antibody detection. (A) Two-step method for ZnONR synthesis: In the first step, using a spin coater, a seed layer is added by dripping $Zn(NO_3)_2$ and HMT aqueous solutions on the FTO substrate, (B) hydrothermal method promotes the ZnONR film growth on the FTO surface at 100 °C, (C) modified electroactive surface (scanning electron microscopy highlighting the structure of ZnONRs on the FTO surface), (D) addition of SARS-CoV-2 recombinant trimeric spike protein ($4~\mu g~mL^{-1}$), (E) surface blocking step is performed with glycine solution ($10~\mu mol~L^{-1}$) to minimize the non-specific adsorption, (F) positive (containing anti-SARS-CoV-2 antibodies) or negative (pre-pandemic) serum samples (1:500 v/v) are placed on the ZnO electrode surface, and (G) read out is performed using an electrochemical workstation.

and dried (FTO-ZnONRs/spike/Gly). After that, 20 μL of blood serum diluted in phosphate buffer (pH 7.4) at a ratio of 1:500 (v/v) was incubated on the electrode surface and then stored for 1 h, rinsed next, and dried (FTO-ZnONRs/spike/Gly/serum). A schematic of the biosensor assembly process is shown in Figure 1. The positive samples (FTO-ZnONRs/spike/Gly/+serum) were analyzed with serum from convalescent and vaccinated individuals, while the negative samples (FTO-ZnONRs/spike/Gly/-serum) were analyzed with serum from prepandemic individuals.

Electron Microscopy and Spectroscopic Characterizations. Scanning electron microscopy (SEM) images were collected using a field-emission scanning electron microscope JMS-6701F (JEOL) situated in the Multiuser Experimental Center of the Federal University of ABC (CEM/UFABC, Santo André, Brazil) with a voltage of 5 kV. The solutions were diluted to the minimum possible concentration to observe the changes on the ZnONR surface and to carry out the observations on a microscope after each immunosensor assembly stage.

Fourier transform infrared spectroscopy (FTIR, Perkin Elmer) was recorded from 700 to 1800 cm^{-1} at room temperature with a spectral resolution of 4 cm^{-1} and an average of 124 data acquisitions. X-ray photoelectron spectroscopy (XPS; ThermoFisher Scientific, K-alpha +) was acquired with monochromatic Al Kα radiation. Carbon (C 1s) was used to calibrate the sample charging for XPS measurements. XPS data were processed using CasaXPS processing software.

Electrochemical Measurements. The electrochemical measurements were conducted with a μAutolab type III potentiostat/galvanostat for Metrohm, using NOVA 2.1 software supplied by Metrohm. In a conventional three-electrode system, an FTO-ZnONR-modified electrode was regarded as a working electrode, a platinum wire as a counter electrode, and a saturated calomel electrode as a reference electrode against which all potentials were

measured. The response readings were performed in 5 mmol L^{-1} $K_4Fe(CN)_6/K_3Fe(CN)_6$ in 0.1 mol L^{-1} KCl (pH 7.3).

Enzyme-Linked Immunosorbent Assay. The ELISA was performed using 96-well high-binding half-area polystyrene plates (Corning, USA) coated overnight at 4 °C with 4 μg mL^{-1} spike protein and diluted in carbonate−bicarbonate buffer (pH 9.6, 0.1 mol L^{-1}). For cross-specificity experiments using pre-COVID-19 pandemic serum samples, plates were coated with 4 μg mL^{-1} RDB proteins of the four endemic human CoVs (229E, OC43, NL63, and HKU1). All HCoV proteins used for ELISA were kindly provided by Boscardin's Laboratory (ICB-USP). After this period, the coating solutions were discarded, and 80 μL of BSA (1%), skim milk powder (5%), and Tween-20 (0.05%) in phosphate-buffered saline (PBS) were added to each well for blocking, carried out at room temperature for 2 h. Serum or plasma samples were thawed at room temperature, incubated at 56 °C for 30 min to inactivate the virus, and diluted (1:100) in BSA (0.25%), skimmed milk powder (5%), and Tween-20 (0.05%) in PBS. 25 μL of this solution was added to each well and incubated at 37 °C for 45 min. After incubation, the plates were washed with Tween-20 (0.05%) in PBS five times. 25 μL of peroxidase-conjugated goat anti-human IgG secondary antibody solutions (Jackson Immunoresearch, USA) diluted 1:10,000 in BSA (0.25%), skim milk powder (5%), and Tween-20 (0.05%) in PBS were added to each well and incubated at 37 °C for 30 min and then washed five times. The o-phenylenediamine dihydrochloride tablets (Sigma, USA) were dissolved in phosphate−citrate buffer (pH 5.0, 0.05 mol L^{-1}) at a concentration of 0.4 mg mL^{-1}. Immediately before use, 5 μL of hydrogen peroxide (30%) was added to the solution. Then, 25 μL of the final solution was added to each well, and the plates were incubated in the dark at room temperature for 30 min. After incubation, the reaction was halted by adding 25 μL of a 2 N H_2SO_4 solution to each well. Plates were then read at 490 nm using a plate reader (GloMax, Promega, USA). All samples were run in
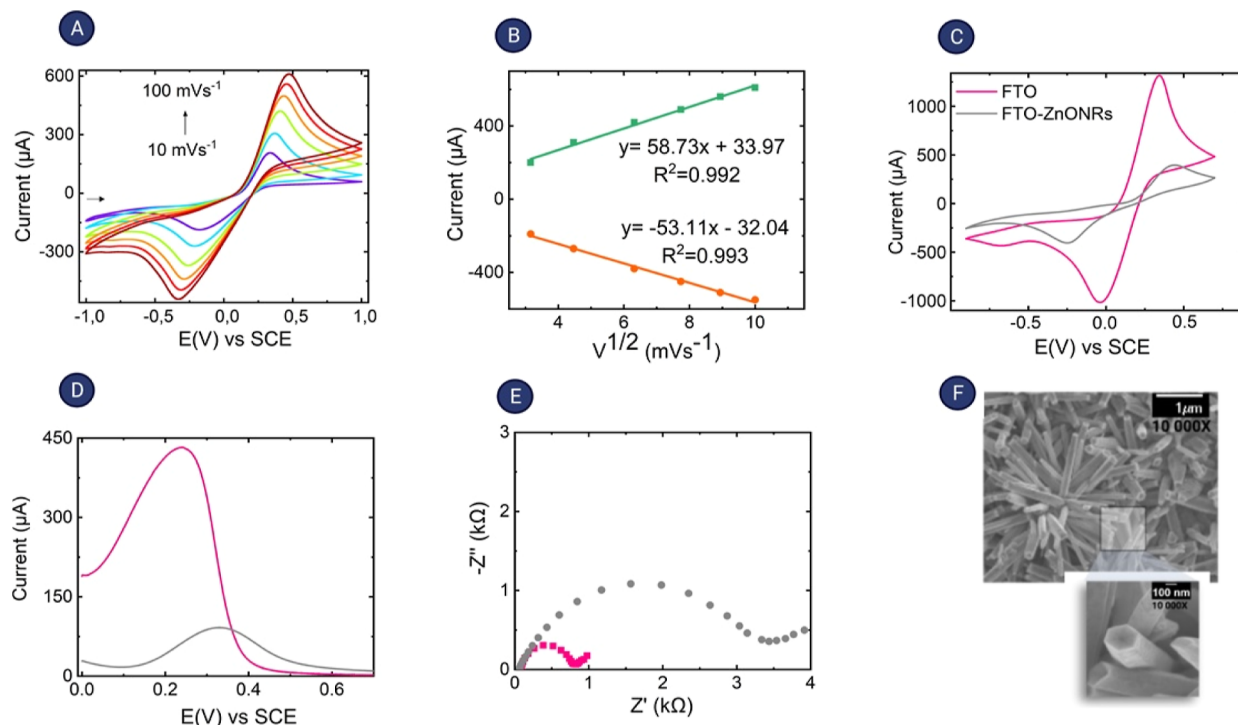
Figure 2. Functional modification of the FTO electrodes. (A) Cyclic voltammograms of the FTO-ZnONR electrode at different scan rates, varying from 10, 20, 40, 60, 80, and 100 mV s^{-1}, (B) plot of peak current versus square root of the scan rate of the FTO-ZnONR electrodes. (C) Cyclic voltammograms in a sweep window of −0.9 to 0.7 V at a scan rate of 50 mV s^{-1}, (D) square wave voltammograms in a sweep window of 0−0.7 V with a modulation amplitude of 20 mV and a frequency of 20 Hz, (E) Nyquist diagram of EIS measurements performed from 30 kHz to 0.1 Hz with an RMS amplitude of 10 mV, demonstrating the electrode surface of FTO (pink) and after functionalization with ZnONRs (Gray). (F) SEM images of the ZnONRs. Electrolyte: solution of 5 mmol L^{-1} K$_4$Fe(CN)$_6$/K$_3$Fe(CN)$_6$ in 0.1 mol L^{-1} KCl.

duplicate. Pre-COVID-19 samples were included as negative controls in the experiments. The values were determined as optical density minus blank, and results are given as the ratio of participant samples/ average of a set of 20 control pre-pandemic samples. An antibody ratio of ≥1.2 was considered positive.

Statistical Analysis. Descriptive statistics, receiver operating characteristics (ROCs), and correlation analysis were performed using GraphPad Prism software version 9, and a *p*-value < 0.05 was considered statistically significant. The variables were analyzed using the Kruskal−Wallis test with Dunn's post-hoc test for multiple comparisons.

RESULTS AND DISCUSSION

Electrochemical Characterization of the FTO-ZnONR Electrode. Cyclic voltammetry (CV) is a powerful electrochemical technique used to assess the oxidation−reduction processes of molecular species and study chemical reactions initiated by electron transfer.[62] It is popularly used in the electrochemical characterization of materials due to its ease of execution and rapid analysis.[63] The electrochemical and morphological performance of the FTO electrode modified with ZnONRs was evaluated and is shown in Figure 2.

The linearity of anodic and cathodic peak currents versus the square root of the scan rate (Figure 2A,B) revealed an efficient diffusion-controlled process, demonstrating a thermodynamically favorable electron transfer with an improved electrochemical signal pattern. As the scan rate increases, oxidation and reduction peak current increases along with a gradual shift of the potential oxidation peak toward a positive direction and reduction rise toward a negative approach. This behavior indicates a limitation in the charge transfer kinetics, characteristic of a quasi-reversible system.[39,64] The observed peak

separation potential, $\Delta E_p = (E_{pa} - E_{pc})$ of 90 mV, was more significant than the value expected for a reversible system. The reversible systems tend to have a peak-to-peak voltage difference of 59/n mV.[65] It is known that for reversible and diffusion-controlled systems, the peak is proportional to the scanning speed according to the Randles−Sevcik equation[66]

$$I_p = (2.69 \times 10^5) n^{3/2} A D^{1/2} C V^{1/2} \tag{1}$$

where: I_p is the peak current, n is the number of electrons transferred during the oxidation or reduction, A is the electroactive area of the electrode (cm^2), D is the coefficient of diffusion (cm^2 s^{-1}), C is the concentration of the electroactive species (mol/cm^3), and V is the scan rate (V s^{-1}). Rearranging the Randles−Sevcik equation, we can find the electroactive area of the electrode

$$A = \frac{I_p}{V^{1/2}} \times \frac{1}{2.69 \times 10^5 n^{3/2} D^{1/2} C} \tag{2}$$

Note that the first term refers to the angular coefficient of the lines obtained in the graph of peak current versus the square root of scan rate (Figure 2B) [Amps/(V s^{-1})$^{1/2}$]. The other variables are $n = 1$, $C = 5 \times 10^{-6}$ mol/cm^3, and the coefficient of potassium ferricyanide diffusion being equal to 6.39×10^{-6} cm^2 s^{-1}. An electroactive area value of 0.017 cm^2 was obtained for the FTO-ZnONR electrode. Similar results have been reported in the literature for the ZnO electrode surface area.[67,68] In contrast, an electroactive area value of 0.039 cm^2 was obtained for the bare FTO (Figure S1). As we can see, the bare FTO electroactive area is higher than that of
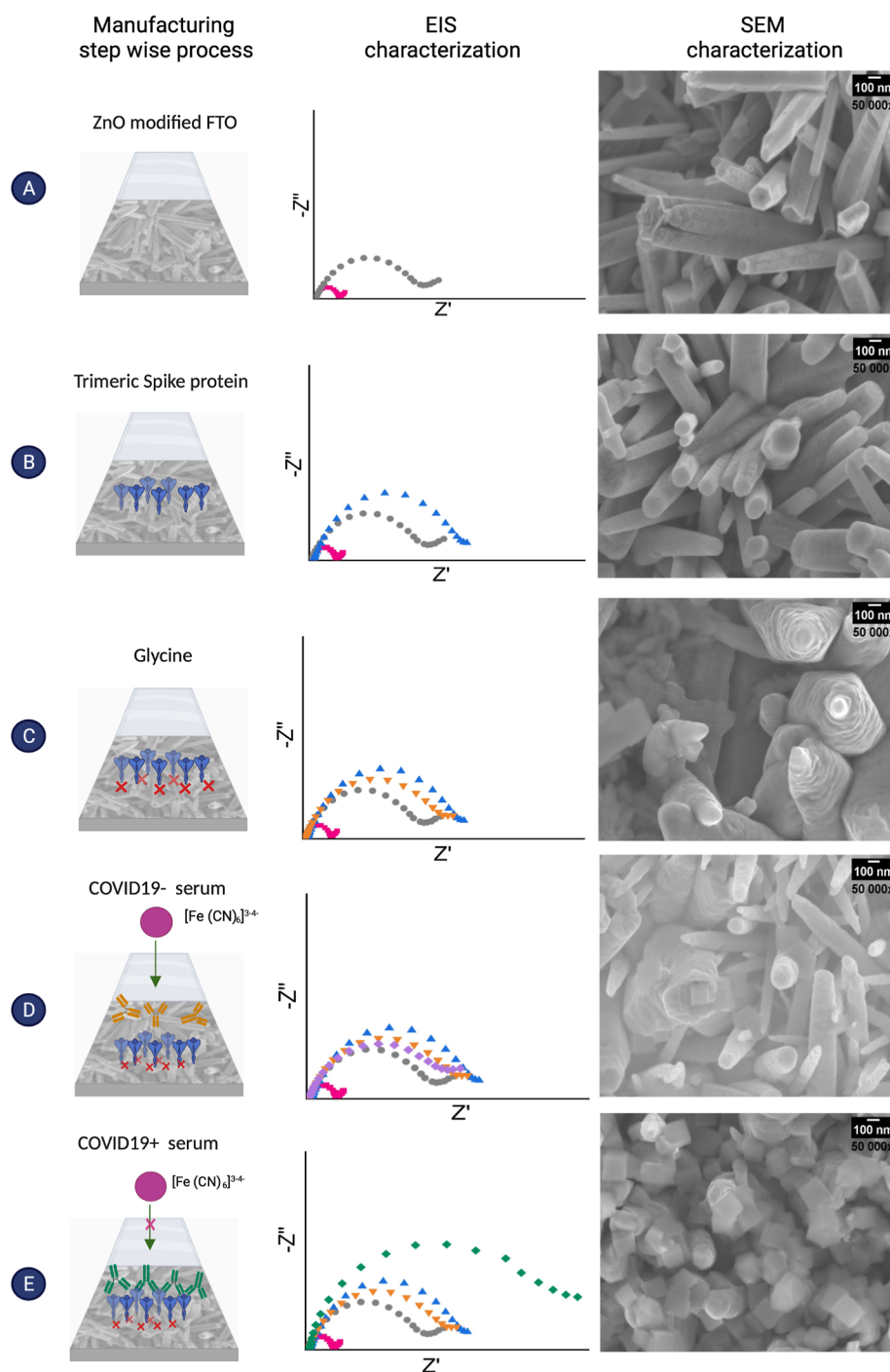
Figure 3. Electronic microscopy characterization of ZnONR immunosensors and EIS measurements at each assembly stage. (A) ZnONRs, (B) after S protein adsorption (4 ng mL^{-1}), (C) after glycine block (10 nmol L^{-1}), (D) in the presence of serum from the pre-pandemic individuals (1:1000 v/v), and (E) in the presence of serum from the convalescent individuals (1:1000 v/v).

FTO-ZnONRs, and it can be assigned to the ZnO semi-conductor properties.[69,70]

On the other hand, CV significantly decreases the peak oxidation current from 1317 μA (bare FTO) to 395 μA after modification with ZnONRs (Figure 2C). We also observed in the square wave voltammetry (SWV) tests (Figure 2D) that the peak intensity had a reduction of approximately 70% with the addition of the nanomaterial, which promoted a shift of the peak to more positive potentials. The Nyquist diagram (Figure 2E) confirms the result that was observed in CV since it shows an increase in the R_{ct} signal from 0.65 kΩ (bare FTO) to 3.37

kΩ when the ZnONRs are deposited on the FTO electrode; similar results have been reported in the literature for electrochemical impedance spectroscopy (EIS) and CV experiments with ZnO electrodes.[40,71]

The results obtained by CV, SWV, and EIS suggest that the matrix of ZnONRs (Figure 2F) offers some resistive path for the flow of electrons from the electrolyte to the substrate. In contrast, a direct transfer of electrons is possible at the bare FTO electrode. However, the ZnO matrix has several advantages: biocompatibility, low toxicity, high electron mobility, chemical stability, high isoelectric point, and easy
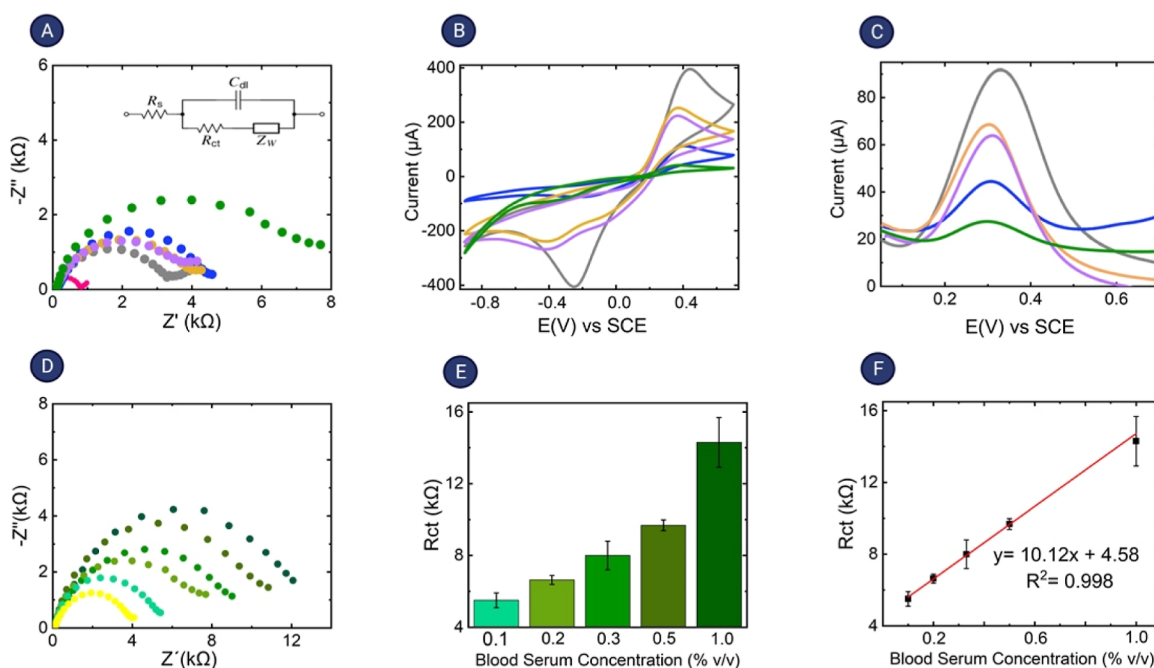
Figure 4. Electrochemical behavior and electrochemical validation of the ZnONRs/spike immunosensor. (A) Nyquist diagram of EIS measurements at each assembly stage performed from 30 kHz to 0.1 Hz with an RMS amplitude of 10 mV. Inset: the equivalent circuit model used for fitting the impedance data, (B) CV at each assembly stage, where the potential was swept from −0.9 to 0.7 V at a scan rate of 50 mV s^{-1}, (C) SWV, swept from 0 to 0.7 with a modulation amplitude of 20 mV and 20 Hz. Being (gray) ZnONRs, (blue) spike trimeric protein (4 μg mL^{-1}), (orange) glycine (10 μmol L^{-1}), (lila) serum from pre-pandemic, and (green) serum from convalescent individuals (1:500 v/v dilution), (D) Nyquist diagram of the calibration study by varying the concentration of positive serum-containing SARS-CoV-2 antibodies (green), dilutions were made in phosphate buffer being 0.1, 0.2, 0.33, 0.5, and 1 (%v/v) and shown in yellow the value refers to a blank (FTO-ZnONRs/spike/Gly), (E) bar graph showing the R_{ct} values obtained using the Nyquist diagrams and the Randles circuit as a function of the concentration of blood serum containing SARS-CoV-2 antibodies, and (F) calibration curve showing the variation of R_{ct} with the concentration of blood serum containing SARS-CoV-2 antibodies. Electrolyte: solution of 5 mmol L^{-1} K$_4$Fe(CN)$_6$/K$_3$Fe(CN)$_6$ in 0.1 mol L^{-1} KCl.

fabrication, turning it into a promising electrochemical biosensing platform.[37,39,54]

Working Principle of the Immunosensor. A method for directly connecting an electronic device to a biological environment is challenging due to the inherent complexity of biosensor development. Nanomaterials enable the miniaturization of devices, enhancing their sensitivity due to their higher surface area and long-range electron conductivity.[72,73] The ZnONRs create a favorable environment for biomolecules adsorption, maintaining their functionality and converting biological events into a stable, selective, and sensitive measurable signal. The SARS-CoV-2 recombinant trimeric spike protein was the biomolecule used to construct the electrochemical biosensing detection platform for anti-spike antibodies as the S protein is the main target antigen component from all structural proteins of SARS-CoV-2.[74] When working at physiological pH (7.4), the IEP of S protein (~5) has a net negative surface charge, and the ZnONR matrix with a high isoelectric point (~9.5) takes a net positive surface charge density. Thus, the negatively charged protein can be immobilized by electrostatic interaction on the surface of the positively charged ZnONR matrix. This principle has been widely used for the development of multiple immunosensors.[43,75−78]

The detection is achieved by measuring the Faradic impedance spectra for the ferro/ferricyanide redox couple [Fe(CN)$_6$]$^{3-/4-}$ after each modification step process of the electrode. Thus, the binding of anti-SARS-CoV-2 antibodies in human blood to the immobilized antigenic protein increases the R_{ct} signal. This increase is attributed to the electrode surface coverage with the bulky-sized antibodies. This coverage of the surface with the antibody retards the access of the ferro/ferricyanide redox couple to the conductive surface, reducing the electron transfer efficiency.

Electron Microscopy and Spectroscopic Characterizations. SEM images of ZnONRs show that the rods have a hexagonal shape with an average diameter of 490 nm, as shown in Figures 2F and 3A. The results are consistent with studies previously published by the group[61,79] and other researchers.[80−82] After SARS-CoV-2 recombinant spike protein immobilization, visual morphological changes were observed. The surface of the nanorods does not look smooth; it seems to be covered, indicating that an optimal immobilized protein profile was achieved (Figure 3B). Subtle modifications on the surface were observed after the blocking step with glycine (Figure 3C). Surprisingly, antigen−antibody complexes (anti-SARS-CoV-2 antibodies bound to immobilized spike proteins) induced dramatic morphological changes on the top of the electrode (Figure 3E). The electrode morphology modified with negative serum from pre-pandemic individuals is very similar to the surface where the spike protein is immobilized with glycine (blocking step), as shown in Figure 3D. This indicates that no SARS-CoV-2 antibodies were present in the tested pre-pandemic samples; consequently, no antigen recognition occurred.

Figure S2 shows FTIR spectra at each stage of device fabrication, and we also compare the spectra obtained in the presence of serum from the pre-pandemic and convalescent

individuals in the range of 1800−700 cm^{-1}. The FTIR spectrum of the ZnO nanostructures shows a broad band around 1600 cm^{-1} and an absorption peak at 1116 cm^{-1} assigned to O−H stretching and deformation vibrations of adsorbed water on the ZnO surface, respectively.[83,84] The band at 1370 cm^{-1} can be correlated to NO$_3$ stretch, which also appeared at 831 cm^{-1} as a weak band.[85] The absorption bands at 1258 and 1203 cm^{-1} correspond to the stretching modes of HMTA used for the growth process of the ZnONRs.[80] The FTIR spectrum from spike-attached ZnONRs shows characteristic bands of amide-I (C=O stretching, 1600−1700 cm^{-1}), amide-II (N−H bending, 1500−1600 cm^{-1}), and amide-III (C−N stretching and N−H bending, 1200−1330 cm^{-1}), which indicates that protein is attached on the surface of the modified electrode.[86−88] In the presence of glycine, no significant change in the FTIR spectrum was observed due to the overlap with the spike protein bands. Also, in the presence of negative serum, the vibrational spectra are very similar to the spike protein immobilized with glycine on the electrode ZnONR surface, as shown in Figure 3D, which correlates with SEM images and EIS spectra (Figure 3D), confirming no interaction has occurred. However, for convalescent serum, a significant increase in the bands at 1560−1464 cm^{-1} associated with IgG, 1420−1289 and 1160−1028 cm^{-1} related to IgM, and 1285−1237 cm^{-1} designed to IgA were detected.[87] These bands were broad and overlapping in the spectrum of the spike-immobilized electrode surface, which can evidence the conjugation of antibodies to the FTO-ZnONRs/spike/Gly interface.

XPS analysis of ZnO electrodes revealed the presence of nitrogen on the surface after functionalization, indicating successful spike protein attachment (Figure S3).[89−91] Furthermore, it is possible to observe an increase in N 1s peak with the incubation of the antibodies anti-SARS-CoV-2 present in human samples (FTO-ZnONRs/spike/Gly/+serum electrode), revealing the binding of antibodies to the electrode surface (Figure S3A). Figure S3B shows the high-resolution spectra for the FTO-ZnONR electrode. The binding energies were calibrated using the carbon C 1s peak (284.6 eV). The high-resolution Zn 2p spectrum peaks at 1043.28 and 1020.18 eV correspond to Zn 2p$_{1/2}$ and Zn 2p$_{3/2}$, respectively. The binding energy variation determined from the XPS study was ~23 eV, confirming that Zn atoms were in a Zn^{2+} oxidation state.[92,93] The O 1s high-resolution spectrum exhibited two Gaussian peaks named O1 and O2. The O1 peak at ~529 eV is related to O^{2-} ions in the wurtzite structure of the hexagonal Zn^{2+}-ion array.[94−96] The peak O2 at 530.78 eV can be attributed to the OH group adsorbed on the surface of the ZnONRs.[94,95] Figure S3C shows the high-resolution core-level spectra of C 1s at each fabrication stage of the electrode, and the peak at 284.6 eV can be attributed to C−C. The binding energy peaks at 286 and 288 eV are related to C−O and C=O bonds, respectively.[97,98] The N 1s high-resolution core-level spectra (Figure S3D) exhibit two peaks at 399 and 400, which can be attributed to the C−N/N=C and N−C=O bonds, respectively.[98] Figure S3E shows the high-resolution core-level spectra of O 1s, where a peak located at 531 eV can be assigned to C=O, the peak at 532 eV can be assigned to C−OH, and the peak at 533 eV can be assigned to O−C=O/O−C−O.[97]

Electrochemical Response Studies of the ZnONRs/ Spike Immunosensor. The EIS, CV, and SWV were used to characterize the electrode at each manufacturing stage (Figure

4). It shows the Faradic impedance spectra for the redox of [Fe(CN)$_6$]$^{3−/4−}$ measured at each manufacturing stage. The imaginary impedance component (Z″) is displayed as a function of the real component of impedance (Z′), as shown in Figure 4A.

These impedance spectra are typical of the theoretical, semicircular shape observed when the data is modeled using a Randles equivalent circuit, a helpful tool for analyzing EIS data that accounts for the resistive and capacitive processes at different frequencies.[99] A modified Randles circuit (inset in Figure 4A) with a constant phase element simulated the experimental diagrams. This equivalent circuit's components are R$_s$, the electrolytic resistance between the modified working electrode and the Pt reference electrode, and C$_{dl}$, the double-layer capacitance. Also, W is the Warburg impedance, and R$_{ct}$ is the charge transfer resistance of the [Fe(CN)$_6$]$^{3−/4−}$ redox probe. In the Faradic impedance measurements, R$_{ct}$ is the most sensitive parameter to describe the electrodes' surface recognition process.[100] As was previously mentioned, the R$_{ct}$ value of the FTO electrode increases from 0.65 kΩ for bare FTO to 3.37 kΩ for FTO-ZnONRs. Despite this increase in the R$_{ct}$ signal, using the ZnONR matrix is advantageous because it provides a biocompatible environment suitable for immobilizing enzymes, proteins, and DNA.[27] Then, after immobilization of SARS-CoV-2 recombinant trimeric spike protein, the semicircle area increases to 4.66 kΩ (FTO-ZnONRs/spike), which can be related to the barriers created on the electrode surface. This increase in the R$_{ct}$ signal suggests that the recombinant spike protein was successfully immobilized on the electrode surface.

The R$_{ct}$ value of the FTO-ZnONRs/spike/Gly was 3.98 kΩ, which is less than that for the FTO-ZnONRs/spike electrode (4.66 kΩ), which can be related to the difference in charge on the surface after attachment of the glycine molecules, which decreases the resistance to the charge transfer. Regarding the negative serum, the R$_{ct}$ signal obtained was 3.99 kΩ (FTO-ZnONRs/spike/Gly/-serum), very similar to the FTO-ZnONRs/spike/Gly signal, suggesting that glycine prevented non-specific interactions, as expected. After dripping the positive serum on the electrode surface (FTO-ZnONRs/ spike/Gly/+serum), the semicircle area increases significantly to 6.72 kΩ. It is assigned to the electrode surface coverage with the bulky-sized antibodies (an average molecular weight of approximately 150 kDa[101]). This surface coverage with the antibody reduces the electron transfer efficiency, increasing the R$_{ct}$. This significant increase in the R$_{ct}$ signal suggests that the antibodies present in the blood serum recognize the S protein immobilized on the electrode surface. Table S1 summarizes the R$_{ct}$ values obtained in each step of the developed immunosensor.

The results obtained in the CV and SWV were confirmed by EIS measurements, as shown in Figure 4B,C. A significant decrease in peak current was observed in the presence of antibodies due to the barriers created on the electrode surface. The bulky protein and antibody retard the redox molecules from reaching the surface. The current increases in the cathodic peak current for the electrode after the attachment of the glycine layer, which can be attributed to the amount of charge variation after the attachment of blocking molecules to the film's surface, affect the mobility of charge carriers of the mediator.

Analytical Sensitivity Analysis. The impedimetric response to different dilutions of human serum samples was
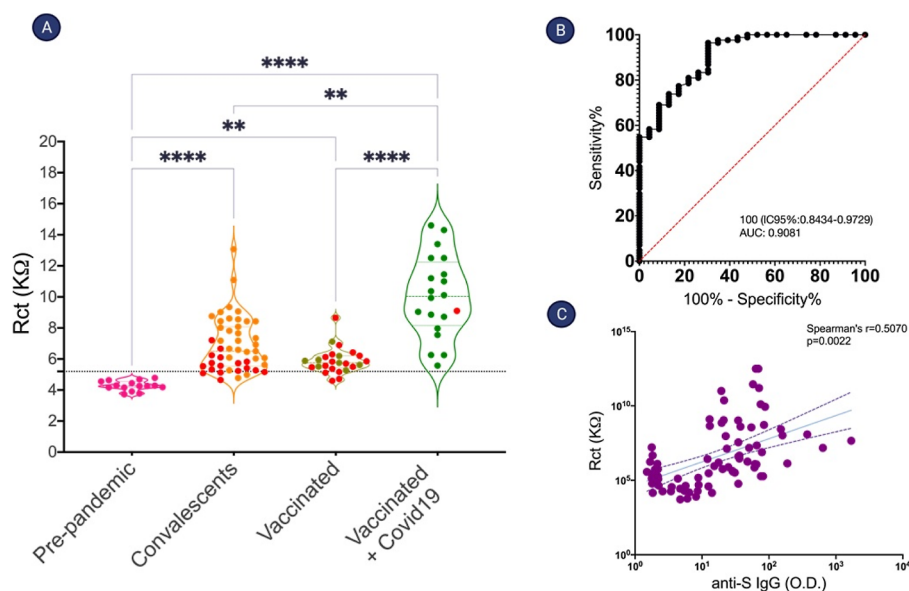
Figure 5. Detection accuracy of the developed electrochemical ZnONRs/spike immunosensor. (A) ZnONRs/spike immunosensor response was compared among a representative set of clinical samples from healthy pre-pandemic individuals, convalescents, and CoronaVac-vaccinated individuals. Serum samples were analyzed using the electrochemical impedance method and data were expressed in charge transfer resistance (R_{ct}). Red color dots indicated previously considered negative samples in anti-S IgG by ELISA test, (B) ROC curve was used to describe the discrimination accuracy of the developed electrochemical immunosensor, and (C) correlations between total antibody response against the SARS-CoV-2 spike protein measured from charge transfer impedance (R_{ct}) via our ZnONRs/spike immunosensor and IgG antibodies against the SARS-CoV-2 spike protein (anti-S IgG) detected using conventional ELISA, in all positive samples analyzed (healthy pre-pandemics, convalescents, and vaccinated individuals).

performed through successive titration to validate the ZnONRs/spike immunosensor for detecting anti-S antibodies in clinical samples. The sera were diluted with phosphate buffer (pH 7.4). The error bars corresponded to the standard deviation of the data points in triple experiments. EIS results are shown in Figure 4D, which presents the Nyquist diagram. The system indicates that the impedance increases with the concentration of the target analyte. The R_{ct} signal increases from 3.98 kΩ for the blank (FTO-ZnONRs/spike/Gly) to 5.04 kΩ after adding serum with a concentration equal to 0.1% v/v. To add a dilution of 0.2% v/v serum, the R_{ct} increases to 6.77 kΩ, and it continues to grow until showing an R_{ct} signal of 13.5 kΩ to add a serum with a concentration of 1.0% v/v. This trend evidences the binding of the antibodies present in human serum to the antigen immobilized on the electrode surface, increasing the hindrance to the movement of redox molecules. The R_{ct} values of the different EIS plots exhibited linear associations, as shown in Figure 4E,F. For the concentration range of 0.1−1% v/v, the correlation coefficient (R) was 0.998. It demonstrates that the biosensor signal is specific and works dose-dependently using a range of blood serum samples containing anti-SARS-CoV-2 spike protein antibodies.

The quantification detection of monoclonal antibodies (mAbs) anti-SARS-CoV spike protein (Clone: 3022) was performed under optimal conditions. EIS results are shown in Figure S2, which presents the Nyquist diagram (Figure S4A). The system clearly shows that the impedance increases with the concentration of the target analyte (Figure S4B). The R_{ct} values of the dose−response curve of IgG mAb were plotted against the IgG mAb concentration (Figure S4C). The linear response of antibodies ranges from 200 to 1200 ng mL^{-1}. The correlation coefficient (R) was calculated to be 0.995. The limit of detection (LOD) was 19.34 ng mL^{-1} using the equation[102]

$$\text{LOD} = 3.3 \times \left(\frac{\text{SD}}{\text{slope}} \right) \tag{3}$$

the value of SD is the standard deviation of the blank FTO-ZnO/spike/Gly bioelectrode under control conditions. The limit of quantification (LOQ) was 58.62 ng mL^{-1} using the equation[103]

$$\text{LOQ} = 10 \times \left(\frac{\text{SD}}{\text{slope}} \right) \tag{4}$$

This biosensor's sensitivity is adequate for detecting COVID-19 seroconversion and was comparable and even better than other immunoassays (Table S2).[20,104−107] Moreover, the device is portable, cheaper, and has shown a great potential to evaluate the humoral immune response in COVID-19 convalescent individuals or post-COVID-19 vaccinated individuals, offering an affordable and powerful alternative compared to the existing COVID-19 serological assays.

Determination of Positive/Negative Cutoff Threshold of Anti-SARS-CoV-2 Antibodies in Clinical Samples. The analytical validation began by establishing a cutoff point or a positive/negative threshold defined as the level of antibody activity that determines the positive or negative reactive status for a serum/plasma sample from a given individual.[108] In this case, the result is positive when a test serum presents an R_{ct} (kΩ) value above that determined in the cutoff. Still, if the result is below the cutoff value, the sample is deemed negative for SARS-CoV-2 antibodies. The cutoff determination was made considering the distribution of the R_{ct} resulting from the analysis of the 15 negative human blood samples (Figure 5A), following the formula below[109]

$$\text{Cut} - \text{off} = \overline{X} + 3 \times \text{SD} \qquad (5)$$

where $\overline{X}$: mean and SD: standard deviation. The value obtained for the cutoff was 5.20 kΩ.

Diagnostic Sensitivity, Specificity, and Determination of Anti-SARS-CoV-2 Antibodies in Clinical Serum Samples. The performance of the developed sensor in detecting the presence of spike SARS-CoV-2 antibodies in clinical samples was determined by analyzing 47 blood serum samples from individuals previously infected and recovered from SARS-CoV-2 (convalescent individuals). Figure 5A shows the R_{ct} obtained from pre-pandemic and convalescent samples with the calculated cutoff (dotted black line). The graphic reveals that the sensor identified the COVID-19 serum samples selectively and exhibited a relevant increase in R_{ct} values compared to pre-pandemic samples. Consequently, the ZnONRs/spike immunosensor discriminated between COVID-19 convalescent (positive) and pre-pandemic (healthy negative) samples. The immunosensor showed a negligible response toward the samples collected from pre-pandemic individuals, which suggests that no SARS-CoV-2 antibodies are found that can bind to the S protein. However, the positive confirmed clinical samples showed a significant relative change in the R_{ct} values. Although all the samples were from convalescent individuals, differences in R_{ct} signals were observed, attributed to the number of antibodies in the samples. The immune response will depend on each person since it is influenced by intrinsic and environmental factors, such as age, sex, genetics, and lifestyle.[11,110] Some individuals can react by getting excellent antibody levels against the SARS-Cov-2 virus, while others do not. Afterward, not all SARS-CoV-2-infected individuals will develop detectable antibodies using regular SARS-CoV-2 antibody tests. For these reasons, we observed a heterogeneous response in our study. Therefore, the antibody levels present in the samples that can effectively bind to the S protein immobilized on the electrode surface is variable for each sample. A higher R_{ct} signal could be interpreted as a more significant number of antibodies in the analyzed samples.

On the other hand, the biosensor was developed to detect positive samples for anti-SARS-CoV-2 spike protein antibodies, even in the negative samples in the ELISA plate wells (Figure S5), which is considered a gold standard test to perform serological diagnosis. Therefore, the diagnostic sensitivity and specificity values were calculated with a defined cutoff, and positive and negative samples were analyzed. For this, the following formulas were used[111]

$$\text{sensitivity} = \left[\frac{a}{(a+c)}\right] \times 100 \qquad (6)$$

$$\text{specificity} = \left[\frac{d}{(b+d)}\right] \times 100 \qquad (7)$$

where a: true-positive, b: false-positive, c: false-negative, and d: true-negative.

The sensitivity is the proportion of individuals with the disease who are accurately diagnosed with a positive test result ("true-positive rate"). In contrast, specificity is the proportion of individuals without the disease who are precisely identified by a negative test result ("true-negative rate").[112] The sensitivity and specificity values for the immunosensor described in this work were 88.7, and 100%, respectively.

Serological Cross-Reactivity with Common Coronavirus (HCoVs) Assessment. A suitable COVID-19 serological sensor must be sensitive and highly specific, ruling out any cross-reactivity with similar coronaviruses such as seasonal endemic HCoVs.[113] Therefore, the seroconversion of HCoVs in pre-COVID-19 pandemic serum samples was evaluated using ELISA to detect specific IgG antibodies against the RDB proteins of the four most common HCoVs (229E, OC43, NL63, and HKU1). ELISA results showed that all pre-pandemic samples analyzed in this study were positive for HCoVs (Figure S6). Simultaneously, using the ZnONRs/spike immunosensor, 100% of the same pre-COVID-19 cohort was found negative, demonstrating that our sensor is precise for SARS-CoV-2. It successfully distinguished the negative samples and eliminated the adverse risk of cross-specificity with human antibodies against HCoVs.

Detection of SARS-CoV-2 Antibodies in Vaccinated Individuals with Inactivated SARS-CoV-2 Vaccine (CoronaVac). To evaluate the applicability of the developed sensor in detecting anti-SARS-CoV-2 antibodies in vaccinated individuals, we analyze 45 human blood serum samples from individuals vaccinated with inactivated SARS-CoV-2 vaccine (CoronaVac vaccine) at least 28 days after the second immunization. From these 45 samples, 25 were from CoronaVac-vaccinated individuals (without previous positive results for COVID-19 disease) and 20 from CoronaVac-vaccinated, previously infected individuals (with a previous positive result for COVID-19 disease). Figure 5A shows the R_{ct} results, demonstrating that the sensor responds to blood serum and increases the R_{ct} values compared to pre-pandemic samples previously tested. It means that our ZnONRS/spike immunosensor could identify the antibody-induced response against SARS-CoV-2 spike protein stimulated by CoronaVac vaccination.

Vaccinated samples presented more homogeneous antibody-induced immune responses. Only slight variation in the R_{ct} values was found compared to that in samples from convalescents. This behavior might be justified because of the higher variability of naturally triggered humoral responses post-viral infection compared to vaccine-induced humoral immunity.[114,115]

The ZnONRs/spike immunosensor readouts (R_{ct} signal) from previously infected individuals followed by two vaccine doses have shown significantly higher R_{ct} values than those from asymptomatic or negative individuals without positive results COVID-19 disease before the immunization protocol, following data already reported.[116]

Our results confirmed recently described data where administration of the inactivated SARS-Cov-2 vaccine, CoronaVac, also induced higher antibody responses in previously naturally infected individuals.[117] According to Wang et al.[118] is expected that vaccination increases all components of the humoral response due to the ongoing antibody somatic mutation, memory B cell clonal turnover, and other general intrinsic factors related to vaccine-induced humoral immune responses.

It is essential to highlight that 16 samples of the 45 analyzed were negative for anti-SARS-CoV-2 spike protein antibodies by ELISA test (Figure S5), with the ZnONRs/spike immunosensor, and 12 samples showed a positive result, showing that the modified electrode has a higher sensitivity and efficiency than the golden standard tests. We can also highlight that the R_{ct} signal for some of these samples was slightly higher than the
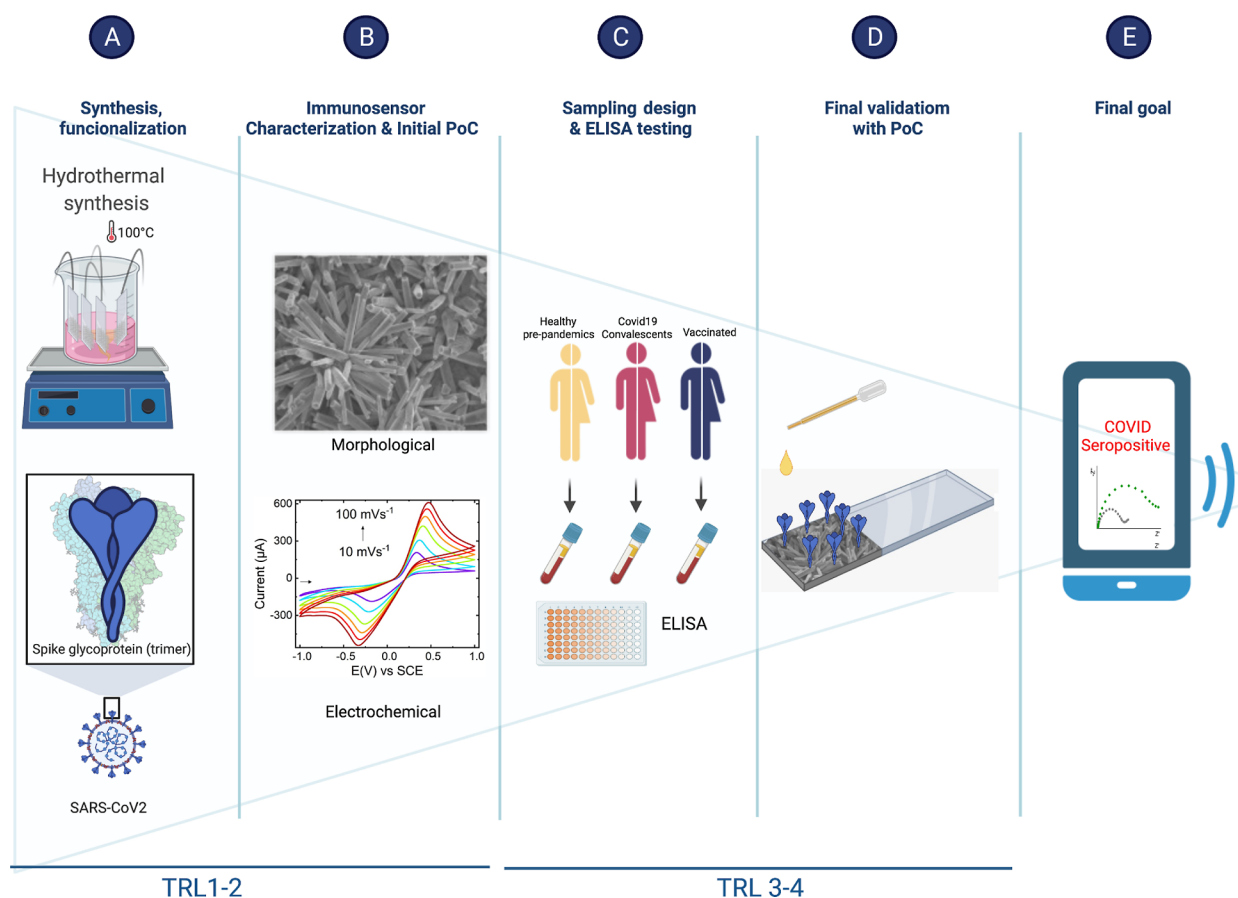
Figure 6. Development and validation of the electrochemical ZnONR immunosensors for anti-SARS-CoV-2 antibody detection. (A) Basic science research. Hydrothermal synthesis of ZnONRs, FTO (fluorine tin oxide) functionalization with viral spike protein, and optimization of sensor architecture and (B) prototype characterization. Morphological, spectroscopic, and electrochemical characterization was performed before and after the biological modification of ZnONR-modified FTO electrodes and (C) concept validation. Sampling design, collection, and confirmation of the clinical status by anti-S IgG ELISA serological analysis. (D) Final validation with the proof of concept. Clinical serum samples from healthy pre-COVID19 individuals, convalescents, and vaccinated patients were applied on the ZnO electrode surface for anti-COVID19 antibody detection and (E) final project goal.

cutoff, suggesting that the antibody titers present in the analyzed samples are relatively low and consistent with a negative ELISA result. Previous studies reported deficient production of vaccine-induced antibody titers after CoronaVac application, especially among elderly and immunocompromised individuals.[12−15] Our results demonstrate that the ZnONRs/spike immunosensor can detect the anti-SARS-CoV-2 spike protein antibody in individuals vaccinated with CoronaVac. This point-of-care technology can specifically aid public health actions in assessing humoral immune response post-COVID-19 vaccination in the countries where this vaccine is applied.

ZnONRs/Spike Immunosensor Detection Performance Analysis. To further explore the potential of our detection system, we use the ROC curve analysis to graphically evaluate the ZnONRs/spike immunosensor detection test (Figure 5B). ROC analysis is a valuable tool for assessing the performance of diagnostic tests and, more generally, for evaluating the accuracy of a statistical model that classifies subjects into one of the two categories, diseased or non-diseased. The area under the ROC curve (AUC) is an overall summary of diagnostic accuracy. The AUC equals 0.5 when the ROC curve corresponds to random chance and 1.0 for perfect accuracy.[119,120]

The ZnONRs/spike immunosensor detection test presented an AUC of 0.9081, evidencing the high accuracy of this assay. Therefore, the developed ZnO detection system offers a viable alternative method for detecting anti-SARS-CoV-2 antibodies in human serum and has a potential application in estimating the prevalence of the SARS-CoV-2 antibodies in a given population. Data acquired from conventional ELISA anti-spike and ZnONRs/spike immunosensor were compared and correlated using Spearman rank correlation (Figure 5C). This correlation coefficient represents the power of the putative linear association among such variables.[121] The spearman coefficient ranged from −1 to 1. Values close to 1 indicate a strong and positive correlation, values relative to −1 indicate a strong, negative correlation, and values close to zero indicate no linear correlation.[122] In our analysis, a correlation coefficient of 0.507 was obtained, showing a positive and moderate correlation between the data obtained using conventional ELISA test and our novel ZnONRs/spike immunosensor. Considering the differences in the biological samples and readout approaches, a result of a moderate correlation with a relevant *P*-value is encouraging. Since different ELISA tests detect anti-S IgG, the ZnONRs/spike immunosensor is a direct assay designed to detect total specific antibodies against COVID-19 without needing a secondary

antibody that specifically binds the species and class (isotype) of the primary antibody. This feature might be an added advantage for the other immunological detection of COVID19 in different animal species.

Evaluation of S Protein Concentration, Reproducibility, and Stability. Studying the impact of S protein concentration as the receptor molecule is critical for better biosensor design and performance. Different concentrations of S protein were immobilized in the range of 1 to 7 μg mL^{-1}. The EIS response was measured to monitor each electrode signal in triple experiments, using a $[\mathrm{Fe(CN)_6}]^{4-/3-}$ solution as the redox probe. Response signal growing was explicitly stopped when the concentration of spike protein was over 4 μg mL^{-1} (Figure S7A), after which device response was linear, indicating the maximum amount of protein that could be absorbed on the electrode surface. Based on this performance, 4 μg mL^{-1} was selected as the ideal concentration in subsequent experiments.

Independent data from five modified electrodes were acquired using a pool of serum samples of COVID-19 convalescent and pre-pandemic individuals, respectively, to determine the immunosensor's reproducibility (Figure S7B). The relative standard deviation (RSD) measurements were 3.11% for pre-pandemic samples and 2.14% (for convalescent individuals), demonstrating outstanding reproducibility of the biodevice. Moreover, the response of the electrode FTO-ZnO/spike/Gly was measured for 10 different electrodes (Figure S7C), obtaining an RSD of 3.20%, validating that the proposed immunosensor has good reproducibility. For this purpose, the EIS response was measured using a $[\mathrm{Fe(CN)_6}]^{4-/3-}$ solution as the redox probe.

The modified electrode was incubated with a serum sample of convalescent individuals (1:500 v/v) and stored at 4 °C to estimate the long-term stability of the device. The sensor showed around an 8.4% change in the impedance response after 15 days (Figure S7D).

In brief, all accomplished developmental phases of the ZnO immunosensor are represented in the schematic diagram (Figure 6). Each column corresponds to a step forward along with the product development and represents an increasing score along with the technology readiness level scale (TRL). The lower line indicates the work already performed and relates to the technology maturity level (TRL) already achieved in the project. The work described here moves the project from the beginning of TRL1 (basic science research) to TRL4 (final validation completion with the proof of concept). Our prospects are to adapt the current technology to be portable for on-site use, allowing the connection of mobile devices to facilitate the detection of COVID-19 antibodies since the future of public health is likely to become increasingly digital.

CONCLUSIONS

In this work, we have successfully developed a ZnONRs/spike immunosensor to detect anti-SARS-CoV-2 antibodies quickly. The fabricated electrode detected antibodies against SARS-CoV-2 spike protein in serum samples in about 5 min and showed a sensitivity of 88.7% and a specificity of 100%. No cross-reactivity with other common coronaviruses was found. The ZnONRs/spike immunosensor is easy to produce and employ, even though the bioreceptor component of the electrode, SARS-CoV-2 recombinant trimeric spike protein, has a high production cost as it requires expensive mammalian

cell expression systems. The electrode's manufacturing cost is relatively cheap, making it a great alternative. The biosensor results revealed a strong concordance with the conventional ELISA test results or even more sensitivity since some of the tested serum samples were considered negative using ELISA and positively detected in our sensor. The novel ZnO-based biosensing platform has shown the potential to evaluate the humoral immune response in COVID-19 convalescent individuals or post-COVID-19 vaccination, supporting efforts for immunosurveillance, aiding the control of future global waves of regional outbreaks of SARS-CoV-2 across the world. The immunosensor presented an AUC of 0.9081, indicating the high accuracy of the assay. The biosensing system is highly reproducible and stable for a practical application (around 15 days). Furthermore, this nanostructured electrode architecture is flexible. It shows great potential for other diagnostic and biomedical applications since the sensor technology can be easily customized using different biomolecules on the ZnONRs or other target analytes.

ASSOCIATED CONTENT

ⓈI Supporting Information

The Supporting Information is available free of charge at https://pubs.acs.org/doi/10.1021/acsbiomaterials.2c00509.

Electrochemical behavior of FTO electrodes; FTIR spectra at each fabrication stage of the electrodes; XPS spectra; quantification detection of mAb anti-SARS-CoV spike protein; ELISA assay for pre-pandemic, convalescents, and vaccinated individuals; ELISA assay HCoVs; optimization, reproducibility, and stability of the immunosensor; fitted parameters of the Nyquist impedance plot at each assembly stage of the ZnONRs immunosensor; and performance comparison of the Covid-19 serological tests (PDF)

AUTHOR INFORMATION

Corresponding Author

Wendel A. Alves − *Centro de Ciências Naturais e Humanas, Universidade Federal do ABC, Santo André, São Paulo 09210-580, Brazil;* ⊙ orcid.org/0000-0002-8394-2751; Email: wendel.alves@ufabc.edu.br

Authors

Freddy A. Nunez − *Centro de Ciências Naturais e Humanas, Universidade Federal do ABC, Santo André, São Paulo 09210-580, Brazil*

Ana C. H. Castro − *Centro de Ciências Naturais e Humanas, Universidade Federal do ABC, Santo André, São Paulo 09210-580, Brazil*

Vivian L. de Oliveira − *Centro de Ciências Naturais e Humanas, Universidade Federal do ABC, Santo André, São Paulo 09210-580, Brazil; Laboratório de Imunologia, LIM19, Instituto do Coração (InCor), Hospital das Clínicas da Faculdade de Medicina da Universidade de São Paulo (HCFMUSP), São Paulo, São Paulo 05403-900, Brazil;* ⊙ orcid.org/0000-0003-2523-0374

Ariane C. Lima − *Departamento de Clínica Médica, Disciplina de Alergia e Imunologia Clínica, Faculdade de Medicina da Universidade de São Paulo, São Paulo, São Paulo 01246-903, Brazil*

Jamille R. Oliveira − *Departamento de Clínica Médica, Disciplina de Alergia e Imunologia Clínica, Faculdade de*

Medicina da Universidade de São Paulo, São Paulo, São Paulo 01246-903, Brazil; ⦿ orcid.org/0000-0002-4993-5494

Giuliana X. de Medeiros − *Departamento de Clínica Médica, Disciplina de Alergia e Imunologia Clínica, Faculdade de Medicina da Universidade de São Paulo, São Paulo, São Paulo 01246-903, Brazil*

Greyce L. Sasahara − *Laboratório de Imunologia, LIM19, Instituto do Coração (InCor), Hospital das Clínicas da Faculdade de Medicina da Universidade de São Paulo (HCFMUSP), São Paulo, São Paulo 05403-900, Brazil*

Keity S. Santos − *Laboratório de Imunologia, LIM19, Instituto do Coração (InCor), Hospital das Clínicas da Faculdade de Medicina da Universidade de São Paulo (HCFMUSP), São Paulo, São Paulo 05403-900, Brazil; Departamento de Clínica Médica, Disciplina de Alergia e Imunologia Clínica, Faculdade de Medicina da Universidade de São Paulo, São Paulo, São Paulo 01246-903, Brazil;* ⦿ orcid.org/0000-0001-5271-4011

Alexandre J. C. Lanfredi − *Centro de Engenharia, Modelagem e Ciências Sociais Aplicadas, Universidade Federal do ABC, Santo André, São Paulo 09210-580, Brazil;* ⦿ orcid.org/0000-0002-8530-8826

Complete contact information is available at:
https://pubs.acs.org/10.1021/acsbiomaterials.2c00509

Author Contributions

F.A.N: methodology, validation, investigation, and writing—original draft. W.A.A., V.L.d.O., and A.C.H.C: conceived the sensing strategy, designed the study, conducted data curation, writing—review and editing, and visualization. A.J.C.L. and F.A.N: conducted SEM and XPS acquirement and analysis. F.A.N and W.A.A: conducted FTIR acquirement and analysis. J.R.O. and A.C.L.: performed ELISA Tests. G.X.d.M and G.L.S: processed laboratory human samples. K.S.S.: immunological resources. W.A.A.: supervising and funding acquisition.

Notes

The authors declare no competing financial interest.

■ ABBREVIATIONS

S Protein, recombinant trimeric spike protein; ELISA, enzyme-linked immunosorbent assay; PCR, polymerase chain reaction; ZnONRs, zinc oxide nanorods; LFA, immunochromatographic lateral flow assay; HMTA, hexamethylenetetramine; FTO, fluorine-doped tin oxide; EIS, electrochemical impedance spectroscopy; CV, cyclic voltammetry; SWV, square-wave voltammetry; ROC, received-operating characteristic curve; AUC, area under the ROC curve

■ REFERENCES

(1) WHO. WHO Coronavirus (COVID-19) Dashboard. https://covid19.who.int/ (accessed 13 04, 2022).

(2) Basto-Abreu, A.; Carnalla, M.; Torres-Ibarra, L.; Romero-Martínez, M.; Martínez-Barnetche, J.; López-Martínez, I.; Aparicio-Antonio, R.; Shamah-Levy, T.; Alpuche-Aranda, C.; Rivera, J. A.; Barrientos-Gutierrez, T.; Cuevas-Nasu, L.; Gaona-Pineda, E. B.; Ávila-Arcos, M. A.; Reyes-Sánchez, F.; Torres-Álvarez, R.; López-Olmedo, N.; Vidaña-Perez, D.; González-Morales, R.; Barrera-Nuñez, D.; Perez-Ferrer, C.; Gaspar-Castillo, C.; Stern, D.; Canto-Osorio, F.; Sanchez-Pájaro, A. Nationally Representative SARS-CoV-2 Antibody Prevalence Estimates after the First Epidemic Wave in Mexico. *Nat. Commun.* **2022**, *13*, 589.

(3) Lalwani, P.; Salgado, B. B.; Filho, I. V. P.; da Silva, D. S. S.; de Morais, T. B. do N.; Jordão, M. F.; Barbosa, A. R. C.; Cordeiro, I. B.; Neto, J. N. de S.; de Assunção, E. N.; dos Santos, R. O.; Carvalho, N. O.; Sobrinho, W. B. S.; da Costa, C. F.; de Souza, P. E.; de Albuquerque, B. C.; Ganoza, C. A.; Araujo-Castillo, R. v.; Filho, S. A.; Lalwani, J. D. B. SARS-CoV-2 Seroprevalence and Associated Factors in Manaus, Brazil: Baseline Results from the DETECTCoV-19 Cohort Study. *Int. J. Infect. Dis.* **2021**, *110*, 141−150.

(4) Rostami, A.; Sepidarkish, M.; Leeflang, M. M.; Riahi, S.; Nourollahpour Shiadeh, M.; Esfandyari, S.; Mokdad, A. H.; Hotez, P. J.; Gasser, R. B.; author Robin Gasser, C. B. SARS-CoV-2 seroprevalence worldwide: a systematic review and meta-analysis. *Clin. Microbiol. Infect.* **2021**, *27*, 331−340.

(5) Wu, M.; Wall, E. C.; Carr, E. J.; Harvey, R.; Townsley, H.; Mears, H. v.; Adams, L.; Kjaer, S.; Kelly, G.; Warchal, S.; Sawyer, C.; Kavanagh, C.; Queval, C. J.; Ngai, Y.; Hatipoglu, E.; Ambrose, K.; Hindmarsh, S.; Beale, R.; Gamblin, S.; Howell, M.; Kassiotis, G.; Libri, V.; Williams, B.; Gandhi, S.; Swanton, C.; Bauer, D. L. Three-Dose Vaccination Elicits Neutralising Antibodies against Omicron. *Lancet* **2022**, *399*, 715−717.

(6) Collie, S.; Champion, J.; Moultrie, H.; Bekker, L.-G.; Gray, G. Effectiveness of BNT162b2 Vaccine against Omicron Variant in South Africa. *N. Engl. J. Med.* **2022**, *386*, 494−496.

(7) Vanaparthy, R.; Mohan, G.; Vasireddy, D.; Atluri, P. Review of Covid-19 Viral Vector-Based Vaccines and Covid-19 Variants. *Infez. Med.* **2021**, *29*, 328−338.

(8) Stamatatos, L.; Czartoski, J.; Wan, Y. H.; Homad, L. J.; Rubin, V.; Glantz, H.; Neradilek, M.; Seydoux, E.; Jennewein, M. F.; MacCamy, A. J.; Feng, J.; Mize, G.; de Rosa, S. C.; Lemos, A.; Cohen, M. P.; Moodie, K. W.; McElrath, Z.; McGuire, M. J.; McGuire, A. T. MRNA Vaccination Boosts Cross-Variant Neutralizing Antibodies Elicited by SARS-CoV-2 Infection. *Science* **2021**, *372*, 1413−1418.

(9) Hitchings, M. D. T.; Ranzani, O. T.; Torres, M. S. S.; de Oliveira, S. B.; Almiron, M.; Said, R.; Borg, R.; Schulz, W. L.; de Oliveira, R. D.; da Silva, P. V.; de Castro, D. B.; Sampaio, V. de S.; de Albuquerque, B. C.; Ramos, T. C. A.; Fraxe, S. H. H.; da Costa, C. F.; Naveca, F. G.; Siqueira, A. M.; de Araújo, W. N.; Andrews, J. R.; Cummings, D. A. T.; Ko, A. I.; Croda, J. Effectiveness of CoronaVac among Healthcare Workers in the Setting of High SARS-CoV-2 Gamma Variant Transmission in Manaus, Brazil: A Test-Negative Case-Control Study. *Lancet Reg. Health. Am.* **2021**, *1*, 100025.

(10) Li, J.; Hou, L.; Guo, X.; Jin, P.; Wu, S.; Zhu, J.; Pan, H.; Wang, X.; Song, Z.; Wan, J.; Cui, L.; Li, J.; Chen, Y.; Wang, X.; Jin, L.; Liu, J.; Shi, F.; Xu, X.; Zhu, T.; Chen, W.; Zhu, F. Heterologous AD5-NCOV plus CoronaVac versus Homologous CoronaVac Vaccination: A Randomized Phase 4 Trial. *Nat. Med.* **2022**, *28*, 401−409.

(11) Jara, A.; Undurraga, E. A.; González, C.; Paredes, F.; Fontecilla, T.; Jara, G.; Pizarro, A.; Acevedo, J.; Leo, K.; Leon, F.; Sans, C.; Leighton, P.; Suárez, P.; García-Escorza, H.; Araos, R. Effectiveness of an Inactivated SARS-CoV-2 Vaccine in Chile. *N. Engl. J. Med.* **2021**, *385*, 875−884.

(12) Medeiros, G. X.; Sasahara, G. L.; Magawa, J. Y.; Nunes, J. P. S.; Bruno, F. R.; Kuramoto, A. C.; Almeida, R. R.; Ferreira, M. A.; Scagion, G. P.; Candido, E. D.; Leal, F. B.; Oliveira, D. B. L.; Durigon, E. L.; Silva, R. C. v.; Rosa, D. S.; Boscardin, S. B.; Coelho, V.; Kalil, J.; Santos, K. S.; Cunha-Neto, E. Reduced T Cell and Antibody

Responses to Inactivated Coronavirus Vaccine Among Individuals Above 55 Years Old. *Front. Immunol.* **2022**, *13*, 812126.

(13) Karamese, M.; Tutuncu, E. E. The Effectiveness of Inactivated SARS-CoV-2 Vaccine (CoronaVac) on Antibody Response in Participants Aged 65 Years and Older. *J. Med. Virol.* **2022**, *94*, 173−177.

(14) Seyahi, E.; Bakhdiyarli, G.; Oztas, M.; Kuskucu, M. A.; Tok, Y.; Sut, N.; Ozcifci, G.; Ozcaglayan, A.; Balkan, I. I.; Saltoglu, N.; Tabak, F.; Hamuryudan, V. Antibody Response to Inactivated COVID-19 Vaccine (CoronaVac) in Immune-Mediated Diseases: A Controlled Study among Hospital Workers and Elderly. *Rheumatol. Int.* **2021**, *41*, 1429−1440.

(15) Vacharathit, V.; Aiewsakun, P.; Manopwisedjaroen, S.; Srisaowakarn, C.; Laopanupong, T.; Ludowyke, N.; Phuphuakrat, A.; Setthaudom, C.; Ekronarongchai, S.; Srichatrapimuk, S.; Wongsirisin, P.; Sangrajrang, S.; Imsuwansri, T.; Kirdlarp, S.; Nualkaew, S.; Sensorn, I.; Sawaengdee, W.; Wichukchinda, N.; Sungkanuparph, S.; Chantratita, W.; Kunakorn, M.; Rojanamatin, J.; Hongeng, S.; Thitithanyanont, A. CoronaVac Induces Lower Neutralising Activity against Variants of Concern than Natural Infection. *Lancet Infect. Dis.* **2021**, *21*, 1352−1354.

(16) Sethuraman, N.; Jeremiah, S. S.; Ryo, A. Interpreting Diagnostic Tests for SARS-CoV-2. *JAMA* **2020**, *323*, 2249−2251.

(17) Liu, P. P.; Zong, Y.; Jiang, S. P.; Jiao, Y. J.; Yu, X. J. Development of a Nucleocapsid Protein-Based ELISA for Detection of Human IgM and IgG Antibodies to SARS-CoV-2. *ACS Omega* **2021**, *6*, 9667−9671.

(18) Yadav, S.; Sadique, M. A.; Ranjan, P.; Kumar, N.; Singhal, A.; Srivastava, A. K.; Khan, R. SERS Based Lateral Flow Immunoassay for Point-of-Care Detection of SARS-CoV-2 in Clinical Samples. *ACS Appl. Bio Mater.* **2021**, *4*, 2974−2995.

(19) Ditte, K.; Nguyen Le, T. A.; Ditzer, O.; Sandoval Bojorquez, D. I.; Chae, S.; Bachmann, M.; Baraban, L.; Lissel, F. Rapid Detection of SARS-CoV-2 Antigens and Antibodies Using OFET Biosensors Based on a Soft and Stretchable Semiconducting Polymer. *ACS Biomater. Sci. Eng.* **2021**, DOI: 10.1021/acsbiomaterials.1c00727.

(20) Funari, R.; Chu, K. Y.; Shen, A. Q. Detection of Antibodies against SARS-CoV-2 Spike Protein by Gold Nanospikes in an Opto-Microfluidic Chip. *Biosens. Bioelectron.* **2020**, *169*, 112578.

(21) Mahshid, S. S.; Flynn, S. E.; Mahshid, S. The Potential Application of Electrochemical Biosensors in the COVID-19 Pandemic: A Perspective on the Rapid Diagnostics of SARS-CoV-2. *Biosens. Bioelectron.* **2021**, *176*, 112905.

(22) da Silva, S. J. R.; da Silva, C. T. A.; Guarines, K. M.; Mendes, R. P. G.; Pardee, K.; Kohl, A.; Pena, L. Clinical and Laboratory Diagnosis of SARS-CoV-2, the Virus Causing COVID-19. *ACS Infect. Dis.* **2020**, *6*, 2319−2336.

(23) Parihar, A.; Ranjan, P.; Sanghi, S. K.; Srivastava, A. K.; Khan, R. Point-of-Care Biosensor-Based Diagnosis of COVID-19 Holds Promise to Combat Current and Future Pandemics. *ACS Appl. Bio Mater.* **2020**, *3*, 7326−7343.

(24) Zhu, X.; Yuri, I.; Gan, X.; Suzuki, I.; Li, G. Electrochemical Study of the Effect of Nano-Zinc Oxide on Microperoxidase and Its Application to More Sensitive Hydrogen Peroxide Biosensor Preparation. *Biosens. Bioelectron.* **2007**, *22*, 1600−1604.

(25) Barbosa, H. P.; Araújo, D. A. G.; Pradela-Filho, L. A.; Takeuchi, R. M.; de Lima, R. G.; Ferrari, J. L.; Sousa Góes, M.; dos Santos, A. L. . *Zinc Oxide as a Multifunctional Material: From Biomedical Applications to Energy Conversion and Electrochemical Sensing*; Springer, 2021; Vol. 55, pp 251−305.

(26) Fortunato, E.; Gonçalves, A.; Pimentel, A.; Barquinha, P.; Gonçalves, G.; Pereira, L.; Ferreira, I.; Martins, R. Zinc Oxide, a Multifunctional Material: From Material to Device Applications. *Appl. Phys. A* **2009**, *96*, 197−205.

(27) Shetti, N. P.; Bukkitgar, S. D.; Reddy, K. R.; Reddy, C. V.; Aminabhavi, T. M. ZnO-Based Nanostructured Electrodes for Electrochemical Sensors and Biosensors in Biomedical Applications. *Biosens. Bioelectron.* **2019**, *141*, 111417.

(28) Dien, N. D. Preparation of Various Morphologies of ZnO Nanostructure through Wet Chemical Methods. *Adv. Mater. Sci.* **2019**, *4*, 1−5.

(29) Wojnarowicz, J.; Chudoba, T.; Lojkowski, W. A Review of Microwave Synthesis of Zinc Oxide Nanomaterials: Reactants, Process Parameters and Morphologies. *Nanomaterials* **2020**, *10*, 1086.

(30) Ellmer, K. Magnetron Sputtering of Transparent Conductive Zinc Oxide: Relation between the Sputtering Parameters and the Electronic Properties. *J. Phys. D: Appl. Phys.* **2000**, *33*, R17.

(31) Maruyama, T.; Shionoya, J. Zinc Oxide Thin Films Prepared by Chemical Vapour Deposition from Zinc Acetate. *J. Mater. Sci. Lett.* **1992**, *11*, 170−172.

(32) Sbrockey, N. M.; Ganesan, S. ZnO thin films by MOCVD. *III-Vs Rev.* **2004**, *17*, 23−25.

(33) Black, K.; Chalker, P. R.; Jones, A. C.; King, P. J.; Roberts, J. L.; Heys, P. N. A New Method for the Growth of Zinc Oxide Nanowires by MOCVD Using Oxygen-Donor Adducts of Dimethylzinc. *Chem. Vap. Deposition* **2010**, *16*, 106−111.

(34) Wang, X.; Li, X.; Zhang, Q.; Lu, Z.; Song, H.; Wang, Y. Electrodeposition of ZnO Nanorods with Synergistic Photocatalytic and Self-Cleaning Effects. *J. Electron. Mater.* **2021**, *50*, 4954−4961.

(35) Kumar, M.; Sasikumar, C. Electrodeposition of Nanostructured ZnO Thin Film: A Review. *Am. J. Mater. Sci.* **2014**, *2*, 18−23.

(36) Inguanta, R.; Garlisi, C.; Spanò, T.; Piazza, S.; Sunseri, C. Growth and Photoelectrochemical Behaviour of Electrodeposited ZnO Thin Films for Solar Cells. *J. Appl. Electrochem.* **2013**, *43*, 199−208.

(37) Ridhuan, N. S.; Abdul Razak, K.; Lockman, Z. Fabrication and Characterization of Glucose Biosensors by Using Hydrothermally Grown ZnO Nanorods. *Sci. Rep.* **2018**, *8*, 13722.

(38) Dai, Z.; Shao, G.; Hong, J.; Bao, J.; Shen, J. Immobilization and Direct Electrochemistry of Glucose Oxidase on a Tetragonal Pyramid-Shaped Porous ZnO Nanostructure for a Glucose Biosensor. *Biosens. Bioelectron.* **2009**, *24*, 1286−1291.

(39) Palomera, N.; Balaguera, M.; Arya, S. K.; Hernández, S.; Tomar, M. S.; Ramírez-Vick, J. E.; Singh, S. P. Zinc Oxide Nanorods Modified Indium Tin Oxide Surface for Amperometric Urea Biosensor. *J. Nanosci. Nanotechnol.* **2011**, *11*, 6683−6689.

(40) Tak, M.; Gupta, V.; Tomar, M. Flower-like ZnO Nanostructure Based Electrochemical DNA Biosensor for Bacterial Meningitis Detection. *Biosens. Bioelectron.* **2014**, *59*, 200−207.

(41) Israr, M. Q.; Sadaf, J. R.; Asif, M. H.; Nur, O.; Willander, M.; Danielsson, B. Potentiometric Cholesterol Biosensor Based on ZnO Nanorods Chemically Grown on Ag Wire. *Thin Solid Films* **2010**, *519*, 1106−1109.

(42) Jang, Y.; Park, J.; Pak, Y. K.; Pak, J. J. Immunosensor Based on the ZnO Nanorod Networks for the Detection of H1N1 Swine Influenza Virus. *J. Nanosci. Nanotechnol.* **2012**, *12*, 5173−5177.

(43) Park, J.; You, X.; Jang, Y.; Nam, Y.; Kim, M. J.; Min, N. K.; Pak, J. J. ZnO Nanorod Matrix Based Electrochemical Immunosensors for Sensitivity Enhanced Detection of Legionella Pneumophila. *Sens. Actuators, B* **2014**, *200*, 173−180.

(44) Tereshchenko, A.; Fedorenko, V.; Smyntyna, V.; Konup, I.; Konup, A.; Eriksson, M.; Yakimova, R.; Ramanavicius, A.; Balme, S.; Bechelany, M. ZnO Films Formed by Atomic Layer Deposition as an Optical Biosensor Platform for the Detection of Grapevine Virus A-Type Proteins. *Biosens. Bioelectron.* **2017**, *92*, 763−769.

(45) Gasparotto, G.; Costa, J. P. C.; Costa, P. I.; Zaghete, M. A.; Mazon, T. Electrochemical Immunosensor Based on ZnO Nanorods-Au Nanoparticles Nanohybrids for Ovarian Cancer Antigen CA-125 Detection. *Mater. Sci. Eng., C* **2017**, *76*, 1240−1247.

(46) Liu, A.; Yin, K.; Mi, L.; Ma, M.; Liu, Y.; Li, Y.; Wei, W.; Zhang, Y.; Liu, S. A Novel Photoelectrochemical Immunosensor by Integration of Nanobody and ZnO Nanorods for Sensitive Detection of Nucleoside Diphosphatase Kinase-A. *Anal. Chim. Acta* **2017**, *973*, 82−90.

(47) Martins, B. R.; Sampaio, T. M.; de Farias, A. K. S. R.; de Paula Martins, R. de P.; Teixeira, R. R.; Oliveira, R. T. S.; Oliveira, C. J. F.; da Silva, M. V.; Rodrigues, V.; Dantas, N. O.; Espindola, F. S.; Silva,

A. C. A.; Alves-Balvedi, R. P. Immunosensor Based on Zinc Oxide Nanocrystals Decorated with Copper for the Electrochemical Detection of Human Salivary Alpha-Amylase. *Micromachines* **2021**, *12*, 657.

(48) Vabbina, P. K.; Kaushik, A.; Pokhrel, N.; Bhansali, S.; Pala, N. Electrochemical Cortisol Immunosensors Based on Sonochemically Synthesized Zinc Oxide 1D Nanorods and 2D Nanoflakes. *Biosens. Bioelectron.* **2015**, *63*, 124−130.

(49) Tabatabaei, M. K.; Fard, H. G.; Koohsorkhi, J.; Mohammadnejad Arough, J. High-performance Immunosensor for Urine Albumin Using Hybrid Architectures of ZnO Nanowire/ Carbon Nanotube. *IET Nanobiotechnol.* **2020**, *14*, 126−132.

(50) Koike, K.; Mukai, K.; Onaka, T.; Maemoto, T.; Sasa, S.; Yano, M. A Potentiometric Immunosensor Based on a ZnO Field-Effect Transistor. *Jpn. J. Appl. Phys.* **2014**, *53*, 05FF04.

(51) Dong, S.; Tong, M.; Zhang, D.; Huang, T. The strategy of nitrite and immunoassay human IgG biosensors based on ZnO@ZIF-8 and ionic liquid composite film. *Mater. Sci. Eng., C* **2017**, *251*, 650−657.

(52) Patella, B.; Moukri, N.; Regalbuto, G.; Cipollina, C.; Pace, E.; Di Vincenzo, S.; Aiello, G.; O'Riordan, A.; Inguanta, R. Electrochemical Synthesis of Zinc Oxide Nanostructures on Flexible Substrate and Application as an Electrochemical Immunoglobulin-G Immunosensor. *Materials* **2022**, *15*, 713.

(53) Yang, T.; Chen, M.; Kong, Q.; Luo, X.; Jiao, K. Toward DNA Electrochemical Sensing by Free-Standing ZnO Nanosheets Grown on 2D Thin-Layered MoS2. *Biosens. Bioelectron.* **2017**, *89*, 538−544.

(54) Wang, C.; Tan, X.; Chen, S.; Yuan, R.; Hu, F.; Yuan, D.; Xiang, Y. Highly-Sensitive Cholesterol Biosensor Based on Platinum-Gold Hybrid Functionalized ZnO Nanorods. *Talanta* **2012**, *94*, 263−270.

(55) Choi, M. S.; Na, H. G.; Shim, G. S.; Cho, J. H.; Kim, M. Y.; Kim, S. i.; Baek, S. H.; Jin, C.; Lee, K. H. Simple and Scalable Synthesis of Urchin-like ZnO Nanoparticles via a Microwave-Assisted Drying Process. *Ceram. Int.* **2021**, *47*, 14621−14629.

(56) Chang, T. H.; Lu, Y. C.; Yang, M. J.; Huang, J. W.; Linda Chang, P. F.; Hsueh, H. Y. Multibranched Flower-like ZnO Particles from Eco-Friendly Hydrothermal Synthesis as Green Antimicrobials in Agriculture. *J. Cleaner Prod.* **2020**, *262*, 121342.

(57) Phuruangrat, A.; Kuntalue, B.; Thongtem, S.; Thongtem, T. Hydrothermal Synthesis of Hexagonal ZnO Nanoplates Used for Photodegradation of Methylene Blue. *Optik* **2021**, *226*, 165949.

(58) Mwankemwa, B. S.; Malevu, T. D.; Sahini, M. G.; Vuai, S. A. Effects of Vertically Aligned ZnO Nanorods Surface Morphology on the Ambient-Atmosphere Fabricated Organic Solar Cells. *Results Mater.* **2022**, *14*, 100271.

(59) Chen, Y. X.; Zhao, X. Q.; Sha, B.; Chen, J. H. Stacking Fault Directed Growth of Thin ZnO Nanobelt. *Mater. Lett.* **2008**, *62*, 2369−2371.

(60) Kołodziejczak-Radzimska, A.; Jesionowski, T. Zinc Oxide-From Synthesis to Application: A Review. *Materials* **2014**, *7*, 2833−2881.

(61) Souza, J. S.; Carvalho, W. M.; Souza, F. L.; Ponce-de-Leon, C.; Bavykin, D. v.; Alves, W. A. Multihierarchical Electrodes Based on Titanate Nanotubes and Zinc Oxide Nanorods for Photoelectro-chemical Water Splitting. *J. Mater. Chem. A* **2016**, *4*, 944−952.

(62) Elgrishi, N.; Rountree, K. J.; McCarthy, B. D.; Rountree, E. S.; Eisenhart, T. T.; Dempsey, J. L. A Practical Beginner's Guide to Cyclic Voltammetry. *J. Chem. Educ.* **2018**, *95*, 197−206.

(63) Huang, M. H.; Mao, S.; Feick, H.; Yan, H.; Wu, Y.; Kind, H.; Weber, E.; Russo, R.; Yang, P. Room-Temperature Ultraviolet Nanowire Nanolasers. *Science* **2001**, *292*, 1897−1899.

(64) Jindal, K.; Tomar, M.; Gupta, V. CuO Thin Film Based Uric Acid Biosensor with Enhanced Response Characteristics. *Biosens. Bioelectron.* **2012**, *38*, 11−18.

(65) Molaakbari, E.; Mostafavi, A.; Beitollahi, H.; Alizadeh, R. Synthesis of ZnO Nanorods and Their Application in the Construction of a Nanostructure-Based Electrochemical Sensor for Determination of Levodopa in the Presence of Carbidopa. *Analyst* **2014**, *139*, 4356−4364.

(66) Wang, J. *Analytical Electrochemistry*, 3rd ed.; Wiley, 2006.

(67) Al-Fandi, M. G.; Alshraiedeh, N. H.; Oweis, R. J.; Hayajneh, R. H.; Alhamdan, I. R.; Alabed, R. A.; Al-Rawi, O. F. Direct Electrochemical Bacterial Sensor Using ZnO Nanorods Disposable Electrode. *Sens. Rev.* **2018**, *38*, 326−334.

(68) Siddegowda, K. S.; Mahesh, B.; Chamaraja, N. A.; Roopashree, B.; Kumara Swamy, N.; Nanjundaswamy, G. S. Zinc Oxide Nanoparticles Supported on Multi-Walled Carbon Nanotube Modified Electrode for Electrochemical Sensing of a Fluoroquinolone Drug. *Electroanalysis* **2020**, *32*, 2183−2192.

(69) Batra, N.; Sharma, A.; Tomar, M.; Gupta, V. Efficient Detection of Total Cholesterol Using (ChEt-ChOx/ZnO/Pt/Si) Bioelectrode Based on ZnO Matrix. *Thin Solid Films* **2014**, *562*, 612−620.

(70) Hou, X.; Wang, L.; He, G.; Hao, J. Synthesis, Optical and Electrochemical Properties of ZnO Nanorod Hybrids Loaded with High-Density Gold Nanoparticles. *CrystEngComm* **2012**, *14*, 5158−5162.

(71) Zhan, F.; Yang, Y.; Liu, W.; Wang, K.; Li, W.; Li, J. Facile Synthesis of FeOOH Quantum Dots Modified ZnO Nanorods Films via a Metal-Solating Process. *ACS Sustainable Chem. Eng.* **2018**, *6*, 7789−7798.

(72) Ferrag, C.; Kerman, K. Grand Challenges in Nanomaterial-Based Electrochemical Sensors. *Front. Sens.* **2020**, *1*, 583822.

(73) Zucolotto, V. Specialty Grand Challenges in Biosensors. *Front. Sens.* **2020**, *1*, 3.

(74) Huang, Y.; Yang, C.; Xu, X.; Xu, W.; Liu, S. Structural and Functional Properties of SARS-CoV-2 Spike Protein: Potential Antivirus Drug Development for COVID-19. *Acta Pharmacol. Sin.* **2020**, *41*, 1141−1149.

(75) Viter, R.; Khranovskyy, V.; Starodub, N.; Ogorodniichuk, Y.; Gevelyuk, S.; Gertnere, Z.; Poletaev, N.; Yakimova, R.; Erts, D.; Smyntyna, V.; Ubelis, A. Application of Room Temperature Photoluminescence from ZnO Nanorods for Salmonella Detection. *IEEE Sens. J.* **2014**, *14*, 2028−2034.

(76) Rodrigues, J.; Pereira, S. O.; Santos, N. F.; Rodrigues, C.; Costa, F. M.; Monteiro, T. Insights on Luminescence Quenching of ZnO Tetrapods in the Detection of HCG. *Appl. Surf. Sci.* **2020**, *527*, 146813.

(77) Viter, R.; Savchuk, M.; Starodub, N.; Balevicius, Z.; Tumenas, S.; Ramanaviciene, A.; Jevdokimovs, D.; Erts, D.; Iatsunskyi, I.; Ramanavicius, A. Photoluminescence Immunosensor Based on Bovine Leukemia Virus Proteins Immobilized on the ZnO Nanorods. *Sens. Actuators, B* **2019**, *285*, 601−606.

(78) Zia, T. ul H.; Shah, A. ul H. A. Label-Free Photo-electrochemical Immunosensor Based on Sensitive Photocatalytic Surface of Sn Doped ZnO for Detection of Hepatitis C (HCV) Anticore MAbs 19D9D6. *Colloids Surf., A* **2021**, *630*, 127586.

(79) Almeida, R. M.; Ferrari, V. C.; Souza, J.; Souza, F. L.; Alves, W. A. Tailoring a Zinc Oxide Nanorod Surface by Adding an Earth-Abundant Cocatalyst for Induced Sunlight Water Oxidation. *ChemPhysChem* **2020**, *21*, 476−483.

(80) McPeak, K. M.; Le, T. P.; Britton, N. G.; Nickolov, Z. S.; Elabd, Y. A.; Baxter, J. B. Chemical Bath Deposition of ZnO Nanowires at Near-Neutral PH Conditions without Hexamethylenetetramine (HMTA): Understanding the Role of HMTA in ZnO Nanowire Growth. *Langmuir* **2011**, *27*, 3672−3677.

(81) Hsu, Y. F.; Xi, Y. Y.; Tam, K. H.; Djurišić, A. B.; Luo, J.; Ling, C. C.; Cheung, C. K.; Ng, A. M. C.; Chan, W. K.; Deng, X.; Beling, C. D.; Fung, S.; Cheah, K. W.; Fong, P. W. K.; Surya, C. C. Undoped P-Type ZnO Nanorods Synthesized by a Hydrothermal Method. *Adv. Funct. Mater.* **2008**, *18*, 1020−1030.

(82) Yan, X.; Li, Z.; Chen, R.; Gao, W. Template Growth of ZnO Nanorods and Microrods with Controllable Densities. *Cryst. Growth Des.* **2008**, *8*, 2406−2410.

(83) Mitra, S.; Patra, P.; Chandra, S.; Debnath, N.; Das, S.; Banerjee, R.; Kundu, S. C.; Pramanik, P.; Goswami, A. Porous ZnO Nanorod for Targeted Delivery of Doxorubicin: In Vitro and in Vivo Response for Therapeutic Applications. *J. Mater. Chem.* **2012**, *22*, 24145−24154.

(84) Klochko, N.; Klepikova, K.; Kopach, V.; Tyukhov, I.; Starikov, V.; Sofronov, D.; Khrypunova, I.; Zhadan, D.; Petrushenko, S.; Dukarov, S.; Lyubov, V.; Kirichenko, M.; Khrypunova, A. Development of Semi-Transparent ZnO/FTO Solar Thermoelectric Nanogenerator for Energy Efficient Glazing. *Sol. Energy* **2019**, *184*, 230−239.

(85) Hernández-Paredes, J.; Glossman-Mitnik, D.; Esparza-Ponce, H. E.; Alvarez-Ramos, M. E.; Duarte-Moller, A. Band Structure, Optical Properties and Infrared Spectrum of Glycine−Sodium Nitrate Crystal. *J. Mol. Struct.* **2008**, *875*, 295−301.

(86) Aydın, E. B.; Aydln, M.; Sezginturk, M. K. New Impedimetric Sandwich Immunosensor for Ultrasensitive and Highly Specific Detection of Spike Receptor Binding Domain Protein of SARS-CoV-2. *ACS Biomater. Sci. Eng.* **2021**, *7*, 3874−3885.

(87) Martinez-Cuazitl, A.; Vazquez-Zapien, G. J.; Sanchez-Brito, M.; Limon-Pacheco, J. H.; Guerrero-Ruiz, M.; Garibay-Gonzalez, F.; Delgado-Macuil, R. J.; de Jesus, M. G. G.; Pereyra-Talamantes, M. A.; Mata-Miranda, A.; Mata-Miranda, M. M. ATR-FTIR Spectrum Analysis of Saliva Samples from COVID-19 Positive Patients. *Sci. Rep.* **2021**, *11*, 19980.

(88) Pramanik, A.; Gao, Y.; Patibandla, S.; Mitra, D.; McCandless, M. G.; Fassero, L. A.; Gates, K.; Tandon, R.; Chandra Ray, P. The Rapid Diagnosis and Effective Inhibition of Coronavirus Using Spike Antibody Attached Gold Nanoparticles. *Nanoscale Adv.* **2021**, *3*, 1588−1596.

(89) Zhao, S.; Qiao, X.; Chen, M.; Li, Y.; Wang, X.; Xu, Z.; Wu, Y.; Luo, X. D. Amino Acid-Based Antifouling Peptides for the Construction of Electrochemical Biosensors Capable of Assaying Proteins in Serum with Enhanced Stability. *ACS Sens.* **2022**, *7*, 1740−1746.

(90) Biswas, S.; Lan, Q.; Li, C.; Xia, X. H. Morphologically Flex Sm-MOF Based Electrochemical Immunosensor for Ultrasensitive Detection of a Colon Cancer Biomarker. *Anal. Chem.* **2022**, *94*, 3013−3019.

(91) Aerathupalathu Janardhanan, J.; Chen, Y. L.; Liu, C. T.; Tseng, H. S.; Wu, P. I.; She, J. W.; Hsiao, Y. S.; Yu, H. H. Sensitive Detection of Sweat Cortisol Using an Organic Electrochemical Transistor Featuring Nanostructured Poly(3,4-Ethylenedioxythiophene) Derivatives in the Channel Layer. *Anal. Chem.* **2022**, *94*, 7584−7593.

(92) Saáedi, A.; Yousefi, R.; Jamali-Sheini, F.; Zak, A. K.; Cheraghizade, M.; Mahmoudian, M. R.; Baghchesara, M. A.; Dezaki, A. S. XPS Studies and Photocurrent Applications of Alkali-Metals-Doped ZnO Nanoparticles under Visible Illumination Conditions. *Phys. E Low-dimens. Syst. Nanostruct.* **2016**, *79*, 113−118.

(93) Ahmad, R.; Tripathy, N.; Khan, M. Y.; Bhat, K. S.; Ahn, M. S.; Hahn, Y. B. Ammonium Ion Detection in Solution Using Vertically Grown ZnO Nanorod Based Field-Effect Transistor. *RSC Adv.* **2016**, *6*, 54836−54840.

(94) Al-Gaashani, R.; Radiman, S.; Daud, A. R.; Tabet, N.; Al-Douri, Y. XPS and Optical Studies of Different Morphologies of ZnO Nanostructures Prepared by Microwave Methods. *Ceram. Int.* **2013**, *39*, 2283−2292.

(95) Wu, Z. W.; Tyan, S. L.; Chen, H. H.; Huang, J. C. A.; Huang, Y. C.; Lee, C. R.; Mo, T. S. Temperature-Dependent Photoluminescence and XPS Study of ZnO Nanowires Grown on Flexible Zn Foil via Thermal Oxidation. *Superlattices Microstruct.* **2017**, *107*, 38−43.

(96) Das, J.; Pradhan, S. K.; Sahu, D. R.; Mishra, D. K.; Sarangi, S. N.; Nayak, B. B.; Verma, S.; Roul, B. K. Micro-Raman and XPS Studies of Pure ZnO Ceramics. *Physica B* **2010**, *405*, 2492−2497.

(97) Das, S. K.; Dickinson, C.; Lafir, F.; Brougham, D. F.; Marsili, E. Synthesis, Characterization and Catalytic Activity of Gold Nanoparticles Biosynthesized with Rhizopus Oryzae Protein Extract. *Green Chem.* **2012**, *14*, 1322−1334.

(98) Kehrer, M.; Duchoslav, J.; Hinterreiter, A.; Cobet, M.; Mehic, A.; Stehrer, T.; Stifter, D. XPS Investigation on the Reactivity of Surface Imine Groups with TFAA. *Plasma Processes Polym.* **2019**, *16*, 1800160.

(99) Rushworth, J. v.; Ahmed, A.; Griffiths, H. H.; Pollock, N. M.; Hooper, N. M.; Millner, P. A. A Label-Free Electrical Impedimetric Biosensor for the Specific Detection of Alzheimer's Amyloid-Beta Oligomers. *Biosens. Bioelectron.* **2014**, *56*, 83−90.

(100) Qi, P.; Wan, Y.; Zhang, D. Impedimetric Biosensor Based on Cell-Mediated Bioimprinted Films for Bacterial Detection. *Biosens. Bioelectron.* **2013**, *39*, 282−288.

(101) Layqah, L. A.; Eissa, S. An Electrochemical Immunosensor for the Corona Virus Associated with the Middle East Respiratory Syndrome Using an Array of Gold Nanoparticle-Modified Carbon Electrodes. *Mikrochim. Acta* **2019**, *186*, 224.

(102) Alafeef, M.; Dighe, K.; Moitra, P.; Pan, D. Rapid, Ultrasensitive, and Quantitative Detection of SARS-CoV-2 Using Antisense Oligonucleotides Directed Electrochemical Biosensor Chip. *ACS Nano* **2020**, *14*, 17028−17045.

(103) Lister, A. S. Validation of HPLC Methods in Pharmaceutical Analysis. *Sep. Sci. Technol.* **2005**, *6*, 191−217.

(104) Zhang, Z.; Wang, X.; Wei, X.; Zheng, S. W.; Lenhart, B. J.; Xu, P.; Li, J.; Pan, J.; Albrecht, H.; Liu, C. Multiplex Quantitative Detection of SARS-CoV-2 Specific IgG and IgM Antibodies Based on DNA-Assisted Nanopore Sensing. *Biosens. Bioelectron.* **2021**, *181*, 113134.

(105) Jiang, M.; Dong, T.; Han, C.; Liu, L.; Zhang, T.; Kang, Q.; Wang, P.; Zhou, F. Regenerable and High-Throughput Surface Plasmon Resonance Assay for Rapid Screening of Anti-SARS-CoV-2 Antibody in Serum Samples. *Anal. Chim. Acta* **2022**, *1208*, 339830.

(106) Yakoh, A.; Pimpitak, U.; Rengpipat, S.; Hirankarn, N.; Chailapakul, O.; Chaiyo, S. Paper-Based Electrochemical Biosensor for Diagnosing COVID-19: Detection of SARS-CoV-2 Antibodies and Antigen. *Biosens. Bioelectron.* **2021**, *176*, 112912.

(107) Qu, J.; Chenier, M.; Zhang, Y.; Xu, C. Q. A Microflow Cytometry-Based Agglutination Immunoassay for Point-of-Care Quantitative Detection of SARS-CoV-2 IgM and IgG. *Micromachines* **2021**, *12*, 433.

(108) Wright, P. F.; Nilsson, E.; Van Rooij, E. M.; Lelenta, M.; Jeggo, M. H. Standardisation and Validation of Enzyme-Linked Immunosorbent Assay Techniques for the Detection of Antibody in Infectious Disease Diagnosis. *Rev. Sci. Tech.* **1993**, *12*, 435−450.

(109) Frey, A.; Di Canzio, J.; Zurakowski, D. A Statistically Defined Endpoint Titer Determination Method for Immunoassays. *J. Immunol. Methods* **1998**, *221*, 35−41.

(110) Brodin, P. Immune Determinants of COVID-19 Disease Presentation and Severity. *Nat. Med.* **2021**, *27*, 28−33.

(111) Trevethan, R. Sensitivity, Specificity, and Predictive Values: Foundations, Pliabilities, and Pitfalls in Research and Practice. *Front. Public Health* **2017**, *5*, 307.

(112) Pewsner, D.; Battaglia, M.; Minder, C.; Marx, A.; Bucher, H. C.; Egger, M. Ruling a Diagnosis in or out with "SpPIn" and "SnNOut": A Note of Caution. *Br. Med. J.* **2004**, *329*, 209−213.

(113) Ravindran, R.; McReynolds, C.; Yang, J.; Hammock, B. D.; Ikram, A.; Ali, A.; Bashir, A.; Zohra, T.; Chang, W. L. W.; Hartigan-O'Connor, D. J.; Rashidi, H. H.; Khan, I. H. Immune Response Dynamics in COVID-19 Patients to SARS-CoV-2 and Other Human Coronaviruses. *PLoS One* **2021**, *16*, No. e0254367.

(114) Lombardi, A.; Bozzi, G.; Ungaro, R.; Villa, S.; Castelli, V.; Mangioni, D.; Muscatello, A.; Gori, A.; Bandera, A. Mini Review Immunological Consequences of Immunization With COVID-19 MRNA Vaccines: Preliminary Results. *Front. Immunol.* **2021**, *12*, 657711.

(115) Pollard, A. J.; Bijker, E. M. A Guide to Vaccinology: From Basic Principles to New Developments. *Nat. Rev. Immunol.* **2021**, *21*, 83−100.

(116) Cerqueira-Silva, T.; Andrews, J. R.; Boaventura, V. S.; Ranzani, O. T.; de Araújo Oliveira, V.; Paixão, E. S.; Júnior, J. B.; Machado, T. M.; Hitchings, M. D. T.; Dorion, M.; Lind, M. L.; Penna, G. O.; Cummings, D. A. T.; Dean, N. E.; Werneck, G. L.; Pearce, N.; Barreto, M. L.; Ko, A. I.; Croda, J.; Barral-Netto, M. Effectiveness of CoronaVac, ChAdOx1 NCoV-19, BNT162b2, and Ad26.COV2.S among Individuals with Previous SARS-CoV-2 Infection in Brazil: A Test-Negative, Case-Control Study. *Lancet Infect. Dis.* **2022**, *22*, 791.

(117) Soysal, A.; Gönüllü, E.; Karabayir, N.; Alan, S.; Atici, S.; Yildiz, I.; Engin, H.; Çivilibal, M.; Karaböcüoğlu, M. Comparison of Immunogenicity and Reactogenicity of Inactivated SARS-CoV-2 Vaccine (CoronaVac) in Previously SARS-CoV-2 Infected and Uninfected Health Care Workers. *Hum. Vaccines Immunother.* **2021**, *17*, 1953344.

(118) Wang, Z.; Muecksch, F.; Schaefer-Babajew, D.; Finkin, S.; Viant, C.; Gaebler, C.; Hoffmann, H. H.; Barnes, C. O.; Cipolla, M.; Ramos, V.; Oliveira, T. Y.; Cho, A.; Schmidt, F.; Da Silva, J.; Bednarski, E.; Aguado, L.; Yee, J.; Daga, M.; Turroja, M.; Millard, K. G.; Jankovic, M.; Gazumyan, A.; Zhao, Z.; Rice, C. M.; Bieniasz, P. D.; Caskey, M.; Hatziioannou, T.; Nussenzweig, M. C. Naturally Enhanced Neutralizing Breadth against SARS-CoV-2 One Year after Infection. *Nature* **2021**, *595*, 426−431.

(119) Hajian-Tilaki, K. Receiver Operating Characteristic (ROC) Curve Analysis for Medical Diagnostic Test Evaluation. *Caspian J. Intern. Med.* **2013**, *4*, 627−635.

(120) Zou, K. H.; O'Malley, A. J.; Mauri, L. Receiver-Operating Characteristic Analysis for Evaluating Diagnostic Tests and Predictive Models. *Circulation* **2007**, *115*, 654−657.

(121) Mukaka, M. M. Statistics Corner: A Guide to Appropriate Use of Correlation Coefficient in Medical Research. *Malawi Med. J.* **2012**, *24*, 69−71.

(122) Schober, P.; Boer, C.; Schwarte, L. A. Correlation Coefficients: Appropriate Use and Interpretation. *Anesth. Analg.* **2018**, *126*, 1763−1768.